

Universidad de Málaga

Escuela Técnica Superior de Ingeniería de Telecomunicación



TESIS DOCTORAL

ANALYSIS OF GAUSSIAN QUADRATIC FORMS  
WITH APPLICATION TO STATISTICAL  
CHANNEL MODELING

Autor:

PABLO RAMÍREZ ESPINOSA

Doctorado en Ingeniería de Telecomunicación

Ph.D. in Telecommunication Engineering

Directores:

EDUARDO MARTOS NAYA


JOSÉ ANTONIO CORTÉS ARRABAL

AÑO 2019



UNIVERSIDAD  
DE MÁLAGA

AUTOR: Pablo Ramírez Espinosa

 <http://orcid.org/0000-0003-1161-0747>

EDITA: Publicaciones y Divulgación Científica. Universidad de Málaga



Esta obra está bajo una licencia de Creative Commons Reconocimiento-NoComercial-SinObraDerivada 4.0 Internacional:

<http://creativecommons.org/licenses/by-nc-nd/4.0/legalcode>

Cualquier parte de esta obra se puede reproducir sin autorización  
pero con el reconocimiento y atribución de los autores.

No se puede hacer uso comercial de la obra y no se puede alterar, transformar o hacer obras derivadas.

Esta Tesis Doctoral está depositada en el Repositorio Institucional de la Universidad de Málaga (RIUMA): [riuma.uma.es](http://riuma.uma.es)





UNIVERSIDAD  
DE MÁLAGA

## AUTORIZACIÓN PARA LA LECTURA DE LA TESIS

D. Eduardo Martos Naya y D. José Antonio Cortés Arrabal, profesores doctores del Departamento de Ingeniería de Comunicaciones de la Universidad de Málaga

### CERTIFICAN

Que D. Pablo Ramírez Espinosa, Ingeniero de Telecomunicación, ha realizado en el Departamento de Ingeniería de Comunicaciones de la Universidad de Málaga, bajo su dirección el trabajo de investigación correspondiente a su TESIS DOCTORAL titulada:

### **"Analysis of Gaussian Quadratic Forms with Application to Statistical Channel Modeling"**

En dicho trabajo, se han propuesto aportaciones originales en el problema de análisis estadístico de formas cuadráticas gaussianas, así como la introducción de un nuevo método de análisis de variables aleatorias. Igualmente, basándose en dichas aportaciones, se han introducido nuevos modelos generalizados de desvanecimientos. Esto ha dado lugar a varias publicaciones científicas, superando el requisito de 1 punto ANECA del programa de doctorado regulado por el Real Decreto 99/2011.

Por todo ello, y dada la unidad temática de las distintas contribuciones y la metodología común seguida en todas ellas, los directores consideran que esta tesis es apta para su presentación al Tribunal que ha de juzgarla y AUTORIZAN la presentación de la tesis por COMPENDIO DE PUBLICACIONES en la Universidad de Málaga. Igualmente, certifican que las publicaciones que avalan la tesis no han sido empleadas en trabajos anteriores a la misma.

Málaga, 26 de septiembre de 2019

Los directores:

Fdo.: Eduardo Martos Naya

Fdo.: José Antonio Cortés Arrabal



UNIVERSIDAD  
DE MÁLAGA

**UNIVERSIDAD DE MÁLAGA**  
**ESCUELA TÉCNICA SUPERIOR DE INGENIERÍA DE**  
**TELECOMUNICACIÓN**

Reunido el tribunal examinador en el día de la fecha, constituido por:

Presidente: Dr. D. \_\_\_\_\_

Secretario: Dr. D. \_\_\_\_\_

Vocal: Dr. D. \_\_\_\_\_

para juzgar la Tesis Doctoral titulada "*Analysis of Gaussian Quadratic Forms with Application to Statistical Channel Modeling*", realizada por D. Pablo Ramírez Espinosa y dirigida por los Dres. D. Eduardo Martos Naya y D. José Antonio Cortés Arrabal,

acordó por \_\_\_\_\_ otorgar la calificación de

\_\_\_\_\_

y, para que conste, se extiende firmada por los componentes del tribunal la presente diligencia.

Málaga, a \_\_\_\_\_ de \_\_\_\_\_ del \_\_\_\_\_

El presidente:

El secretario:

El vocal:

Fdo.: \_\_\_\_\_

Fdo.: \_\_\_\_\_

Fdo.: \_\_\_\_\_



UNIVERSIDAD  
DE MÁLAGA

*"I have no special talent. I am only passionately curious."*

Albert Einstein





UNIVERSIDAD  
DE MÁLAGA

# *Agradecimientos*

Me gustaría dar las gracias, en primer lugar, a mis directores de tesis, Eduardo y José Antonio, por guiarme a lo largo de estos años. Mucho de lo que he aprendido a lo largo de mi doctorado se lo debo a ellos, desde esas charlas aparentemente infinitas sobre variables aleatorias hasta profundas lecciones acerca de cómo redactar y preparar documentos científicos. Me siento afortunado de haber contado con ellos como directores, pues son ejemplo no sólo de profesores, sino de personas.

No podría olvidarme tampoco de otras personas que me han aportado tanto en este tiempo. En especial, querría agradecer a Javier y a José Paris todo lo que se han implicado conmigo; pues sin ser mis directores han actuado como tal, enseñándome y guiándome a lo largo del proceso. Igualmente, quisiera agradecer a Laureano todo su apoyo, tanto como compañero en la Universidad de Málaga como desde la distancia en su aventura investigadora en Hong Kong.

Gracias también a David, por haber sido mi apoyo profesional y personal durante mi estancia en Queen's University. Siempre es un placer trabajar junto a investigadores de su calibre.

Y por último, pero quizás lo más importante de todo, gracias a mi familia, en especial a mis padres, por el incondicional apoyo ya no sólo durante el doctorado sino durante toda mi vida. Gracias por creer en mí.



UNIVERSIDAD  
DE MÁLAGA

## *Abstract*

This thesis provides novel and tight approximations to the distribution of both real and complex non-central Gaussian quadratic forms (GQFs). To that end, a new method to analyze random variables is proposed, which is based on the analysis of a suitably defined sequence of auxiliary random variables that converges in distribution to the target one. Consequently, the major advantage of this proposal is that the resulting expressions always represent a valid distribution, in contrast to classical approximation methods based on series expansions.

By leveraging such convergence, simple and recursive approximations for the probability density function (PDF) and the cumulative distribution function (CDF) of positive definite real GQFs are given. In the context of indefinite complex GQFs, the application of the proposed technique leads to very tractable approximants for their first order statistics in terms of elementary functions, i.e., exponentials and powers. Thus, the obtained expressions are more useful for further analytical purposes than other solutions available in the literature. This tractability is exemplified through the performance analysis of maximal ratio combining systems over correlated Rice channels, providing closed-form approximations for the outage probability and the bit error.

Moreover, in the context of channel modeling, the proposed methodology of analysis of variables gives rise to two generalizations of the well-know  $\kappa$ - $\mu$  shadowed fading model. These new models, namely the fluctuating Beckmann and the correlated  $\kappa$ - $\mu$  shadowed models, include as particular cases the vast majority of fading distributions, ranging from the classical ones such as Rayleigh and Rice models to more refined extensions as the Beckmann distribution or the  $\eta$ - $\mu$  model. The statistical characterization of both distributions is provided, giving closed-form expressions for their moment generating function (MGF), PDF and CDF; along with the formulation of the second order statistics of the fluctuating Beckmann model.



UNIVERSIDAD  
DE MÁLAGA

## Resumen

En esta tesis se presenta una nueva aproximación a la distribución de formas cuadráticas gaussianas (FCGs) no centrales tanto en variables reales como complejas. Para ello, se propone un nuevo método de análisis de variables aleatorias que, en lugar de centrarse en el estudio de la variable en cuestión, se basa en la caracterización estadística de una secuencia de variables aleatorias auxiliares convenientemente definida. Como consecuencia, las expresiones obtenidas, con independencia del grado de precisión adquirido, siempre representan una distribución válida, siendo ésta su principal ventaja frente a otros métodos de aproximación clásicos basados en expansiones en series.

Aplicando este método, se obtienen simples expresiones recursivas para la función densidad de probabilidad (PDF) y la función de distribución (CDF) de las FCGs reales definidas positivas. En el caso de las formas complejas, esta nueva forma de análisis conduce a aproximaciones para los estadísticos de primer orden en términos de funciones elementales (exponenciales y potencias), siendo más convenientes para cálculos posteriores que otras soluciones disponibles en la literatura. La tratabilidad matemática de estos resultados se ejemplifica mediante el análisis de sistemas de combinación por razón máxima (MRC) sobre canales Rice correlados, proporcionando aproximaciones cerradas para la probabilidad de *outage* y la probabilidad de error de bit.

Finalmente, en el contexto de modelado de canal, la metodología de análisis de variables propuesta permite obtener dos nuevas generalizaciones del conocido modelo de desvanecimiento  $\kappa$ - $\mu$  *shadowed*. Estas dos nuevas distribuciones, nombradas Beckmann fluctuante y  $\kappa$ - $\mu$  *shadowed* correlado, incluyen como casos particulares a la gran mayoría de distribuciones de desvanecimientos usadas en la literatura, abarcando desde los modelos clásicos de Rayleigh y Rice hasta otros más generales y complejos como el Beckmann y el  $\eta$ - $\mu$ . Para ambas distribuciones, se presenta su caracterización estadística de primer orden, i.e., función generadora de momentos (MGF), PDF y CDF; así como los estadísticos de segundo orden del modelo Beckmann fluctuante.



UNIVERSIDAD  
DE MÁLAGA

# Contents

<b>1</b>	<b>Introduction</b>	<b>1</b>
1.1	Objectives . . . . .	3
1.2	Organization . . . . .	3
1.3	Publications . . . . .	4
<b>2</b>	<b>Background</b>	<b>5</b>
2.1	General notation . . . . .	5
2.2	Some results on random variables . . . . .	6
2.2.1	Convergence between sequences of random variables . . . . .	7
2.2.2	The Gaussian distribution . . . . .	9
2.2.3	The $\chi^2$ distribution . . . . .	10
2.2.4	The gamma distribution . . . . .	11
2.2.5	Classical approximations to the distribution of random variables . . . . .	13
2.3	Gaussian quadratic forms . . . . .	19
2.3.1	Definition . . . . .	19
2.3.2	Statistical characterization of non-central Gaussian quadratic forms . . . . .	21
2.4	Fading models overview . . . . .	28
2.4.1	Classical fading models . . . . .	28
2.4.2	Generalized fading models . . . . .	32
<b>3</b>	<b>Summary of Results</b>	<b>37</b>
3.1	Analysis of random variables through confluence . . . . .	37
3.1.1	Proposed approach . . . . .	38
3.1.2	Application to non-central real Gaussian quadratic forms . . . . .	41
3.1.3	Application to non-central complex Gaussian quadratic forms . . . . .	45
3.2	Generalizations of the $\kappa$ - $\mu$ shadowed distribution . . . . .	55
3.2.1	The fluctuating Beckmann fading model . . . . .	55
3.2.2	The $\kappa$ - $\mu$ shadowed fading model with intercluster correlation . . . . .	64
<b>4</b>	<b>Conclusions and future work</b>	<b>69</b>
4.1	Conclusions . . . . .	69
4.2	Future work . . . . .	70
<b>A</b>	<b>Publications</b>	<b>73</b>



A.1	New approximation to distribution of positive random variables applied to Gaussian quadratic forms . . . . .	73
A.2	A new approach to the statistical analysis of non-central complex Gaussian quadratic forms with applications . . . . .	75
A.3	An extension of the $\kappa$ - $\mu$ shadowed fading model: statistical characterization and applications . . . . .	77
A.4	The $\kappa$ - $\mu$ shadowed fading model with arbitrary intercluster correlation . .	79
<b>B</b>	<b>Resumen en Castellano</b>	<b>81</b>
B.1	Introducción y motivación . . . . .	81
B.2	Análisis de variables aleatorias por confluencia . . . . .	82
B.2.1	Método propuesto . . . . .	82
B.2.2	Aplicación a formas cuadráticas gaussianas (FCG) reales no centrales	84
B.2.3	Aplicación a FCG complejas no centrales . . . . .	86
B.3	Generalizaciones del modelo de desvanecimientos $\kappa$ - $\mu$ <i>shadowed</i> . . . . .	90
B.3.1	El modelo Beckmann fluctuante . . . . .	91
B.3.2	El modelo $\kappa$ - $\mu$ <i>shadowed</i> con correlación . . . . .	94
B.4	Conclusiones y líneas futuras . . . . .	96
	<b>Bibliography</b>	<b>99</b>

# List of Figures

2.1	PDF and CDF of gamma distribution for different values of $m$ and $\Omega = 1$ .	13
3.1	PDF of $Q_R$ for different values of $\alpha, \rho$ and $\bar{x}$ . The proposed approximation in (3.13) is compared with the power series expansion in and with Monte Carlo simulations. $N$ denotes the number of terms calculated in the power series. . . . .	43
3.2	CDF of $Q_R$ for $\alpha=0.7, \rho = 0.5$ and $\bar{x} = (2, 1, -1, 0.6, -0.9)$ . Our proposed method in (3.14) with $m = 100$ is compared with the $\chi^2$ expansion in (2.65) and with Monte Carlo simulations. $N$ denotes the number of terms calculated in the $\chi^2$ series expansion. . . . .	43
3.3	CDF of $Q_R$ at $x = 1$ for distinct quadratic form order, $n$ . Our proposed expression in (3.14) is compared with the Laplace approximation in (2.64) with $\beta_L = 10$ and with Monte Carlo simulations. . . . .	44
3.4	CDF of $Q_R$ for different values of $n, \alpha, \rho$ and $\bar{x}$ . The proposed method is compared with the power series in (2.62), the Laguerre expansion in (2.64) and the $\chi^2$ expansion in (2.65) and contrasted with Monte Carlo simulations. Parameters: $\beta_L = 9$ for $n = 15$ and $\beta_L = 12$ for $n = 30$ . . . . .	45
3.5	CDF of $Q_C$ for $n = 6, \lambda = (-3, -1.8, -1, 1, 2.1, 3)$ and $\mu = (8.5, 7.4, 4, 5, 6.8, 7.9)$ . Exact (simulated) CDF is compared with the proposed approximation in (3.25) and Raphaeli's approach in (2.70) with $N$ terms computed. . . . .	49
3.6	CDF of $Q_C$ for different parameters. Exact (simulated) CDF is compared with the proposed approximation in (3.25) with $m = 50$ and the saddle-point approach in (2.78). Data: $\lambda_1 = [0.2, 1, 1.4, 3, 5], \lambda_2 = [0.1, 0.6, 1], \mu_1 = [0.6, 7.4, 3, 2.6, 5.5]$ and $\mu_2 = [1, 0.8, 3.4]$ . . . . .	50
3.7	Complementary $P_{\text{out}}$ vs. $\bar{\gamma}/\gamma_{\text{th}}$ for $P = 2$ , different values of $\rho$ and different values of $K$ at each path. Solid lines correspond to theoretical calculation with $m = 40$ for $\mathbf{k} = (1, 0.5)$ and $m = 100$ for $\mathbf{k} = (6, 4)$ , while markers correspond to Monte Carlo simulations. . . . .	53
3.8	$P_{\text{out}}$ vs. $\bar{\gamma}/\gamma_{\text{th}}$ for $P = 4$ , different values of $\rho$ and different values of $K$ at each path. Solid lines correspond to theoretical calculation while markers correspond to Monte Carlo simulations. For theoretical calculation, $m = 40$ for $\mathbf{k} = (0.5, 0.25, 0.25, 0)$ and $m = 200$ for $\mathbf{k} = (8, 7, 6, 6)$ . . . . .	53

3.9	BER vs. $\bar{\gamma}$ for 16-QAM, $P = 4$ and different values of $\rho$ and $\mathbf{k}$ . Solid lines correspond to theoretical calculation with $m = 40$ for $\mathbf{k} = (0.5, 0.25, 0.25, 0)$ and $m = 150$ for $\mathbf{k} = (8, 7, 6, 6)$ , while markers correspond to Monte Carlo simulations. . . . .	54
3.10	FB signal envelope distribution for different values of $\eta$ and $m$ in weak LoS scenario ( $\kappa = 1$ ) with $\varrho = 0.1$ , $\mu = 1$ and $\Omega = \mathbb{E}[R^2] = 1$ . Solid lines correspond to the exact PDF, while markers correspond to Monte Carlo simulations. . . . .	61
3.11	FB signal envelope distribution for different values of $\varrho$ and $m$ in strong LoS scenario ( $\kappa = 10$ ) with $\eta = 0.1$ , $\mu = 2$ and $\Omega = \mathbb{E}[R^2] = 1$ . Solid lines correspond to the exact PDF, while markers correspond to Monte Carlo simulations. . . . .	62
3.12	FB signal envelope distribution for different values of $\varrho$ and $\eta$ in strong LoS scenario ( $\kappa = 10$ ) with $m = 1$ , $\mu = 1$ and $\Omega = \mathbb{E}[R^2] = 1$ . Solid lines correspond to the exact PDF, while markers correspond to Monte Carlo simulations. . . . .	63
3.13	Normalized LCR vs threshold value $u(\text{dB})$ for different values of $\kappa$ , $\eta$ and $\mu$ , with $m = 1$ , $\varrho \rightarrow \infty$ and $\Omega = \mathbb{E}[R^2] = 1$ . Solid lines correspond to theoretical calculations, while markers correspond to Monte Carlo simulations. . . . .	63
3.14	Normalized AFD vs threshold value $u(\text{dB})$ for different values of $\kappa$ , $\eta$ and $\mu$ , with $m = 1$ , $\varrho \rightarrow \infty$ and $\Omega = \mathbb{E}[R^2] = 1$ . Solid lines correspond to theoretical calculations, while markers correspond to Monte Carlo simulations. . . . .	64
3.15	Signal envelope distribution for different values of $\mu$ and $\rho$ with $\kappa = 1$ , $m = 1$ and $\mathbb{E}[R^2] = 1$ . Solid lines correspond to the exact PDF while markers correspond to Monte Carlo simulations. . . . .	67
3.16	Signal envelope distribution for different values of $\mu$ , $\rho$ and $m$ with $\kappa = 4$ and $\mathbb{E}[R^2] = 1$ . Solid lines correspond to the exact PDF while markers correspond to Monte Carlo simulations. . . . .	68
B.1	PDF de $Q_R$ para distintos valores de $\alpha$ , $\rho$ y $\bar{\mathbf{x}}$ . El método propuesto se compara con distintas técnicas alternativas y con simulaciones de Monte Carlo. $N$ denota el número de términos computados en cada una de las aproximaciones. . . . .	85
B.2	$P_{\text{out}}$ en función de $\bar{\gamma}/\gamma_{\text{th}}$ para $P = 4$ y distintos valores de $\rho$ y $K_i$ . Las líneas sólidas corresponden con los resultados teóricos mientras que los marcadores representan los resultados simulados. Para los cálculos teóricos se ha empleado un valor de $m = 40$ para $\mathbf{k} = (0.5, 0.25, 0.25, 0)$ y de $m = 200$ para $\mathbf{k} = (8, 7, 6, 6)$ . . . . .	89

B.3	BER para una constelación 16-QAM para $P = 4$ y distintos valores de $\rho$ y $K_i$ . Las líneas sólidas corresponden con los resultados teóricos mientras que los marcadores representan los resultados simulados. Para los cálculos teóricos se ha empleado un valor de $m = 40$ para $\mathbf{k} = (0.5, 0.25, 0.25, 0)$ y de $m = 150$ para $\mathbf{k} = (8, 7, 6, 6)$ . . . . .	90
B.4	Amplitud recibida según modelo BF para distintos valores de $\eta$ y $m$ con $\kappa = 1$ , $\varrho = 0.1$ , $\mu = 1$ y $\Omega = 1$ . Las líneas continuas corresponden con los valores teóricos, mientras que los marcadores corresponden a los resultados de la simulación. . . . .	94
B.5	LCR normalizado para distintos valores de $\kappa$ , $\eta$ y $\mu$ con $m = 1$ , $\varrho \rightarrow \infty$ y $\Omega = 1$ . Las líneas continuas corresponden con los valores teóricos, mientras que los marcadores corresponden a los resultados de la simulación. . .	95
B.6	Distribución de la amplitud recibida para distintos valores de $\mu$ , $\rho$ y $m$ para $\kappa = 4$ y $\mathbb{E}[R] = 1$ . Las líneas continuas corresponden a los cálculos teóricos mientras que los marcadores representan el valor de las simulaciones. . .	97



UNIVERSIDAD  
DE MÁLAGA

# List of Acronyms

<b>AFD</b>	<b>A</b> verage <b>F</b> ade <b>D</b> uration
<b>AWGN</b>	<b>A</b> dditive <b>W</b> hite <b>G</b> aussian <b>N</b> oise
<b>BER</b>	<b>B</b> it <b>E</b> rror <b>R</b> ate
<b>CDF</b>	<b>C</b> umulative <b>D</b> istribution <b>F</b> unction
<b>CF</b>	<b>C</b> haracteristic <b>F</b> unction
<b>CGF</b>	<b>C</b> umulant <b>G</b> enerating <b>F</b> unction
<b>FB</b>	<b>F</b> luctuating <b>B</b> eckmann
<b>GQF</b>	<b>G</b> aussian <b>Q</b> uadratic <b>F</b> orm
<b>i.i.d.</b>	<b>I</b> ndependent and <b>I</b> dentically <b>D</b> istributed
<b>LCR</b>	<b>L</b> evel <b>C</b> rossing <b>R</b> ate
<b>LoS</b>	<b>L</b> ine-of- <b>S</b> ight
<b>MGF</b>	<b>M</b> oment <b>G</b> enerating <b>F</b> unction
<b>MIMO</b>	<b>M</b> ultiple- <b>I</b> nter <b>M</b> ultiple- <b>O</b> utput
<b>ML</b>	<b>M</b> aximum <b>L</b> ikelihood
<b>MRC</b>	<b>M</b> aximal <b>R</b> atio <b>C</b> ombining
<b>MSE</b>	<b>M</b> ean <b>S</b> quared <b>E</b> rror
<b>NLoS</b>	<b>N</b> on <b>L</b> ine-of- <b>S</b> ight
<b>OSTBC</b>	<b>O</b> rthogonal <b>S</b> pace <b>T</b> ime <b>B</b> lock <b>C</b> oding
<b>PDF</b>	<b>P</b> robability <b>D</b> ensity <b>F</b> unction
<b>QAM</b>	<b>Q</b> uadrature <b>A</b> mplitude <b>M</b> odulation
<b>SNR</b>	<b>S</b> ignal-to- <b>N</b> oise <b>R</b> atio



UNIVERSIDAD  
DE MÁLAGA

## Chapter 1

# Introduction

Gaussian random variables — both real and complex — are massively used in communications and signal processing mostly as a consequence of the central limit theorem, which states that the sum of independent random variables is asymptotically Gaussian distributed [1]. However, this interest does not only lie in the widespread use of the Gaussian distribution as a limiting case, but also in the analysis of random variables arising from normal ones.

Among these variables, linear combinations of squares of Gaussian variables, known as Gaussian quadratic forms (GQFs), have a remarkable relevance. Their importance is due to their wide number of applications, not only in the communication and signal processing fields, but also in statistics. For instance, they naturally arise in problems related to the detection of signals in Gaussian noise [2][3, sec. 13.5], the spectral detection of normally distributed stationary processes,  $\chi^2$  tests [4, sec. 7], analysis of variance [5], performance analysis of adaptive filter algorithms [6], energy detection [7] or performance analysis of maximum likelihood (ML) estimators [8]. In general, any statistical test based on Euclidean distances or any application of the method of least squares when the involved variables are Gaussian will automatically bring a GQF [4, chap. 7].

In communications, GQFs play an important role when analyzing differential modulation schemes [9], non-coherent modulations [10], diversity techniques [11]–[14], orthogonal space time block coding (OSTBC) [15] or relay systems [16], since the signal-to-noise ratio (SNR) at the output of these systems is given in terms of a GQF when the channel gains are assumed to be Gaussian distributed.

Moreover, GQFs have also a considerable importance in channel modeling, although little attention has traditionally been paid to them in this context. Classically, in wireless channels, it has been assumed that the number of reflections arriving to the receiver is sufficiently large so that the central limit theorem can be applied, modeling the received complex baseband signal as Gaussian [17]–[19]. Depending on the choice of the parameters of this underlying Gaussian variable (mean and variance of its real and imaginary parts), different fading models arose in the related literature, e.g., Rayleigh, Rice and Hoyt. All these classical distributions, including some generalizations introduced tens of



years ago such as Nakagami- $m$  model (with integer  $m$ ) [20], can be seen as very particular cases of a GQF.

In the last years, with the increased interest on channel modeling due to the emergence of new scenarios and technologies, as the use of millimeter waves [21]–[24], large intelligent surfaces [25], [26] and underwater communications [27], several novel distributions have been proposed [28]–[31]. Many of them, which aim to improve the fitting to measured data in these emerging scenarios and to provide more flexibility than classical fading models, can also be regarded as particular cases of a more general GQF. Therefore, the analysis of GQFs would unify the vast majority of fading models nowadays available in the literature, sometimes with slight differences between them.

Unfortunately, despite their large number of applications, no closed-form expressions are known for the distribution of arbitrary GQFs, and only a few particular cases admit a closed formulation. Therefore, inherent to GQFs is the classical problem of approximating the distribution of random variables, for which several approaches have been given in the literature over the years. These proposed methods include, among others, the saddle-point technique [32]–[35], Edgeworth series [35]–[38], series expansions in terms of orthogonal polynomials [39] or approximations in terms of other random variables [40]–[45].

Although many of these classical techniques have been applied to the analysis of GQFs, all the derived results suffer from the same common drawback: the resulting expressions *do not* represent a proper distribution, i.e., the approximated probability density functions (PDFs) may not have unit area and probabilities greater than one (or even negative) can be obtained [39, p. 731][38, sec. 2]. In addition, the accuracy of these techniques typically depends on the parametrization of the target variable, leading in some cases to poor approximations or rendering convergence issues.

Motivated by the aforementioned importance of GQFs in communications and signal processing, and taking into account that deriving exact expressions for the distribution of such an intricate variables may pose a challenge from an analytic point of view, this thesis revisits the problem of analyzing non-central GQFs. Along this line, a new method to characterize these variables is proposed, aiming to circumvent the major drawbacks of classical approaches and seeking simple and tractable approximations for the PDF and cumulative density function (CDF) of both real and complex GQFs. The proposed approach is later leveraged to be applied to arbitrary positive random variables, showing the potential of the method and highlighting its main advantage: it ensures, for any level of accuracy, that the resulting expressions represent a *valid distribution*.

Finally, exploiting the connection between GQFs and the distinct fading models, part of this thesis is also devoted to the analysis of fading distributions, providing very general and versatile — albeit tractable — models that unify the majority of the existing distributions emerging from the application of the central limit theorem.

## 1.1 Objectives

This thesis has two clearly defined objectives: *i)* proposing a new method to approximate the distribution of both real and complex non-central GQFs, and *ii)* unifying most of the fading distributions available in the literature under the umbrella of very general models. Although these objectives seem apparently unconnected, it will be later shown that in fact they are considerably related, and both are achieved by applying the same underlying methodology. More specifically, the main objectives in the context of the analysis of GQFs are as follows:

- Derivation of novel general approximations for both the PDF and CDF of positive random variables which guarantee that the resulting expressions represent a valid distribution.
- Application of the proposed method to positive definite real GQFs in order to provide new simple expressions that outperform the alternative results given in the literature.
- Providing a new approximation to the distribution of complex GQFs that are tractable enough to be useful for analytical purposes and its application to the performance analysis of maximal ratio combining (MRC) systems with correlated branches over line-of-sight (LoS) channels.

Regarding the second aforementioned objective, this thesis aim to propose new fading models that generalizes the majority of fading distributions arising from the central limit theorem. To this end, the versatile and popular  $\kappa$ - $\mu$  shadowed distribution will be used as starting point due to its tractability and empirical validation, and more general (yet tractable) expansions will be sought.

## 1.2 Organization

This is a compilation thesis composed by several publications and some chapters that provide coherence to the whole document. Therefore, the organization varies with respect to the more classical structure of a monograph thesis. Specifically, it is organized in four main chapters and the appendix section as follows:

1. Chapter 1. The current chapter, which contains the introduction and motivation of the thesis, along with the objectives and organization of the rest of the document.
2. Chapter 2 provides the necessary background to understand the main contributions of the thesis. It includes some basic concepts of probability, an overview of the techniques classically employed to approximate the distribution of random variables, an introduction to GQFs and a review of their state of the art and finally a brief summary of both the classical and some of the generalized fading models available in the literature.

3. Chapter 3 summarizes the distinct publications gathered in this thesis, presenting their main contributions and discussing their results.
4. Chapter 4. The last chapter, containing the conclusions and some future research lines arisen from this thesis.

Finally, the publications included in the compilation are attached in Appendix A.

### 1.3 Publications

The following is a list of publications in refereed journals and conference proceedings included as part of the compilation of this thesis:

- [46] P. Ramírez-Espinosa, D. Morales-Jimenez, J. A. Cortés, J. F. París, and E. Martos-Naya, “New approximation to distribution of positive RVs applied to Gaussian quadratic forms”, *IEEE Signal Process. Lett.*, vol. 26, no. 6, pp. 923–927, Jun. 2019. DOI: 10.1109/LSP.2019.2912295.
- [47] P. Ramírez-Espinosa, L. Moreno-Pozas, J. F. París, J. A. Cortés, and E. Martos-Naya, “A new approach to the statistical analysis of non-central complex Gaussian quadratic forms with applications”, *IEEE Trans. Veh. Technol.*, vol. 68, no. 7, pp. 6734–6746, Jul. 2019. DOI: 10.1109/TVT.2019.2916725.
- [48] P. Ramírez-Espinosa, F. J. López-Martínez, J. F. París, M. D. Yacoub, and E. Martos-Naya, “An extension of the  $\kappa$ - $\mu$  shadowed fading model: Statistical characterization and applications”, *IEEE Trans. Veh. Technol.*, vol. 67, no. 5, pp. 3826–3837, May 2018. DOI: 10.1109/TVT.2017.2787204.
- [49] P. Ramírez-Espinosa, J. F. París, J. A. Cortés, and E. Martos-Naya, “The  $\kappa$ - $\mu$  shadowed fading model with arbitrary intercluster correlation”, in *2018 15th Int. Symp. Wireless Commun. Syst. (ISWCS)*, Aug. 2018, pp. 1–5. DOI: 10.1109/ISWCS.2018.8491099.

Publications [46] and [47] gather the results referring to the approximation to the distribution of random variables and the analysis of GQFs, while papers [48] and [49] present the new general fading models.

## Chapter 2

# Background

The purpose of this chapter is to introduce several preliminary results and definitions, providing the necessary background to understand the results that will be later presented.

It is organized as follows. Section 2.1 introduces the general notation, while in Section 2.2 some well-known results on random variables are introduced along with a couple of relevant statistical distributions that will be used throughout this thesis. In addition, some of the most classical approaches that are used to approximate the distribution of random variables are summarized. Section 2.3 deals with Gaussian quadratic forms, considering both the real and complex cases and providing an overview of the different approaches given in the literature to approximate their distribution. Finally, Section 2.4 revisits several models that have been traditionally used to characterize fading in wireless environments, along with new distributions recently proposed to that end.

## 2.1 General notation

### Notation for common sets

$j$	imaginary unit, $\sqrt{-1}$ .
$\text{Re}\{\cdot\}, \text{Im}\{\cdot\}$	Real and imaginary parts.
$\mathbb{C}, \mathbb{R}, \mathbb{N}$	Complex, reals and natural numbers.
$\mathbb{R}^+, \mathbb{N}^+$	Positive real and integers numbers excluding 0.

**Notation for used functions**

$\ln$	Natural logarithm.
$\max, \min$	Maximum and minimum.
$\lim$	Limit.
$\forall$	For all.
$\triangleq$	Defined as.
$ \cdot $	Absolute value.
$\ \cdot\ $	Modulus.
$I_\nu(\cdot)$	Modified Bessel function of first kind [50, eq. (9.6.18)].
$\Gamma(\cdot)$	Gamma function [50, eq. (6.1.1)].
$\gamma(\cdot, \cdot)$	Lower incomplete gamma function [50, eq. (6.5.2)].
${}_1F_1(\cdot; \cdot; \cdot)$	Kummer's hypergeometric function [51, eq. (9.210 1)].
$\mathcal{L}\{\cdot\}, \mathcal{L}^{-1}\{\cdot\}$	Laplace transform and inverse Laplace transform.

**Notation for probability and asymptotics**

$P\{\cdot\}$	Probability.
$\mathbb{E}[\cdot]$	Expectation operator.
$\sim$	Statistically distributed as.
$f_X(x)$	PDF of $X$ .
$F_X(x)$	CDF of $X$ .
$M_X(s)$	MGF of $X$ .

**Matrix-vector notation**

$\mathbf{x}, \mathbf{X}$	Vectors and matrices are denoted with bold lower and upper case, respectively.
$\mathbb{R}^{m \times n}, \mathbb{C}^{m \times n}$	Real and complex $m \times n$ matrices.
$(\mathbf{X})_{i,j}$	$(i, j)$ -th element of the matrix $\mathbf{X}$ .
$\mathbf{I}_n$	$n \times n$ identity matrix.
$\mathbf{0}_{n \times m}$	$n \times m$ matrix of all zeroes.
$(\cdot)^T, (\cdot)^\dagger$	Transpose, conjugate-transpose.

**2.2 Some results on random variables**

This section defines some types of convergence of random variables, focusing on the relationships between them. Moreover, the Gaussian, the  $\chi^2$  and the gamma distribution are revisited, not only providing their first order statistics but also presenting the connection between them as well as some properties that will be used later. Finally,

this section briefly summarizes some of the most widely used techniques to approximate the distribution of random variables, i.e., the saddle-point technique, Gram-Charlier and Edgeworth series and expansions in terms of orthogonal polynomials and other density functions.

### 2.2.1 Convergence between sequences of random variables

Many of the most relevant results in probability, e.g., the central limit theorem [1, sec. 27] or Lévy's continuity theorem (also known as Lévy's convergence theorem) [52, chap. 18], are related to the asymptotic behavior of distributions of random variables. The work presented in this thesis is also partially based on the limit behavior of sequences of random variables and the concept of convergence. Thus, different types of convergence are defined next, as well as the relationships between them.

#### Weak convergence

Let  $\{X_n : n \in \mathbb{N}^+\}$  be a sequence of real random variables. Then,  $\{X_n\}^1$  converges weakly, or converges in distribution, to the random variable  $X \in \mathbb{R}$  if

$$\lim_{n \rightarrow \infty} F_{X_n}(x) = F_X(x) \quad (2.1)$$

at every continuity point  $x$ , with  $F_{X_n}(x)$  and  $F_X(x)$  denoting the CDF of  $X_n$  and  $X$ , respectively [1, sec. 25]. This is expressed as  $\{X_n\} \Rightarrow X$ .

Note that weak convergence ensures that the sequence  $\{F_{X_n}(x)\}$  has a limit  $F_X(x)$ , but it does not guarantee the convergence of the respective PDFs. The conditions under which weak convergence also implies that of PDFs are given in [53]. Specifically, let  $f_{X_n}(x)$  and  $f_X(x)$  denote the PDFs of  $X_n$  and  $X$ , respectively. Therefore, if  $\{X_n\} \Rightarrow X$  and

- i  $f_{X_n}(x)$  and  $f_X(x)$  are continuous functions,
- ii  $f_{X_n}(x)$  is bounded, i.e.,  $\sup_n f_{X_n}(x) \leq a < \infty$  for all  $x$  with  $a$  any number,
- iii  $\{f_{X_n}(x)\}$  is equicontinuous, i.e., for each point  $x$  and  $y$ , there exists  $g(x, \epsilon)$  and  $h(x, \epsilon)$  with  $\epsilon > 0$  such that  $|x - y| < g(x, \epsilon)$  implies that  $|f_{X_n}(x) - f_{X_n}(y)| < \epsilon$  for all  $n \geq h(x, \epsilon)$ ,

then  $\lim_{n \rightarrow \infty} f_{X_n}(x) = f_X(x)$ . In turn, convergence of PDFs always implies that of CDFs by virtue of Scheffe's theorem [54].

<sup>1</sup>For simplicity, the notation for sequences of random variables is simplified when no confusion may arise.

Moreover, consider  $\{X_n\} \Rightarrow X$  and let  $g : \mathbb{R} \rightarrow \mathbb{R}$  be any continuous and bounded function. Therefore, from Helly-Bray theorem [55, sec. 1.3], we have that

$$\lim_{n \rightarrow \infty} \mathbb{E}[g(X_n)] = \mathbb{E}[g(X)]. \quad (2.2)$$

### Convergence in probability

Consider again a sequence of real random variables defined as  $\{X_n : n \in \mathbb{N}^+\}$ . Then,  $\{X_n\}$  converges in probability to another random variable  $X \in \mathbb{R}$  if

$$\lim_{n \rightarrow \infty} P\{|X_n - X| > \epsilon\} = 0 \quad (2.3)$$

for  $\epsilon > 0$  [56, sec. 6.2]. It is denoted by  $\{X_n\} \xrightarrow{p} X$ .

It can be proved that condition in (2.3) is more restrictive than that in (2.1). In fact, if  $\{X_n\} \xrightarrow{p} X$  then  $\{X_n\} \Rightarrow X$ , although the converse does not hold in general [1, thm. 25.2]. Convergence in distribution implies convergence in probability when the limit random variable is a constant, i.e.,  $X = c$ . Under this condition,  $\{X_n\} \Rightarrow c$  also implies  $\{X_n\} \xrightarrow{p} c$  [1, thm. 25.3].

### $L_p$ convergence

The last type of convergence here presented is the  $L_p$  convergence. It is said that a sequence of real random variables  $\{X_n : n \in \mathbb{N}^+\}$  converges in  $L_p$  to a limit random variable  $X \in \mathbb{R}$  if

$$\lim_{n \rightarrow \infty} \mathbb{E}[|X_n - X|^p] = 0 \quad (2.4)$$

for  $p \in \mathbb{N}^+$  [56, sec. 6.5], and it is expressed as  $\{X_n\} \xrightarrow{L_p} X$ .

The most common types of  $L_p$  convergence are for  $p = 1, 2$ . If  $\{X_n\} \xrightarrow{L_p} X$  for  $p = 1$ , then it is said that  $\{X_n\}$  converges in mean to  $X$ , and if it does for  $p = 2$  then  $\{X_n\}$  converges in mean square to  $X$ . Moreover,  $L_p$  convergence for a certain value of  $p$  ensures that (2.4) holds for any  $p'$  such that  $p > p' \geq 1$ .

An important remark is that  $L_p$  convergence for  $p \geq 1$  implies convergence in probability and, consequently, convergence in distribution. This can be straightforwardly proved by applying Markov's inequality [52, sec. 6.4] to (2.3):

$$\lim_{n \rightarrow \infty} P\{|X_n - X| > \epsilon\} \leq \lim_{n \rightarrow \infty} \frac{\mathbb{E}[|X_n - X|^p]}{\epsilon^p} \stackrel{(a)}{=} 0, \quad (2.5)$$

where  $L_p$  convergence is assumed in (a).

### 2.2.2 The Gaussian distribution

Gaussian random variables (both real and complex) appear in a multitude of applications in communications and signal processing, mainly as a limit distribution due to the central limit theorem. Hence, the Gaussian distribution is used, e.g., to characterize random noise [57] and channel gains in wireless communications [17], [18], to mention but a couple of relevant examples. Its importance in this thesis is also relevant, since most of the random variables here considered are based on the Gaussian distribution.

#### The real case

A real random variable  $X$  follows a Gaussian distribution with mean  $\mu$  and variance  $\sigma^2$ , i.e.,  $X \sim \mathcal{N}(\mu, \sigma^2)$ , if its PDF is expressed as [19, eq. (2.3-8)]

$$f_X(x) = \frac{1}{\sqrt{2\pi\sigma^2}} e^{-(x-\mu)^2/(2\sigma^2)}. \quad (2.6)$$

Its CDF is calculated by integrating (2.6) as

$$F_X(x) = \int_{-\infty}^x \frac{1}{\sqrt{2\pi\sigma^2}} e^{-(x-\mu)^2/(2\sigma^2)} dx = 1 - Q\left(\frac{x-\mu}{\sigma}\right) \quad (2.7)$$

where  $Q(\cdot)$  is the Gaussian  $Q$ -function [18, eq. (4.1)].

#### The complex case

Consider now two independent real Gaussian random variables  $X_1$  and  $X_2$  such that  $X_1 \sim \mathcal{N}(\mu_1, \sigma_1^2)$  and  $X_2 \sim \mathcal{N}(\mu_2, \sigma_2^2)$ . Then, the random variable  $X = X_1 + jX_2$  follows a complex Gaussian distribution with mean  $\mu = \mu_1 + j\mu_2$ , variance  $\sigma^2 = \sigma_1^2 + \sigma_2^2$  and pseudovariance  $c^2 = \sigma_1^2 - \sigma_2^2$ , i.e.,  $X \sim \mathcal{CN}(\mu, \sigma^2, c^2)$ . The PDF of  $X$  is readily obtained due to the independence between  $X_1$  and  $X_2$  as

$$f_X(x) = \frac{1}{\pi\sqrt{\sigma^4 - c^4}} \exp\left(-\frac{\sigma^2\|x-\mu\|^2}{\sigma^4 - c^4} + \operatorname{Re}\left\{\frac{c^2(x-\mu)^2}{\sigma^4 - c^4}\right\}\right). \quad (2.8)$$

If  $\sigma_1^2 = \sigma_2^2 = \sigma^2/2$ , then (2.8) simplifies to [58, eq. (2)]

$$f_X(x) = \frac{1}{\pi\sigma^2} e^{\|x-\mu\|^2/\sigma^2} \quad (2.9)$$

and the shorthand notation  $X \sim \mathcal{CN}(\mu, \sigma^2)$  is used.

Of special interest in many cases is the analysis of circularly symmetric Gaussian variables. A complex random variable  $X$  is said to be circularly symmetric if  $f_X(x) = f_Y(y)$  with  $Y = e^{j\phi}X$  for all  $\phi \in \mathbb{R}$ , requiring thus that  $\mu = c^2 = 0$  [59]. However, in



some applications (e.g., channel modeling), non-circularly symmetric Gaussian variables are also relevant.

### 2.2.3 The $\chi^2$ distribution

The  $\chi^2$  distribution plays an important role in many statistics applications, specially in hypothesis and goodness-of-fit testing [60, chap. 30]. Closely related to the Gaussian distribution, the  $\chi^2$  distribution describes the statistical behavior of the sum of  $n$  independent squared Gaussian random variables. Thus, consider

$$X = \sum_{i=1}^n Z_i^2 \quad (2.10)$$

where  $Z_i$  are independent and real Gaussian random variables. Then  $X$  follows a  $\chi^2$  distribution with  $n$  degrees of freedom [19, sec. 2.3]. Depending on whether  $Z_i$  have zero mean or not, we differentiate between the central and the non-central case.

#### The central $\chi^2$ distribution

If  $Z_i$  in (2.10) have zero mean and equal variance  $\sigma^2$  for all  $i$ , i.e.,  $Z_i \sim \mathcal{N}(0, \sigma^2) \forall i$ , then  $X$  follows a central  $\chi^2$  distribution with PDF [19, eq. (2.3-21)]

$$f_X(x) = \frac{1}{2^{n/2} \Gamma(n/2) \sigma^n} x^{n/2-1} e^{-x/(2\sigma^2)} \quad (2.11)$$

where  $\Gamma(\cdot)$  is the gamma function [50, eq. (6.1.1)], and it is denoted by  $X \sim \chi_n^2(\sigma^2)$ . Its CDF can be directly obtained by integrating (2.11) as

$$F_X(x) = \frac{2^{-n/2}}{\sigma^n \Gamma(\frac{n}{2})} \int_0^x y^{n/2-1} e^{-y/(2\sigma^2)} dy = \frac{1}{\Gamma(\frac{n}{2})} \int_0^{\frac{x}{2\sigma^2}} u^{n/2-1} e^{-u} du = \frac{1}{\Gamma(\frac{n}{2})} \gamma\left(\frac{n}{2}, \frac{x}{2\sigma^2}\right) \quad (2.12)$$

where  $\gamma(\cdot, \cdot)$  is the lower incomplete gamma function [50, eq. (6.5.2)].

Finally, the moment generating function (MGF) of  $X$  is calculated using [51, eq. (3.381 4)] as

$$M_X(s) = \int_0^\infty f_X(x) e^{sx} dx = (1 - 2\sigma^2 s)^{-n/2}, \quad (2.13)$$

which is valid for all  $s \in \mathbb{C}$  such that  $\text{Re}\{s\} < 1/(2\sigma^2)$ .

### The non-central $\chi^2$ distribution

In case  $Z_i$  in (2.10) have non-zero mean but equal variances, i.e.,  $Z_i \sim \mathcal{N}(\mu_i, \sigma^2) \forall i$ , then the PDF of  $X$  is given by [19, eq. (2.3-29)]

$$f_X(x) = \frac{1}{2\sigma^2} \left(\frac{x}{\delta^2}\right)^{(n-2)/4} \exp\left(-\frac{x + \delta^2}{2\sigma^2}\right) I_{n/2-1}(\delta/\sigma^2 \sqrt{x}) \quad (2.14)$$

where  $I_\nu(\cdot)$  is the modified Bessel function of the first kind [50, eq. (9.6.18)] and  $\delta^2 = \sum_{i=1}^n \mu_i^2$  is the non-centrality parameter. We denote that by  $X \sim \chi_n^2(\sigma^2, \delta^2)$ .

The MGF of  $X$  in this case can be obtained from (2.14) by using [51, eqs. (6.643 2), (9.220 2) and (9.215 1)] as

$$M_X(s) = \int_0^\infty f_X(x) e^{sx} dx = \frac{\exp\left(\frac{\delta^2 s}{1-2\sigma^2 s}\right)}{(1-2\sigma^2 s)^{n/2}}, \quad \text{Re}\{s\} < 1/(2\sigma^2). \quad (2.15)$$

### 2.2.4 The gamma distribution

Due to its mathematical tractability and its connection to the exponential and Gaussian distribution, the gamma distribution is extensively used in a wide variety of applications in physics, statistics and communications, e.g., waiting times in queues [61], electromigration for submicron interconnects [62] and wireless channel modeling [18], to mention but some relevant examples. The gamma distribution is also of special interest to the main results derived in this thesis.

#### Definition and first order statistics

A random variable  $X$  follows a gamma distribution with shape parameter  $m \in \mathbb{R}^+$  and scale parameter  $\theta \in \mathbb{R}^+$ , i.e.,  $X \sim \Gamma(m, \theta)$ , if its PDF is expressed as [63, eq. (17.23)]

$$f_X(x) = \frac{1}{\Gamma(m)\theta^m} x^{m-1} e^{-x/\theta}. \quad (2.16)$$

Comparing (2.11) and (2.16), it can be observed that the gamma distribution generalizes the central  $\chi^2$  distribution by letting the  $m$  parameter (equivalent to the degrees of freedom in the  $\chi^2$  distribution) take any positive real value instead of only natural numbers.

As with the  $\chi^2$  distribution, the CDF of  $X$  is directly obtained by integrating (2.16) as

$$F_X(x) = \frac{1}{\Gamma(m)\theta^m} \int_0^x t^{m-1} e^{-t/\theta} dt = \frac{1}{\Gamma(m)} \int_0^{x/\theta} y^{m-1} e^{-y} dy = \frac{1}{\Gamma(m)} \gamma(m, x/\theta). \quad (2.17)$$

Moreover, the MGF of gamma distribution is readily calculated from (2.16) as

$$M_X(s) = \int_0^\infty f_X(x) e^{sx} dx, \quad (2.18)$$

where the application of [51, eq. (3.381 4)] leads to

$$M_X(s) = (1 - \theta s)^{-m}, \quad \text{Re}\{s\} < 1/\theta, \quad (2.19)$$

obtaining an expression very similar to (2.13). Finally, from (2.19), the  $n$ -th moment of the distribution are derived as

$$\mathbb{E}[X^n] = \left. \frac{d^n}{ds^n} M_X(s) \right|_{s=0} = \frac{\Gamma(m+n)}{\Gamma(m)} \theta^n. \quad (2.20)$$

The gamma distribution is alternatively formulated in terms of the shape parameter  $m$  and the rate parameter  $\beta = 1/\theta$ , or in terms of  $m$  and  $\Omega = \mathbb{E}[X] = m\theta$ . Expressions for the MGF, PDF and CDF of the gamma distribution with the distinct formulations are straightforwardly obtained from (2.16), (2.17) and (2.19) just by applying the equivalences between the different parameters.

### Gamma distribution with integer parameters

An interesting particular case of the gamma distribution is that in which the shape parameter  $m$  is a positive integer, i.e.,  $m \in \mathbb{N}^+$ . If so, then the gamma random variable  $X$  can be generated from independent and identically distributed (i.i.d.) real Gaussian random variables as

$$X = \sum_{i=1}^{2m} Z_i^2, \quad (2.21)$$

where  $Z_i \in \mathbb{R}$  follow a Gaussian distribution with zero mean and variance  $\theta/2$ , i.e.,  $Z \sim \mathcal{N}(0, \theta/2)$ . As stated before, this case corresponds to the central  $\chi^2$  distribution with  $n = 2m$  degrees of freedom and  $\sigma^2 = \theta/2$ .

Remarkably, the CDF of gamma distribution (and that of the central  $\chi^2$  distribution when  $n$  is even) can be simplified under the assumption of  $m \in \mathbb{N}^+$  by applying [51, eq. (3.351 1)] to the integral in (2.17), obtaining

$$F_X(x) = 1 - e^{-x/\theta} \sum_{k=0}^{m-1} \frac{x^k}{k! \theta^k} \quad (2.22)$$

and considerably improving the mathematical tractability of the distribution.

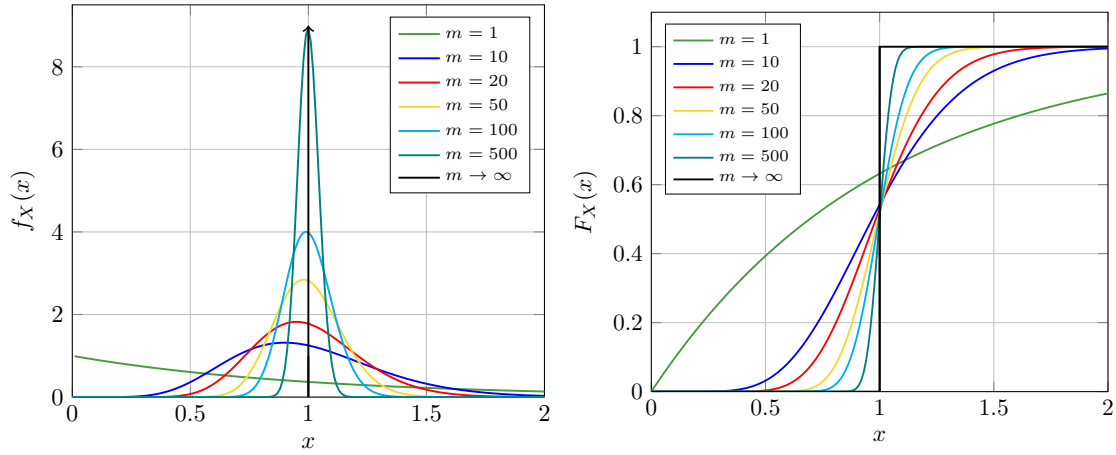


FIGURE 2.1: PDF and CDF of gamma distribution for different values of  $m$  and  $\Omega = 1$

### Degeneration of the gamma distribution

Of special interest to this thesis is the property of the gamma distribution of becoming a degenerate distribution. It is said that a distribution is degenerate if its corresponding random variable  $X \in \mathbb{R}$  has only one possible value  $x_0$  with probability  $P(X = x_0) = 1$  [64, sec. 3.1]<sup>2</sup>. Consequently, the PDF of  $X$  is a delta function at  $x_0$ .

That can be achieved in the case of the gamma distribution by letting  $m \rightarrow \infty$ . To prove that, consider first the sequence  $\{X_m : m \in \mathbb{N}^+\}$  where  $X_m$  is gamma distributed with shape parameter  $m$  and  $\mathbb{E}[X_m] = \Omega$  and whose characteristic function (CF) is given by

$$\phi_{X_m}(jt) = \mathbb{E}[e^{jtX_m}] = M_{X_m}(jt) = \left(1 - \frac{j\Omega t}{m}\right)^{-m} \quad (2.23)$$

where  $j$  denotes the imaginary number  $j = \sqrt{-1}$ . Taking the limit in (2.23) leads to

$$\lim_{m \rightarrow \infty} \phi_{X_m}(jt) = e^{j\Omega t}, \quad (2.24)$$

which correspond to the CF of the constant variable  $C = \Omega$ . Therefore, by virtue of Levy's convergence theorem [52, chap. 18], we have that  $\{X_m\} \Rightarrow C$ . That is, increasing the value of  $m$  leads to a reduction in the variance of the gamma distribution and, in the limit, it becomes a constant variable whose PDF is a delta function at  $x = \Omega$  (equivalently, its CDF tends to the step function). This behavior is shown in Fig. 2.1, where both the PDF and CDF of a gamma distribution is depicted for distinct  $m$ .

### 2.2.5 Classical approximations to the distribution of random variables

As introduced in Chapter 1, approximating the distribution of a random variable is a classical problem in applied statistics, mainly because of the difficulty of deriving exact

<sup>2</sup>Note that this definition only applies for 1-dimensional distributions.

and tractable expressions for the PDF and CDF of many random variables, e.g., GQFs [4]. Therefore, several efforts have been devoted to providing general methods that allow to approximate the distribution of such intricate variables. Most of these techniques are based on the knowledge of either the moments or the CF (or, equivalently, the MGF) of the target variable. This subsection aims to present a brief overview of the most classical methods to obtain approximations to distributions, highlighting their main flaws.

### The saddle-point technique

The saddle-point technique (or method of steepest descent) is a generalization of Laplace's method to approximate integrals of the form

$$I = \int_{\mathcal{C}} f(t) e^{\alpha g(t)} dt \quad (2.25)$$

where  $\mathcal{C}$  is a contour on the complex plane and  $\alpha$  is a large number. It is extensively used in statistics to approximate the distribution of random variables from its MGF or its characteristic function by means of the inversion theorem [1, sec. 26]. Therefore, since the MGF can be seen as the Laplace transform of the PDF, the latter is calculated by performing the inverse transform as

$$f_X(x) = \frac{1}{j2\pi} \int_{\tau-j\infty}^{\tau+j\infty} e^{-sx} M_X(s) ds \quad (2.26)$$

with  $\tau \in \mathbb{R}$ . The above integral is rewritten as

$$f_X(x) = \frac{1}{j2\pi} \int_{\tau-j\infty}^{\tau+j\infty} \exp(K_X(s) - sx) ds \quad (2.27)$$

where  $K_X(s) = \ln M_X(s)$  is the cumulant generating function (CGF). Expanding  $K_X(s) - sx$  in Taylor series around a point  $s = t_0(x)$  such that  $K'_X(t_0(x)) = x$ , we have

$$f_X(x) \approx \frac{1}{j2\pi} \exp(K_X(t_0(x)) - t_0(x)x) \int_{\tau-j\infty}^{\tau+j\infty} \exp\left(\frac{1}{2}(s - t_0(x))^2 K''_X(t_0(x))\right) ds. \quad (2.28)$$

The point  $s = t_0(x)$  is a saddle-point of  $K_X(s) - sx$ , where the function is constant in the imaginary direction and has an extreme in the real one [32]. Hence, choosing  $\tau = t_0(x)$ , the integral in (2.28) is dominated by the value of the integrand at this point, and the approximation is tight. Solving the integral we obtain the saddle-point approximation for  $f_X(x)$  as [32, eq. (21)]

$$f_X(x) \approx \exp(K_X(t_0(x)) - t_0(x)x) \sqrt{\frac{1}{2\pi K''_X(t_0(x))}}. \quad (2.29)$$

Similarly, the saddle-point technique can also be used to derive approximations for the CDF of  $X$  (see [32]–[35] for a more detailed explanation of this technique).

Despite it is widely used in statistics, the above approximation has two main drawbacks. First, there is no guarantee that (2.29) represents a valid distribution (generally it does not), i.e., the approximated PDF may not have unit area and probabilities greater than one might be obtained. Second, increasing the accuracy of the approximation is not trivial since it implies considering higher terms in the Taylor series, considerably complicating the calculation of the integral in (2.28).

### Gram-Charlier and Edgeworth series

Gram-Charlier and Edgeworth series are used to approximate the PDF and CDF of a random variable, whose moments or cumulants are known, from another baseline distribution. We here present the formulation given in [35, chap. 3][36, chap. 5], although alternative formulations can be found in other works (see e.g. [37], [38]).

Consider two random variables  $X$  and  $Y$  with PDFs  $f_X(x)$  and  $f_Y(y)$  and MGFs  $M_X(s)$  and  $M_Y(t)$ , respectively. The MGF of  $X$  can be expressed in terms of a power series as [35, p. 32]

$$M_X(s) = M_Y(s) \sum_{i=0}^{\infty} \mu_i \frac{s^i}{i!}, \quad (2.30)$$

where  $\mu_i$  are the moments of the distribution whose cumulants are given by the difference of those of  $X$  and  $Y$ . Hence, defining  $\kappa_j^x$  and  $\kappa_j^y$  as the cumulants of  $X$  and  $Y$  respectively,  $\mu_i$  are calculated as [65]

$$\mu_i = \sum_{j=0}^{i-1} \binom{i-1}{j} \mu_j (\kappa_{i-j}^x - \kappa_{i-j}^y) \quad (2.31)$$

for  $i > 1$  with  $\mu_0 = 1$  and  $\mu_1 = \kappa_1^x - \kappa_1^y$ . Formally,  $\mu_i$  are not true moments of a distribution, since  $\kappa_j^x - \kappa_j^y$  do not necessarily represent the cumulants of any random variable [36, p. 153].

To obtain the approximation to  $f_X(x)$  is necessary to invert (2.30) term by term, taking into account that from the definition of the MGF the first term is  $f_Y(x)$ . For the other terms, it can be proved that, if  $f_Y(x)$  is uniformly continuous, then [36, eq. (38)]

$$\int_{-\infty}^{\infty} e^{sx} f_Y^{(n)}(x) dx = s^n (-1)^n M_Y(s) \quad (2.32)$$

and, therefore, the PDF of  $X$  is expanded as

$$f_X(x) = \sum_{i=0}^{\infty} f_Y^{(i)}(x) \frac{(-1)^i \mu_i}{i!} = f_Y(x) \sum_{i=0}^{\infty} g_i(x) \frac{\mu_i}{i!}, \quad (2.33)$$

where  $g_i(x) = (-1)^i f_Y^{(i)}(x)/f_Y(x)$ . The complexity of the series expansions is thus determined by the computation of the derivatives of the baseline PDF,  $f_Y(x)$ . If  $Y$  is chosen to follow a standard Gaussian distribution, i.e.,  $Y \sim \mathcal{N}(0, 1)$ , then the expansion in (2.33) is known as Gram-Charlier series and  $g_i(x)$  is given by

$$g_i(x) = 2^{-i/2} H_i(x/\sqrt{2}), \quad (2.34)$$

with  $H_i(\cdot)$  the  $i$ -th order Hermite polynomial [51, eq. (8.950 1)]. Similarly, the CDF of  $X$  can be expanded in the same way just by dividing by  $s$  both terms in (2.30).

Although useful in some cases (e.g., the sum of independent and identically distributed random variables), Edgeworths series have important flaws. First, as with the saddle-point method, the approximated functions are not guaranteed to be proper PDFs (in fact negative probabilities may be obtained), and the accuracy is typically low in the tails of the distribution (the method ensures an absolute error but not a relative one) [35, chap. 3]. Therefore, if we are interested in estimating low probabilities (as in performance analysis in communications and signal detection), this type of approximations may lead to large errors. Moreover, under certain conditions, increasing the number of terms that are computed does not necessary increase the accuracy of the approximation [38, p. 14].

### Orthogonal polynomials series

Another classical way of approximating the distribution of a random variable  $X \in \mathbb{R}$  is expressing its PDF as a series of the form

$$f_X(x) = g(x) \sum_{i=0}^{\infty} \omega_i h_i(x) \quad (2.35)$$

where  $g(x)$  is a known function,  $\omega_i$  are constants and  $h_i(x)$  is a sequence of orthogonal polynomials. Gram-Charlier series in (2.33) belongs to these type of expansions, for which  $g(x)$  is the standard Gaussian PDF and  $h_i(x)$  are the Hermite polynomials.

Expansions of the form (2.35) in terms of Lagrange and Laguerre polynomials are derived in [66, chap. 7][39] under some conditions. As with Edgeworth series, the moments of  $X$  (or its cumulants, since they are related as proved in [65]) are needed to build these approximations.

Specifically, consider a random variable  $X$  whose PDF has finite domain  $[-1, 1]$  and whose  $n$ -th moment is given by  $\mu_n^x$ . Therefore,  $f_X(x)$  admits the following expansion [39, eq. (1)]

$$f_X(x) = \sum_{i=0}^{\infty} \lambda_i P_i(x), \quad (2.36)$$

with  $P_i(x)$  the  $i$ -th order Legendre polynomial [51, eq. (8.911 1)] and

$$\lambda_i = \frac{2i+1}{2^{i+1}} \sum_{j=0}^{\lceil i/2 \rceil} (-1)^j \frac{(2i-2j)!}{j!(i-j)!(i-2j)!} \mu_{i-2j}^x, \quad (2.37)$$

where  $\lceil \cdot \rceil$  is the ceiling function, i.e., for any real number  $\alpha$  it gives the least integer greater than or equal to  $\alpha$ .

The approximant in (2.36) can be generalized to any random variable  $Y$  defined in a closed interval  $[a, b]$  with moments  $\mu_j^y$  by performing the change of variables

$$\hat{X} = \frac{2Y - (a+b)}{b-a} \quad (2.38)$$

such that  $\hat{X} \in [-1, 1]$ . Using now (2.36) and reverting the change of variables the PDF of  $Y$  is expressed as

$$f_Y(y) = \frac{2}{b-a} \sum_{i=0}^{\infty} \hat{\lambda}_i P_i \left( \frac{2y - (a+b)}{b-a} \right), \quad (2.39)$$

where  $\hat{\lambda}_i$  are calculated as in (2.37) but replacing  $\mu_j^x$  by the moments of  $\hat{X}$ , which are obtained from those of  $Y$  as

$$\mu_j^{\hat{X}} = \frac{1}{(b-a)^j} \sum_{k=0}^j \binom{j}{k} 2^k \mu_k^y (-1)^{j-k} (a+b)^{j-k}. \quad (2.40)$$

Moreover, for positive random variables  $X \in \mathbb{R}^+$  with moments  $\mu_n^x$  and whose PDF has domain  $[0, \infty)$ , a similar expansion can be obtained for  $f_X(x)$  based on Laguerre polynomials, which is given by [39, eq. (27)]

$$f_X(x) = \frac{(x-a)^v e^{-y/c}}{c^{v+1}} \sum_{i=0}^{\infty} \delta_i L_i^\alpha(y/c) \quad (2.41)$$

with  $c = (\mu_2^x - (\mu_1^x)^2)/\mu_1^x$ ,  $v = \mu_1^x/c - 1$ ,  $L_i^\alpha(\cdot)$  the  $i$ -th order Laguerre polynomial [51, eq. (8.970 1)] and

$$\delta_i = \sum_{k=0}^i (-1)^k \frac{i! \mu_{i-k}^x}{c^{i-k} k! (i-k)! \Gamma(v+i-k+1)}. \quad (2.42)$$

Expansions (2.39) and (2.41) are in general more tractable than other approximations arising, e.g., from the application of saddle-point technique, being therefore useful for further analytical purposes. However, once again, these series need to be truncated in order to be computed, rendering expressions which do not represent a proper distribution. In addition, the accuracy of the approximation strongly depends on the random variable under analysis. Thus, expansions of the type (2.41) are only recommended when the tail behavior of the target distribution is similar to that of the gamma distribution [66, p. 301].



### Series expansions as mixtures of other densities

As already stated, the main drawback of the aforementioned techniques is that the resulting expressions do not represent proper distributions [40]. Aiming to overcome this issue, several efforts have been devoted in the related literature to seeking alternative approximants that fulfill the condition of being valid PDFs themselves. In this context, approximations based on mixture of density functions have been proposed [40]–[45], specially to fit the distribution of empirical data, providing approximants to a target PDF  $f_X(x)$  of the form [41, eq. (1.4)]

$$f_X(x) \approx \sum_{i=1}^n w_i g(x; \theta_i) \quad (2.43)$$

where  $g(x; \theta_i)$  is the PDF of the baseline distribution depending on a set of parameters  $\theta_i$  and  $w_i$  are constants such that  $\sum_{i=1}^n w_i = 1$ . The issue is now the choice of the baseline density function and the calculation of the mixture parameters, namely  $n$ ,  $w_i$  and  $\theta_i$ . Unfortunately, due to the generality of the problem, it is remarkably difficult to provide a general method to approximate an arbitrary distribution by (2.43).

Due to its mathematical properties and its practical importance, one of the most common choices for  $g(\cdot)$  is the Gaussian distribution. In fact, it can be proved that any random variable can be obtained as the limit of a linear combination of Gaussian variables [43], [44]. However, other distributions such as gamma [42] or exponential [41, chap. 3] have also been proposed to approximate positive variables.

Similarly, several techniques have been classically used to estimate the mixture parameters. The method of moments is perhaps the most widely-extended preference, imposing that the first  $p$  moments of the mixture must be equal to those of the target distribution. Hence, a system of equations given by

$$\mu_j = \sum_{i=1}^n w_i \hat{\mu}_j(\theta_i), \quad j = 1, \dots, p \quad (2.44)$$

arise, where  $\mu_j$  and  $\hat{\mu}_j$  denote the exact and mixture moments, respectively. This system can be solved to determine  $w_i$  and  $\theta_i$  for a given  $n$ , although for relatively large  $n$  it may be extremely tedious.

When the mixture model is used to approximate the distribution of empirical data, the distinct parameters can be estimated by solving the optimization problem that minimizes the  $L^p$  distance between the empirical and the mixture PDFs, defined as

$$L^p = \mathbb{E} \left[ \left| \hat{f}_X(\mathbf{x}) - \sum_{i=1}^n w_i g(\mathbf{x}; \theta_i) \right|^p \right] \quad (2.45)$$

where  $\mathbf{x}$  is the observed data. Another alternative is using the ML estimation [41, chap. 1]. Bayesian estimation has also been proposed to seek the mixture parameters when

characterizing stochastic non-linear systems [45] and linear systems with non-Gaussian noise [40].

On the whole, although approximants based on mixtures of density functions are a good alternative to the other techniques, the lack of a general methodology and the difficulty in estimating the mixture parameters ultimately limit their usefulness.

## 2.3 Gaussian quadratic forms

Due to their vast number of applications, and because one of the main purposes of this thesis is the analysis of GQFs, this section summarizes some of their most relevant properties, as well as the distinct methods that have been proposed to their statistical characterization.

### 2.3.1 Definition

#### The real case

Let  $\bar{\mathbf{x}} \in \mathbb{R}^{n \times 1}$  be a constant vector,  $\mathbf{A} \in \mathbb{R}^{n \times n}$  be a symmetric matrix and  $\mathbf{x} \in \mathbb{R}^{n \times 1}$  be a random vector following a multivariate normal distribution with zero mean and covariance matrix  $\Sigma \in \mathbb{R}^{n \times n}$ , i.e.,  $\mathbf{x} \sim \mathcal{N}_n(\mathbf{0}_{n \times 1}, \Sigma)$ . Then, the real random variable

$$Q_R = (\mathbf{x} + \bar{\mathbf{x}})^T \mathbf{A} (\mathbf{x} + \bar{\mathbf{x}}) \quad (2.46)$$

is a real GQF [4, eq. (3.1.1)]. If all the entries of  $\bar{\mathbf{x}}$  are zero, i.e.,  $\bar{\mathbf{x}} = \mathbf{0}_{n \times 1}$ , then  $Q_R$  is a central quadratic form. In turn, if  $\bar{\mathbf{x}} \neq \mathbf{0}_{n \times 1}$ , it is non-central. Moreover,  $Q_R$  is said to be definite or indefinite depending on whether  $\mathbf{A}$  is definite or not, respectively.

The quadratic form  $Q_R$  admits an alternative formulation in terms of independent standard Gaussian variables, which can be derived by applying simple algebraic transformations to (2.46). Thus, consider any decomposition of the form  $\Sigma = \mathbf{C}\mathbf{C}^T$ , e.g.,  $\mathbf{C} = \Sigma^{1/2}$ , and the vector  $\mathbf{s} = \mathbf{C}\mathbf{z}$  where  $\mathbf{z} \sim \mathcal{N}_n(\mathbf{0}_{n \times 1}, \mathbf{I}_n)$ . It can be easily proved that  $\mathbf{s}$  is Gaussian distributed with

$$\mathbb{E}[\mathbf{s}] = \mathbf{C}\mathbb{E}[\mathbf{z}] = \mathbf{0}_{n \times 1} = \mathbb{E}[\mathbf{x}], \quad (2.47)$$

$$\mathbb{E}[\mathbf{s}\mathbf{s}^T] = \mathbf{C}\mathbb{E}[\mathbf{z}\mathbf{z}^T]\mathbf{C}^T = \Sigma = \mathbb{E}[\mathbf{x}\mathbf{x}^T] \quad (2.48)$$

and, therefore,  $Q_R$  can be expressed as

$$Q_R = (\mathbf{z} + \mathbf{C}^{-1}\bar{\mathbf{x}})^T \mathbf{C}^T \mathbf{A} \mathbf{C} (\mathbf{z} + \mathbf{C}^{-1}\bar{\mathbf{x}}). \quad (2.49)$$

Since  $\mathbf{C}^T \mathbf{A} \mathbf{C}$  is symmetric, it can be diagonalized as  $\mathbf{C}^T \mathbf{A} \mathbf{C} = \mathbf{U}\mathbf{\Lambda}\mathbf{U}^T$ , where  $\mathbf{U}$  is an orthogonal matrix and  $\mathbf{\Lambda}$  is a diagonal matrix whose entries,  $\lambda_i$  for  $i = 1, \dots, n$  are

the eigenvalues of  $\mathbf{C}^T \mathbf{A} \mathbf{C}$  (or, equivalently, those of  $\mathbf{\Sigma} \mathbf{A}$ ) [67, chap. 2]. Hence, relabeling  $\mathbf{y} = \mathbf{U}^T \mathbf{z}$  and  $\mathbf{b} = \mathbf{U}^T \mathbf{C}^{-1} \bar{\mathbf{x}}$ , we finally have

$$Q_R = (\mathbf{y} + \mathbf{b})^T \mathbf{\Lambda} (\mathbf{y} + \mathbf{b}) = \sum_{i=1}^n \lambda_i (y_i + b_i)^2 \quad (2.50)$$

where  $y_i$  and  $b_i$  are the entries of  $\mathbf{y}$  and  $\mathbf{b}$  respectively. Note that, since  $\mathbf{U}$  is orthogonal, the distribution of  $\mathbf{y}$  is the same as that of  $\mathbf{z}$ , i.e.,  $\mathbf{y} \sim \mathcal{N}_n(\mathbf{0}_{n \times 1}, \mathbf{I}_n)$ . Therefore,  $Q_R$  is expressed as a linear combination of independent squared Gaussian random variables with means  $b_i$ , or equivalently, as a linear combination of independent noncentral  $\chi^2$  distributions of the form

$$Q_R = \sum_{i=1}^n \lambda_i Y_i, \quad Y_i \sim \chi_1^2(1, b_i^2). \quad (2.51)$$

Also, regarding (2.50), it can be observed that if  $\lambda_i = 0$  for some  $i$ , then  $Q_R$  is equivalent to another quadratic form of less order. That corresponds to the case in which either or both  $\mathbf{A}$  and  $\mathbf{\Sigma}$  are rank deficient, and consequently the rank of  $\mathbf{C}^T \mathbf{A} \mathbf{C}$  is  $r < n$  and  $\lambda_i = 0$  for  $i = r + 1, \dots, n$ . For simplicity, and without any loss of generality, hereinafter we will assume that both  $\mathbf{A}$  and  $\mathbf{\Sigma}$  are full-rank. Moreover, if  $\mathbf{A}$  is positive or negative definite then  $\lambda_i > 0$  and  $\lambda_i < 0$  for all  $i$ , respectively, and equivalently  $\lambda_i$  can take both positive and negative values if  $\mathbf{A}$  is indefinite.

### The complex case

Analogously to the real case, GQFs in complex variables are defined as

$$Q_C = (\mathbf{v} + \bar{\mathbf{v}})^\dagger \mathbf{A} (\mathbf{v} + \bar{\mathbf{v}}) \quad (2.52)$$

where, in this case,  $\bar{\mathbf{v}} \in \mathbb{C}^{n \times 1}$  is a constant vector representing the mean of  $\mathbf{v}$ ,  $\mathbf{A} \in \mathbb{C}^{n \times n}$  is an Hermitian matrix and  $\mathbf{v} \in \mathbb{C}^{n \times 1}$  is complex multivariate Gaussian vector with zero mean and covariance matrix  $\mathbf{\Sigma} \in \mathbb{C}^{n \times n}$ , i.e.  $\mathbf{v} \sim \mathcal{CN}_n(\mathbf{0}_{n \times 1}, \mathbf{\Sigma})$ .

By following similar steps as in the real case,  $Q_C$  can also be written in terms of independent Gaussian variables. To that end, consider again any decomposition of  $\mathbf{\Sigma}$  such that  $\mathbf{\Sigma} = \mathbf{C} \mathbf{C}^\dagger$ , e.g., the Cholesky factorization [68, p. 441], and diagonalize  $\mathbf{C}^\dagger \mathbf{A} \mathbf{C}$  as  $\mathbf{C}^\dagger \mathbf{A} \mathbf{C} = \mathbf{U} \mathbf{\Lambda} \mathbf{U}^\dagger$ , where  $\mathbf{U}$  is an unitary matrix and  $\mathbf{\Lambda}$  is a diagonal matrix whose entries are the eigenvalues of  $\mathbf{C}^\dagger \mathbf{A} \mathbf{C}$ . Note that since  $\mathbf{C}^\dagger \mathbf{A} \mathbf{C}$  is Hermitian, all its eigenvalues are real [67, p. 42]. By doing so and naming  $\bar{\mathbf{h}} = \mathbf{U}^\dagger \mathbf{C}^{-1} \bar{\mathbf{v}}$ , we obtain

$$Q_C = (\mathbf{s} + \bar{\mathbf{h}})^\dagger \mathbf{\Lambda} (\mathbf{s} + \bar{\mathbf{h}}) \quad (2.53)$$

where  $\mathbf{s}$  is a complex multivariate standard Gaussian vector, i.e.,  $\mathbf{s} \sim \mathcal{CN}_n(\mathbf{0}_{n \times 1}, \mathbf{I}_n)$ . Furthermore, denoting by  $s_i = x_i + jy_i$  and  $h_i = p_i + jq_i$  the entries of  $\mathbf{s}$  and  $\bar{\mathbf{h}}$  respectively,

with  $x_i, y_i \sim \mathcal{N}(0, 1/2) \forall i$ ,  $Q_C$  can be finally expressed as

$$Q_C = \sum_{i=1}^n \lambda_i \|s_i + h_i\|^2 = \sum_{i=1}^n \lambda_i [(x_i + p_i)^2 + (y_i + q_i)^2]. \quad (2.54)$$

Comparing (2.54) and (2.50), it is clear that a complex quadratic form is equivalent to a real one of double order  $n$  for which the eigenvalues  $\lambda_i$  are equal in pairs. As with  $Q_R$ ,  $Q_C$  can also be expressed as a linear combination of independent non-central  $\chi^2$  distributions as

$$Q_C = \sum_{i=1}^n \lambda_i Y_i, \quad Y_i \sim \chi^2_2(1/2, \|h_i\|^2). \quad (2.55)$$

Moreover, if  $p_i = q_i = 0 \forall i$ , then (2.54) corresponds to the gamma distribution with integer parameters in (2.21) by mapping  $n = m$  and  $\lambda_i = \theta \forall i$ . Lastly, note that as in the real case, if  $\mathbf{C}^\dagger \mathbf{A} \mathbf{C}$  is rank deficient then some  $\lambda_i$  are zero, and  $Q_C$  is equivalent to another quadratic form of order  $r < n$ .

### 2.3.2 Statistical characterization of non-central Gaussian quadratic forms

Although the MGF of both real and complex GQFs can be straightforwardly obtain from that of the  $\chi^2$  distribution, closed-form expressions for their PDF and CDF remain unknown for the general case. In the real case, exact closed-form expressions can only be obtained under certain conditions (e.g.,  $\mathbf{A} = \mathbf{\Sigma} = \mathbf{I}$ , the identity matrix), remaining in complicated integral form for the general case, even when the involved random variables have zero mean. Quadratic forms in complex Gaussian variables are slightly more tractable, allowing a simple formulation for the main statistics in the central case. However, only approximated solutions have been given in the non-central one.

Due to the vast number of applications of both real and complex GQFs and the challenge that poses their statistical characterization, considerable efforts have been devoted in the last decades to their study [4], [5], [11], [69]–[79]. This section aims to provide a brief overview of the distinct approximations given in the literature to the distribution of these type of variables, focusing on the non-central case due to its generality. The real and complex cases are reviewed separately, although as stated before, any complex GQF can be considered as a real one with the eigenvalues given in pairs, so the analysis for real variables actually includes both cases.

#### The real case

Since any real GQF can be expressed as a linear combination of independent non-central  $\chi^2$  distributions as in (2.51), the MGF of  $Q_R$  is readily calculated as the product of

the individual MGFs of the  $\chi^2$  random variables. Thus, from (2.15) we obtain

$$M_{Q_R}(s) = \prod_{i=1}^n \exp\left(\frac{b_i^2 \lambda_i s}{1 - 2\lambda_i s}\right) (1 - 2\lambda_i s)^{-1/2}, \quad \lambda_i \operatorname{Re}\{s\} < 1/2 \forall i. \quad (2.56)$$

Note that in the central case, i.e.,  $b_i = 0 \forall i$ , then the exponential term vanishes.

As for the PDF and the CDF, their analysis can be traced back to the work by Robbins and Pitman [69], where the distribution of positive definite central quadratic forms was expressed as a mixture of central  $\chi^2$  densities. A similar expansion was proposed and extended to the ratio of central GQFs in [5] in the context of the analysis of variances. Ruben [80] generalized the analysis by presenting another approximation in terms of non-central  $\chi^2$  variables which is also valid in the non-central case, although the restriction of positive definiteness still holds.

Other types of series expansions were proposed, e.g., by Gurland [74], who proposed an approximant of the form (2.36) in terms of Laguerre polynomials in the positive definite central case and in terms of more complicated polynomials in the non-central case. In [72], Shah extended the work by Gurland, considering by first time the most general case, i.e., indefinite non-central GQFs, giving expressions for the PDF and CDF in terms of intricate orthogonal polynomials. Unfortunately, the challenging computation of such polynomials and the complexity of the derived expressions considerably limit the usefulness of the proposed results. Imhof also considered the indefinite non-central case [73], proposing the inversion of the CF by numerical integration.

All the above series expansions were unified (although restricted to the positive definite case) by Kotz et al. for both the central [70] and non-central case [71], and revisited several years later in [4], providing a general method to seek approximations for positive definite real GQFs in terms of powers, orthogonal polynomials and  $\chi^2$  densities. This general method aims to find a series expansion for the PDF of the form [71, eq. (106)]

$$f_{Q_R}(x) = \sum_{k=0}^{\infty} c_k h_k(x) \quad (2.57)$$

where  $c_k$  are constants and  $\{h_k(x) : k \in \mathbb{N}\}$  is a sequence of known functions. Therefore, if

$$\sum_{k=0}^{\infty} c_k h_k(x) \leq \sum_{k=0}^{\infty} |c_k| |h_k(x)| \leq \beta e^{\alpha x} \quad (2.58)$$

for all  $x \in \mathbb{R}^+$  with  $\alpha$  and  $\beta$  real constants, then the Laplace transform of  $f_{Q_R}(x)$  is calculated as [4, lem. 4.2a.1]

$$\mathcal{L}\{f_{Q_R}(x)\} \triangleq \hat{f}(s) \triangleq \sum_{k=0}^{\infty} c_k \hat{h}_k(s), \quad \operatorname{Re}\{s\} > \alpha \quad (2.59)$$

where  $\hat{h}_k(s)$  denotes the Laplace transform of  $h_k(x)$ .

The method is then based on choosing  $h_k(s)$  such that (2.58) holds and

$$\hat{h}_k(s) = g(s)\eta^k(s) \quad (2.60)$$

with  $g(s)$  an analytic, non-vanishing function and  $\eta(s)$  is analytic for  $\text{Re}\{s\} > \alpha$  and has inverse function  $\phi(s)$ , i.e.  $\eta(\phi(s_0)) = s_0$ .

Once the baseline sequence of functions  $\{h_k(x)\}$  is chosen, the coefficients  $c_k$  are obtained from equating (2.59) with (2.56). Moreover, the CDF can be obtained by integrating term by term (2.57). At this point, different series arise depending on this choice:

- **Power series.** In this case  $h_k(s)$  is given by

$$h_k(x) = (-1)^k \frac{x^{n/2+k-1}}{\Gamma(n/2+k)} \quad (2.61)$$

and, therefore,  $g(s) = s^{-n/2}$  and  $\eta(s) = (-s)^{-1}$ . With this choice, the CDF of real non-central Gaussian quadratic forms is expressed as [4, eq. (4.2b.13)]

$$F_{Q_R}(x) = \sum_{i=0}^{\infty} c_k (-1)^k \frac{x^{n/2+k-1}}{\Gamma(n/2+k)} \quad (2.62)$$

where  $c_k$  are calculated as in [4, eqs. (4.2b.5), (4.2b.8) and (4.2b.10)]. The major limitation of (2.62) is the calculation of  $c_k$ , since numerical issues could be significantly relevant. The problem is that, although  $c_k$  usually take small values for all  $k$ , they are calculated as the difference of large numbers, which is a challenging task due to the limited floating-point precision in calculation software [71, p. 840].

- **Laguerre series.** This particular case arises when choosing

$$h_k(x) = \frac{k!}{2\beta_L \Gamma(n/2+k)} \left(\frac{x}{2\beta_L}\right)^{n/2-1} e^{-x/2} L_k^{n/2-1} \left(\frac{x}{2\beta_L}\right) \quad (2.63)$$

with  $L_k^\alpha(\cdot)$  the  $k$ -th order Laguerre polynomial [51, eq. (8.970 1)] and  $\beta$  a real constant such that  $\beta_L > \lambda_{\max}/2$ , where  $\lambda_{\max} = \max_i\{\lambda_i\}$ . With that, and using [70, eq. (47)], we can straightforwardly identify  $g(s) = (1 + 2s\beta_L)^{-n/2}$  and  $\eta(s) = 2s\beta_L/(1 + 2s\beta_L)$ , obtaining an expansion for the CDF of  $Q_R$  of the form [71, eq. (132)]

$$F_Q(x) = F(n, \beta_L, x) + \sum_{k=1}^{\infty} c_k \frac{\Gamma(k)}{\Gamma(k + \frac{n}{2})} \left(\frac{x}{2\beta_L}\right)^{n/2} e^{-x/(2\beta_L)} L_{k-1}^{n/2} \left(\frac{x}{2\beta_L}\right) \quad (2.64)$$

where  $F(n, \beta_L, x)$  is given in [4, p. 109] and coefficients  $c_k$  are calculated according to [4, eqs. (4.2b.5) and (4.2c.14)].

An important drawback of this approximation is the choice of  $\beta_L$ , which controls the convergence of the series. In [70], [71], a value of  $\beta_L = (\lambda_{\max} + \lambda_{\min})/2$  is recommended. However, this value may render numerical errors depending on

the parameters of the quadratic form, preventing the series convergence. Hence, it is not clear how to find the value of  $\beta_L$  that yields the best approximation in each case.

- **Expansion in  $\chi^2$  densities.** The baseline function  $h_k(x)$  is now the PDF of the central  $\chi^2$  distribution (2.11) with order  $n + 2k$  and variance  $\beta_\chi$ , where  $\beta_\chi$  is a real parameter controlling the series convergence. Thus, from (2.13), it is readily observed that  $g(s) = (1 + 2s\beta_\chi)^{-n/2}$  and  $\eta(s) = (1 + 2s\beta_\chi)^{-1}$ . This choice leads to a series expansion given by

$$F_{Q_R}(x) = \sum_{k=0}^{\infty} c_k \frac{1}{\Gamma(n/2 + k)} \gamma\left(\frac{n}{2} + k, \frac{x}{2\beta_\chi}\right), \quad (2.65)$$

which is valid for  $0 < \beta_\chi < \lambda_{\min}$  with  $c_k$  given by [4, eqs. (4.2b.8) and (4.2b.9)]. The choice of  $\beta_\chi$  in this case seems less problematic than in the Laguerre series, observing that higher values in the given interval accelerate the series convergence in all cases.

The above method also allows another types of approximants based on non-central  $\chi^2$  densities or hypergeometric functions, but the mathematical tractability of the resulting expressions is considerably reduced.

An alternative approximation for the distribution of real GQFs was recently given in [11, eq. (46)], where the saddle-point technique is applied to approximate the integral that defines the CDF. However, the results are restricted to the central case. Moreover, it inherits the drawbacks of this type of approximations, i.e., difficulty in increasing the accuracy of the approximation and probability values that may be greater than one.

### The complex case

Although they can be seen as a particular case of the real case, complex GQFs have interest by themselves due to their massive number of applications, specially in communications and signal detection, where most of the involved random variables are complex (e.g. the Gaussian noise) [6]–[16]. Therefore, considerable efforts have been also devoted to their study.

The MGF of  $Q_C$  can be derived from (2.55) and (2.15) in the same way as in the real case, obtaining [76, eq. (4b)]

$$M_{Q_C}(s) = \prod_{i=1}^n \exp\left(\frac{\mu_i \lambda_i s}{1 - \lambda_i s}\right) (1 - \lambda_i s)^{-1}, \quad \lambda_i \operatorname{Re}\{s\} < 1 \quad \forall i \quad (2.66)$$

where  $\mu_i = \|h_i\|^2$ .

Note that, since a complex quadratic form is equivalent to a real one with the eigenvalues given in pairs, as stated in Section 2.3.1, the exponent of the terms  $(1 - \lambda_i s)$  is



always an integer number, in contrast to that in (2.56). Consequently,  $M_{Q_C}(s)$  is given by a rational function in the central case, where the exponential term vanishes, allowing to obtain exact closed-form expressions for both the PDF and the CDF by directly inverting  $M_{Q_C}(s)$ . However, in the non-central case, no closed-form expressions are known in the general case and thus it is necessary to rely on approximations to both statistics.

Most of these approximations arise, similarly as those in the real case, by the inversion of the MGF or, equivalently, the CF [77]–[79], rendering different approximated expressions for the PDF and CDF of complex GQFs.

The work by Biyari and Lindsey considers a particular case of non-central quadratic form which is of special interest in communications [77]. Specifically, it analyzes the quadratic form resulting from the sum of  $L$  independent and identically distributed quadratic forms of order  $n = 2$  and inverts its MGF by solving some convolution integrals. As a result, the PDF and CDF of this specific quadratic form are given in terms of an infinite sum of Laguerre polynomials.

A more general approximation is given by Raphaeli, where the indefinite non-central case is considered [78]. He uses the residue theorem to invert the MGF of  $Q_C$ , expressing the residues as infinite series in order to circumvent the essential singularities of  $M_{Q_C}(s)$ . Therefore, the CDF of  $Q_C$  is calculated as [78, eq. (26)]

$$F_{Q_C}(x) = 1 + \frac{1}{2\pi j} \int_{\mathcal{C}} \frac{1}{s} e^{-sx} M_{Q_C}(s) ds \quad (2.67)$$

where  $\mathcal{C}$  is a contour circling the right half plane but excluding the imaginary axis if  $x > 0$  and circling the left half plane when  $x < 0$ . Thus, applying the residue theorem we have

$$F_{Q_C}(x) = \begin{cases} 1 + \sum_{\lambda_k > 0} \text{Res} \left\{ \hat{F}_k(0) \right\} & \text{if } x > 0 \\ - \sum_{\lambda_k < 0} \text{Res} \left\{ \hat{F}_k(0) \right\} & \text{if } x < 0 \end{cases}, \quad (2.68)$$

with [78, eq. (27)]

$$\hat{F}_k(s) = \frac{1}{s + \lambda_k^{-1}} \exp(-x(s + \lambda_k^{-1})) M_{Q_C}(s + \lambda_k^{-1}). \quad (2.69)$$

Note that, for each  $\hat{F}_k(s)$ , the pole at  $s = \lambda_k^{-1}$  is translated to  $s = 0$  for convenience. Also, this procedure assumes that all the eigenvalues  $\lambda_k$  are distinct with multiplicities  $m_k$ .

The next step is expressing  $\hat{F}_k(s)$  as the product of two functions  $\hat{g}_k(s, x)$  and  $f_k(s)$  as in [78, eq. (30)], and then expanding  $f_k(s)$  in Laurent series and  $\hat{g}_k(s, x)$  in Taylor series. By doing that, the residues of  $\hat{F}_k(s)$  can therefore be computed recursively, and the CDF



of  $Q_C$  is finally expressed as [78, eq. (32)]

$$F_{Q_C}(x) = 1 + \exp \left( \sum_{j=1}^N \mu_j \right) \sum_{\lambda_k > 0} \frac{1}{(-\lambda_k/2)^{m_k-1}} e^{-x/\lambda_k} \sum_{i=m_k-1}^{\infty} \hat{g}_k^{(i)}(0, x/2) \frac{(2\mu_k/\lambda_k)^{i-m_k+1}}{i!(i-m_k+1)!} \quad (2.70)$$

for  $x > 0$  with  $N$  denoting the number of distinct eigenvalues  $\lambda_k$ . If  $x < 0$ , then the sum is over all  $\lambda_k < 0$  as stated in (2.68). The derivatives of  $\hat{g}_k(s, x)$  are calculated according to [78, eqs. (18-21) and (31)] but taking into account that, due to slight differences in the definitions of  $\lambda_k$  and  $\mu_k$ , we should replace  $\underline{\lambda}_k = \lambda_k/2$  and  $\underline{\mu}_k^2 = 2\mu_k$ , where the parameters in [78] have been underlined in order to avoid confusion. Note that these equivalences have been already applied in (2.70).

A very similar expansion for the PDF is given in [78, eq. (25)], but due to the recursion that involves the independent variable  $x$  the expression is not useful for further analytic purposes, e.g., the calculation of expectations over the quadratic form. Being aware of this issue, Raphaeli proposed an alternative approximation for the PDF [78, eq. (38)] in terms of an infinite sum of modified Bessel functions. In this case, although the recursion does not involve  $x$ , the Bessel functions considerably limit the tractability of the series.

Another approximation was given by Tziritis in [79], where he considered the positive definite case and proposed series expansions for the PDF and CDF in terms of other distributions. Specifically, the gamma and the non-central  $\chi^2$  distributions are considered in the central and non-central case, respectively. Remarkably, the results are valid for both real and complex quadratic forms (with slight modifications).

Hence, focusing on the non-central case, the proposed baseline density is

$$f(x) = \frac{x^{a/2}}{bc^a} \exp \left( -\frac{x+c^2}{b} \right) I_a(2c\sqrt{x}/b), \quad (2.71)$$

which corresponds to the PDF of  $X = bY/2$  with  $Y \sim \chi_{2(a+1)}^2(1, 2c^2/b)$ . The parameters  $a$ ,  $b$  and  $c$  are chosen so that the first three moments of  $X$  are equal to those of  $Q_C$ . With that, the resulting series expansion for the CDF is given by [79, eq. (40)]

$$F_{Q_C}(x) = \sum_{i=0}^{\infty} c_i \binom{a+i}{i} \sum_{k=0}^i \binom{i}{k} \left( \frac{-b}{\beta} \right)^k \left[ 1 - Q_{a+1} \left( \sqrt{\frac{2}{b}}c, \sqrt{\frac{2x}{b}} \right) \right], \quad (2.72)$$

where  $Q_M(\alpha, \delta)$  is the generalized Marcum  $Q$  function [18, eq. (4.59)],  $\beta$  is a real constant that controls the series convergence and must satisfies [79, eq. (23)]

$$\beta^{-1} > 2(b^{-1} - \lambda_{\max}^{-1}) \quad \text{in the complex case,} \quad (2.73)$$

$$\beta^{-1} > 2(b^{-1} - (2\lambda_{\max})^{-1}) \quad \text{in the real case,} \quad (2.74)$$

and  $c_i$  are constants that are obtained recursively according to [79, eqs. (26-28)]. The main drawback of this approximation is its complexity, i.e., the intricate recursion of constants

$c_i$  that involves infinite sums and the required calculation of several Marcum  $Q$  functions undoubtedly limit the usefulness of (2.72). Moreover, when truncated, the series does not represent a valid CDF.

Taking into account the limitations of the direct inversion methods above introduced, since the solutions provided for the PDF and the CDF are difficult to compute and not suitable for any further insightful analysis, very recently, Al-Naffouri et al. presented a different approach [11]. They applied a transformation to the inequality that defines the CDF of  $Q_C$ , and approximated the resulting integral by the saddle-point technique.

Hence, the starting point is the integral definition of the CDF, expressed as [11, eq. (9)]

$$F_{Q_C}(x) = \int_{\mathcal{A}} f_{\mathbf{s}}(\mathbf{s}) d\mathbf{s} = \int_{-\infty}^{\infty} f_{\mathbf{s}}(\mathbf{s}) u\left(x - (\mathbf{s} + \bar{\mathbf{h}})^{\dagger} \mathbf{\Lambda} (\mathbf{s} + \bar{\mathbf{h}})\right) d\mathbf{s} \quad (2.75)$$

where  $\mathcal{A}$  is the area in the  $n$ -dimensional complex plane defined by the inequality  $Q_C < x$ ,  $u(\cdot)$  is the unit step function whose value is 1 if the argument is non-negative and 0 otherwise, and  $\mathbf{s}$ ,  $\bar{\mathbf{h}}$  and  $\mathbf{\Lambda}$  are the parameters of the quadratic form defined in (2.53).

Manipulating (2.75) and using [11, eq. (14)] we have

$$F_{Q_C}(x) = \frac{1}{2\pi} \int_{-\infty}^{\infty} \frac{1}{\det(\mathbf{I}_n + (j\omega + \beta)\mathbf{\Lambda})} \frac{e^{x(j\omega + \beta)}}{j\omega + \beta} e^{-c(\omega)} d\omega \quad (2.76)$$

where  $\beta$  is a positive real constant and

$$c(\omega) = \bar{\mathbf{h}}^{\dagger} \left( \mathbf{I}_n + \frac{1}{j\omega + \beta} \mathbf{\Lambda}^{-1} \right)^{-1} \bar{\mathbf{h}}. \quad (2.77)$$

Since the above integral cannot be put in closed-form, the authors in [11] applied the saddle-point technique described in Section 2.2.5, obtaining

$$F_{Q_C}(x) \approx \frac{1}{2\pi} \exp(s(\omega_0)) \sqrt{\frac{2\pi}{\|s''(\omega_0)\|}} \quad (2.78)$$

where

$$s(\omega) = x(j\omega + \beta) - c(\omega) - \ln(j\omega + \beta) - \sum_{i=1}^n \ln(1 + \lambda_i(j\omega + \beta)) \quad (2.79)$$

and  $\omega_0$  is a complex point such that  $s'(\omega_0) = 0$ .

Despite the compactness of the expression in (2.78), that approximation has the same drawbacks as the previous ones, i.e., it does not represent a valid CDF. Moreover, it is difficult to increase the accuracy of the approximation and it is not clear how to obtain the PDF of  $Q_C$  by using this approach.

Finally, for reader's convenience, a summary of the aforementioned methods to approximate the CDF of non-central complex GQFs is given in Table 2.1.

TABLE 2.1: Summary of the distinct approximations to the CDF,  $F_{Q_C}(x)$ , of non-central complex QFs.

Reference	Type of approximation	Main drawbacks
[77]	Infinite sum of Laguerre polynomials	Only valid for a particular complex QF Not a proper CDF when the series is truncated
[78]	Infinite series of elementary functions	Recursion involving the independent variable $x$ Not a proper CDF when the series is truncated
[79]	Double infinite series of Marcum functions	Coefficients involve intricate recursions Not a proper CDF when the series is truncated Computation of several Marcum functions is required
[11]	Saddle-point approximation	Not a proper CDF Increasing the accuracy is difficult

## 2.4 Fading models overview

In wireless environments, the radio signal is affected by a number of random phenomena (reflection, diffraction and scattering among others) as it travels from transmitter to receiver. Consequently, the received signal appears as a linear combination of multipath waves, each of which with their own (random) amplitudes and phases. This constructive and destructive addition of the distinct multipath waves renders strong and rapidly-varying fluctuations in the received signal amplitude, known as *fast fading*. Due to the multipath propagation, the complex based-band signal can therefore be written as [81, eq. (1)]

$$\tilde{V} = \sum_{i=1}^N V_i e^{j\phi_i}, \quad (2.80)$$

where  $N$  denotes the number of multipath waves,  $V_i$  their amplitudes and  $\phi_i$  their phases.

Aiming to analyze and improve the performance of wireless communication systems, considerable efforts have been devoted to the characterization of fading. Consequently, a wide variety of models have been developed in the related literature in order to describe the statistical behavior of the received signal amplitude  $R = \|\tilde{V}\|$ , including both the classical fading models along with more general models. In the following, a brief overview of most widely used fading distributions is given. Note that we consider only flat-fading models, i.e., those employed to characterize fading which affects narrowband wireless systems.

### 2.4.1 Classical fading models

When  $N$  is sufficiently large, the baseband voltage  $\tilde{V}$  in (2.80) can be regarded as a complex Gaussian random variable because of the central limit theorem [1, sec. 27]. Depending on the choice of the parameters characterizing this complex Gaussian variable,

namely the mean and variance of the in-phase and quadrature components, different classical fading models emerge. A more detailed review of these classical models can be found in standard reference books, e.g., [17, chap. 2] and [18, chap. 2].

### Rayleigh

Rayleigh model assumes that all the multipath components in (2.80) have similar amplitudes and independent phases which are uniformly distributed. Therefore, under the central limit theorem assumption, the received signal envelope  $R$  is model as the magnitude of a zero mean circularly-symmetric complex Gaussian random variable, i.e.,

$$R = \|\sigma X + j\sigma Y\| \quad (2.81)$$

where  $X$  and  $Y$  are independent standard Gaussian random variables, i.e.,  $X, Y \sim \mathcal{N}(0, 1)$  and  $\sigma$  is a positive real constant. The PDF of  $R$  is then given by

$$f_R(r) = \frac{2r}{\Omega} \exp\left(-\frac{r^2}{\Omega}\right), \quad (2.82)$$

with  $\Omega = \mathbb{E}[R^2] = 2\sigma^2$ .

Due to its mathematical simplicity, Rayleigh distribution is massively used to model fading arising from non line of sight (NLoS) scenarios, where all the multipath components are assumed to have the same average power.

### Rice

In contrast to Rayleigh model, Rice model (also known as Nakagami- $n$  or Rician) considers that the complex Gaussian random variable arising from the application of the central limit theorem has non-zero mean, i.e.,

$$R = \|\sigma X + j\sigma Y + p + jq\| \quad (2.83)$$

with  $X, Y \sim \mathcal{N}(0, 1)$  and  $p, q$  and  $\sigma$  real constants.

The PDF of  $R$  is therefore given by [82, eq. (3.12)]

$$f_R(r) = \frac{2r(1+K)e^{-K}}{\Omega} \exp\left(-\frac{r^2(1+K)}{\Omega}\right) I_0\left(2r\sqrt{\frac{K(1+K)}{\Omega}}\right) \quad (2.84)$$

where  $\Omega = \mathbb{E}[R^2] = p^2 + q^2 + 2\sigma^2$  and  $K = (p^2 + q^2)/(2\sigma^2)$  is the Rice factor, which corresponds to the ratio of the power of the dominant component to the average power of the scattering. Since for  $K = 0$  the Rayleigh distribution is obtained, Rice model can be seen as the natural extension of the Rayleigh model to LoS scenarios.

## Hoyt

Neither Rayleigh nor Rice models take into account the effect of the power imbalance between the in-phase and the quadrature components of the received signal, i.e., both of them assumes that the real and imaginary part of the complex Gaussian random variable have equal variances. This effect is considered by the Hoyt (Nakagami- $q$ ) distribution, according to which the received amplitude is modeled as

$$R = \|\sigma_x X + j\sigma_y Y\| \quad (2.85)$$

where  $X, Y \sim \mathcal{N}(0, 1)$  and  $\sigma_x, \sigma_y \in \mathbb{R}^+$ .

The PDF of Hoyt distribution is given by [83, eq. (3.4)]

$$f_R(r) = \frac{(1 + \eta)r}{\sqrt{\eta}\Omega} \exp\left(-\frac{(1 + \eta)^2 r^2}{4\eta\Omega}\right) I_0\left(\frac{(1 - \eta^2)r^2}{4\eta\Omega}\right) \quad (2.86)$$

with  $\Omega = \mathbb{E}[R^2]$  and  $\eta = \sigma_x^2/\sigma_y^2$  representing the ratio of the powers of  $X$  (in-phase component) and  $Y$  (quadrature component)<sup>3</sup>. Note that if  $\eta = 1$ , then (2.86) reduces to (2.82).

Hoyt distribution is one of the distribution employed to model the so-called worse-than-Rayleigh fading conditions, i.e., scenarios where the fading conditions are more severe than those given by Rayleigh distribution [18], [84].

## Beckmann

Although not very used due to its mathematical complexity, the Beckmann model [85] is the most general fading model arising from the central limit theorem assumption, taking into account not only the power imbalance between the scattering components but also between the LoS component. Therefore, the received signal amplitude is described as

$$R = \|\sigma_x X + j\sigma_y Y + p + jq\| \quad (2.87)$$

where  $X, Y$  are independent random variables such as  $X, Y \sim \mathcal{N}(0, 1)$  and  $\sigma_x, \sigma_y \in \mathbb{R}^+$  and  $p, q \in \mathbb{R}$  are constants.

<sup>3</sup>Traditionally,  $\eta$  is also denoted as  $q^2$ . However, we here prefer the first notation in order to be coherent with the definition of equivalent parameters in more general fading models.

Due to its generality, the PDF of the Beckmann distribution is only given in terms of double infinite sums of products of Bessel functions or in integral form

$$f_R(r) = \frac{r(1+\eta)(1+K)}{2\pi\Omega\sqrt{\eta}} \times \int_0^{2\pi} \exp \left[ -\frac{\left( r\cos\theta - \sqrt{\frac{\varrho^2 K \Omega}{(1+\varrho^2)(1+K)}} \right)^2}{\frac{2\eta\Omega}{(1+\eta)(1+K)}} - \frac{\left( r\sin\theta - \sqrt{\frac{K\Omega}{(1+\varrho^2)(1+K)}} \right)^2}{\frac{2\Omega}{(1+\eta)(1+K)}} \right] d\theta \quad (2.88)$$

with  $\Omega = \mathbb{E}[R^2] = \sigma_x^2 + \sigma_y^2 + p^2 + q^2$  and

$$K = \frac{p^2 + q^2}{\sigma_x^2 + \sigma_y^2}, \quad \eta = \frac{\sigma_x^2}{\sigma_y^2}, \quad \varrho^2 = \frac{p^2}{q^2}. \quad (2.89)$$

Parameter  $K$  is directly related to the Rice factor, since it corresponds to the ratio of the power of the dominant component to that of the scattering, and parameter  $\eta$  is also equivalent to that in Hoyt distribution. Finally,  $\varrho$  determines the power imbalance in the dominant component. Remarkably, if  $\eta = 1$  and/or  $K = 0$ , then it can be proved that  $\varrho$  vanishes in (2.88).

Beckmann distribution includes as particular cases the three aforementioned classical models: Rayleigh ( $K = 0, \eta = 1, \forall \varrho$ ), Rice ( $K = K_{\text{Rice}}, \eta = 1, \forall \varrho$ ) and Hoyt ( $K = 0, \eta = \eta_{\text{Hoyt}}, \forall \varrho$ ).

### Nakagami- $m$

Nakagami- $m$  model was introduced in [20] with the aim of generalizing Rayleigh model to improve the fitting to data measurement. Although the model accurately characterize the propagation conditions in many scenarios, no physical justification is given for its use. The PDF of Nakagami- $m$  distribution is given by

$$f_R(r) = \frac{2m^m r^{2m-1}}{\Omega^m \Gamma(m)} e^{-mr^2/\Omega}, \quad (2.90)$$

where  $m > 1/2$  is the Nakagami parameter and  $\Omega = \mathbb{E}[R^2]$ . If  $m = 1$ , then we obtain the Rayleigh distribution. Also, for  $m \in \mathbb{N}^+$ , the received signal amplitude can be obtained from the same underlying Gaussian model than the previous distributions as

$$R = \left( \sum_{i=1}^m \|\sigma X_i + j\sigma Y_i\|^2 \right)^{1/2} \quad (2.91)$$

where  $X_i$  and  $Y_i \forall i$  are independent standard Gaussian random variables.

Because of its good agreement with empirical data and its mathematical tractability, the Nakagami- $m$  distribution is one of the most employed to characterize fading conditions in a wide variety of scenarios. Moreover, it can approximate both Hoyt and Rice distribution by the mapping given in [18, eqs. (2.25) and (2.26)].

An important remark is the connection between Nakagami- $m$  and Gamma distributions. Specifically, if  $X$  is Nakagami- $m$  distributed, then  $Y = X^2$  is Gamma distributed with shape parameter  $m$  and scale parameter  $\Omega/m$ , i.e.,  $Y \sim \Gamma(m, \Omega/m)$ .

### 2.4.2 Generalized fading models

As introduced before, aiming to provide more flexibility when attempting to characterize fading conditions in more intricate scenarios (e.g. underwater acoustic or millimeter wave propagation) as well as to unify the distinct classical fading distributions under the umbrella of more general models, several distributions have been proposed in the last years.

These general fading models not only increase the accuracy of fittings to data measurement, but they also sometimes improve the mathematical tractability of the classical models. We here revisit some of these general distributions, focusing on their connections to other fading models.

#### Rician shadowed

The Rician shadowed model was originally proposed in [86] as a generalization of Rice model to describe fading behavior in land mobile satellite link [18, chap. 2]. It considers that the dominant (LoS) component is no longer deterministic but instead log-normally distributed. However, Rician shadowed model inherits the complicated formulation of lognormal distribution, and its PDF is only given in integral form [86, eq. (6)].

Aiming to gain mathematical tractability but maintaining the closeness to measured data, an alternative formulation of Rician shadowed model was given in [87], in which the LoS component is Gamma distributed, describing the received signal amplitude as

$$R = \|\sigma X + j\sigma Y + \xi(p + jq)\| \quad (2.92)$$

with  $X, Y \sim \mathcal{N}(0, 1)$ ,  $\xi^2 \sim \Gamma(m, 1/m)$  and  $\sigma_x, \sigma_y, p$  and  $q$  constants as in Rice model. Note that all the involved random variables are independent. The PDF of  $R$  is therefore given by

$$f_R(r) = \left(\frac{m}{m+K}\right)^m \frac{2r(1+K)}{\Omega} e^{-r^2(1+K)/\Omega} {}_1F_1\left(m; 1; \frac{r^2 K(1+K)}{\Omega(m+K)}\right) \quad (2.93)$$

where  $K = (p^2 + q^2)/(2\sigma^2)$ ,  $\Omega = \mathbb{E}[R^2] = p^2 + q^2 + 2\sigma^2$  and  ${}_1F_1(\cdot)$  is the Kummer's hypergeometric function [51, eq. (9.210 1)].

The addition of the random variable  $\xi$  introduces a random fluctuation in the dominant component that characterizes the shadowing. This fluctuation is controlled by parameter  $m$ , reducing its severity as  $m$  becomes larger. If  $m \rightarrow \infty$ , then Rice model is obtained, as can be easily proved by taking the limit in (2.93) and applying [50, eq. (13.3.1)].

### $\kappa$ - $\mu$

The  $\kappa$ - $\mu$  model [28], [88] was introduced as a generalization of the Rice distribution in the same way as Nakagami- $m$  extends Rayleigh model. In [28], a physical explanation for such generalization is given, according to which the received signal amplitude is built out of the superposition of clusters of waves. The power of the LoS component is distinct within each cluster, but the scattered waves of all clusters are assumed to have the same power. Therefore, the received signal amplitude is given by [28, eq. (6)]

$$R = \left( \sum_{i=1}^{\mu} \|\sigma X_i + j\sigma Y_i + p_i + jq_i\|^2 \right)^{1/2} \quad (2.94)$$

where  $X_i, Y_i \sim \mathcal{N}(0, 1) \forall i, \sigma \in \mathbb{R}^+$  and  $p_i, q_i \in \mathbb{R}$  are constants and  $\mu \in \mathbb{N}^+$  is the parameter that effectively generalizes Rice distribution, being equivalent to  $m$  in the Nakagami- $m$  model.

The PDF of  $R$  is given in a similar form to that of the Rice distribution as [28, eq. (1)]

$$f_R(r) = \frac{2\mu(1+\kappa)^{\mu/2+1/2}}{\kappa^{\mu/2-1/2}e^{\mu\kappa}} \frac{r^\mu}{\Omega^{\mu/2+1/2}} e^{-r^2\mu(1+\kappa)/\Omega} I_{\mu-1} \left( 2\mu r \sqrt{\frac{\kappa(1+\kappa)}{\Omega}} \right) \quad (2.95)$$

with

$$\kappa = \frac{\sum_{i=1}^{\mu} p_i^2 + q_i^2}{2\mu\sigma^2}, \quad \Omega = \mathbb{E}[R^2] = \sum_{i=1}^{\mu} p_i^2 + q_i^2 + 2\mu\sigma^2. \quad (2.96)$$

Note that the meaning of  $\kappa$  is similar to that of the Rice  $K$ -factor, corresponding to the ratio of the power of the LoS component to that of the diffuse component.

The physical model in (2.94) forces  $\mu$  to be a positive integer number. However, (2.95) is valid for  $\mu \in \mathbb{R}^+$  although it loses its physical meaning.

Nevertheless, the extra parameter compared to Rice model (which is obtained by setting  $\mu = 1$  and  $\kappa = K$ ) provides a better accuracy in fitting data measurements but maintaining the mathematical tractability of the original model. In addition, it also includes Nakagami- $m$  distribution as particular case ( $\mu = m, \kappa = 0$ ).

An important remark is that  $R^2$  in (2.94) can be identified as a particular case of the complex Gaussian quadratic form in (2.52) in which  $\mathbf{A} = \mathbf{\Sigma} = \mathbf{I}_\mu$ . Therefore, the  $\kappa$ - $\mu$



model, as well as all the fading distributions derived from it, can be analyzed as part of a more general problem.

### $\eta$ - $\mu$

Similarly as the  $\kappa$ - $\mu$  distribution generalizes the Rice model, the  $\eta$ - $\mu$  distribution arises as an extension of the Hoyt model under the same physical argument of clustering of waves [28]. Therefore, the received signal envelope is built as

$$R = \left( \sum_{i=1}^{\mu} \|\sigma_x X_i + j\sigma_y Y_i\|^2 \right)^{1/2} \quad (2.97)$$

where  $\mu$  is the same parameter as in the  $\kappa$ - $\mu$  model,  $X_i, Y_i \sim \mathcal{N}(0, 1) \forall i$  and  $\sigma_x, \sigma_y \in \mathbb{R}^+$  correspond to the variance of the in-phase and quadrature scattering components, respectively. Some details should be pointed out here: (i) the author in [28] proposed two different formats for the  $\eta$ - $\mu$  distribution, and the physical model in (2.97) corresponds to what he called *format one*; (ii) the number of clusters in this format was originally denoted by  $2\mu$ , but we here prefer to redefine the parameter  $\mu$  in order to be coherent with that in  $\kappa$ - $\mu$  fading model. Therefore, according to (2.97), the PDF of  $R$  is given by

$$f_R(r) = \left( \frac{\mu(1+\eta)}{2\Omega} \right)^{\frac{\mu+1}{2}} \frac{2\sqrt{\pi}(1-\eta)^{\frac{1-\mu}{2}}}{\Gamma(\mu/2)\sqrt{\eta}} r^{\mu} \exp\left(-\frac{r^2\mu(1+\eta)^2}{4\Omega\eta}\right) I_{\frac{\mu-1}{2}}\left(r^2\frac{\mu(1-\eta^2)}{4\Omega\eta}\right) \quad (2.98)$$

with  $\eta = \sigma_x^2/\sigma_y^2$  being consistent with the corresponding parameter in Hoyt model and  $\Omega = \mathbb{E}[R^2] = \mu(\sigma_x^2 + \sigma_y^2)$ .

As the  $\kappa$ - $\mu$  model with Rice, the  $\eta$ - $\mu$  distribution generalizes the Hoyt model ( $\mu = 1$ ,  $\eta = \eta_{Hoyt}$ ) without penalizing the mathematical tractability. Moreover, it also includes Nakagami- $m$  model as a particular case ( $\mu = m$ ,  $\eta = 1$ ). However, both  $\kappa$ - $\mu$  and  $\eta$ - $\mu$  models fail when attempting to characterize the power imbalance of the LoS component as the Beckmann distribution does.

### $\kappa$ - $\mu$ shadowed

The  $\kappa$ - $\mu$  shadowed was originally proposed in [29] as a natural extension of the  $\kappa$ - $\mu$  model in which the deterministic component representing the LoS contribution is allowed to randomly fluctuate, similarly as the Rician shadowed model arises from the Rice distribution. Later, the author in [89] proposed the same distribution in the context of device-to-device communications, although from another physical model that was finally proved to be wrong [90]. According to [29], the received signal amplitude under

TABLE 2.2: Connections between the  $\kappa$ - $\mu$  shadowed fading model and others models in the literature. In order to avoid confusion, the parameters corresponding to the  $\kappa$ - $\mu$  shadowed distribution are underlined.

Channels	$\kappa$ - $\mu$ shadowed parameters
Rayleigh	$\underline{\kappa} = 0, \underline{\mu} = 1, \forall \underline{m}$
Rice	$\underline{\kappa} = K, \underline{\mu} = 1, \underline{m} \rightarrow \infty$
Nakagami- $m$	$\underline{\kappa} = 0, \underline{\mu} = m, \forall \underline{m}$
Hoyt	$\underline{\kappa} = (1 - \eta)/(2\eta), \underline{\mu} = 1, \underline{m} = 0.5$
$\kappa$ - $\mu$	$\underline{\kappa} = \kappa, \underline{\mu} = \mu, \underline{m} \rightarrow \infty$
$\eta$ - $\mu$	$\underline{\kappa} = (1 - \eta)/(2\eta), \underline{\mu} = 2\mu, \underline{m} = \mu$
Rician shadowed	$\underline{\kappa} = K, \underline{\mu} = 1, \underline{m} = m$

$\kappa$ - $\mu$  shadowed fading is given by

$$R = \left( \sum_{i=1}^{\mu} \|\sigma X_i + j\sigma Y_i + \xi(p_i + jq_i)\|^2 \right)^{1/2} \quad (2.99)$$

where  $\mu$  denotes the number of clusters,  $X_i, Y_i \sim \mathcal{N}(0, 1) \forall i$ ,  $\sigma \in \mathbb{R}^+$  and  $p_i, q_i \in \mathbb{R}$  are constants and  $\xi$  is a random variable such that  $\xi^2 \sim \Gamma(m, 1/m)$ . All the involved random variables are assumed to be independent. Note that, conditioned on  $\xi$ , (2.99) corresponds to the physical model of the  $\kappa$ - $\mu$  distribution in (2.94). The PDF of  $R$  under  $\kappa$ - $\mu$  shadowed fading is therefore calculated by averaging (2.95) over all possible states of  $\xi$ , obtaining [29, eq. (4)]

$$f_R(r) = \frac{2\mu^\mu m^m (1 + \kappa)^\mu}{\Omega^\mu \Gamma(\mu) (\mu\kappa + m)^m} r^{2\mu-1} \exp\left(-\frac{\mu(1 + \kappa)r^2}{\Omega}\right) {}_1F_1\left(m; \mu; \frac{\mu^2 \kappa (1 + \kappa)r^2}{(\mu\kappa + m)\Omega}\right) \quad (2.100)$$

where parameters  $\kappa$  and  $\Omega$  are defined as in the  $\kappa$ - $\mu$  model (2.96). As in the latter, (2.100) is a valid PDF even for  $\mu \in \mathbb{R}^+$ , although it loses its physical meaning. Moreover, if  $m \rightarrow \infty$ , it is easy to prove by taking the limit and using [50, eq. (13.3.1)] that (2.100) reduces to  $\kappa$ - $\mu$  PDF (2.95).

Remarkably, the  $\kappa$ - $\mu$  shadowed distribution does not only include the underlying fading models derived from the  $\kappa$ - $\mu$  model but also, somehow counterintuitively, the  $\eta$ - $\mu$  and the Hoyt distributions [91]. Hence, it unifies most of the here presented fading models, providing a large versatility on modeling propagation conditions [29], [89], [92]. The connections between the  $\kappa$ - $\mu$  shadowed fading model and the others distributions are summarized in Table 2.2.

Furthermore, it was proved in [30] that  $\kappa$ - $\mu$  shadowed distribution, under the assumption of  $\mu$  and  $m$  being positive integers, can be given in terms of a mixture of

Nakagami- $m$  distributions as

$$f_R(r|m, \mu \in \mathbb{N}^+) = \sum_{i=0}^M C_i f_{\mathcal{N}}(m_i, \Omega_i m_i; r) \quad (2.101)$$

where  $f_{\mathcal{N}}(m_i, \Omega_i m_i; r)$  denotes the Nakagami- $m$  PDF (2.90) with parameter  $m_i$  and mean power  $\Omega_i m_i$ , and  $M, m_i$  and  $\Omega_i$  are constants depending on the  $\kappa$ - $\mu$  shadowed parameters as given in [30, Table 1]. Therefore, any result given in the literature for Nakagami- $m$  distribution can straightforwardly leveraged to the  $\kappa$ - $\mu$  shadowed.

## Chapter 3

# Summary of Results

This chapter presents the main results obtained in this thesis. A twofold contribution is provided: *i)* a new method to approximate the distribution of random variables and its application to the statistical analysis of both complex and real non-central GQFs, and *ii)* two generalizations of the already versatile  $\kappa$ - $\mu$  shadowed fading model. Although these contributions seem a priori unconnected, it will be later shown that both actually share the same underlying methodology.

The chapter is organized as follows. Section 3.1.1 introduces the proposed method to approximate the distribution of random variables, providing general expressions for the PDF and CDF of arbitrary positive variables. This technique is applied to both real and complex GQFs in sections 3.1.2 and 3.1.3, respectively. Finally, the two proposed fading models are presented in sections 3.2.1 and 3.2.2.

### 3.1 Analysis of random variables through confluence

Most of the approaches to approximate the distribution of random variables presented in Chapter 2 have the same main drawback: the resulting expressions does not represent a valid distribution, i.e., the approximated PDF does not necessarily integrate to one and the probabilities may be negative [39, p. 731][38, sec. 2]. Moreover, in the case of the saddle-point technique, it is not obvious how to increase the accuracy of the approximation.

The only exception are the approximants arising from mixtures of distributions, which in fact ensure that the resulting function is a valid PDF. However, as pointed out in Section 2.2.5, the calculation of the mixture parameters may be extremely difficult, and the lack of a general method considerably limits its usefulness.

These limitations are also present in the distinct series expansions given for the PDF and CDF of GQFs in Section 2.3, along with other downsides such as the numerical issues in some cases (e.g., power series expansions), the convergence problems associated with the introduction of artificial parameters and the strong dependence between the required number of terms to be computed and the parameters of the quadratic form.

Motivated by all the above-mentioned drawbacks, one of the main goals of this thesis is to provide a new approach that circumvents these limitations, giving as a result alternative and more robust approximations not only for the distribution of GQFs but also for that of any random variable.

### 3.1.1 Proposed approach

The new method is desired to have the following properties: *i)* the resulting expressions always represent a valid distribution and *ii)* any target level of accuracy can be achieved independently of the parameters of the random variable under analysis. Taking into consideration these requirements, it is clear that we have to disregard any method based on series expansions. Therefore, instead of approximating a certain statistic of a random variable by an infinite series, we analyze a sequence of auxiliary random variables that, in the limit, converges in distribution to the target one. That is, given a random variable  $X \in \mathbb{R}$ , we aim to find a sequence  $\{X_m : m \in \mathbb{N}^+\}$  such that  $\{X_m\} \Rightarrow X$ .

Once the sequence is suitably defined, we can leverage this convergence and approximate the CDF (and the PDF if the conditions given in Section 2.2.1 hold) by that of the auxiliary variables, ensuring that, for any value of  $m$ , the resulting expressions will represent a valid distribution since they are the statistics of another random variable.

The problem is now how to define the auxiliary sequence. Ideally,  $\{X_m\}$  should be chosen so that it converges rapidly to  $X$  and it is mathematically tractable, i.e., the PDF and CDF of  $X_m$  should be easily obtainable for all  $m$ . To that end, we propose defining  $X_m$  by somehow perturbing  $X$ , i.e., introducing an artificial random fluctuation in  $X$  so that it simplifies its statistical analysis. In order to achieve the desired convergence, this fluctuation should vanish in the limit.

Due to the mathematical tractability of the gamma distribution and its limit property of converging to a constant, this artificial fluctuation is chosen to be gamma distributed. Specifically, we will generate the sequence  $\{X_m\}$  from  $X$  by letting its mean or variance to randomly fluctuate according to a gamma distribution. If  $X$  is built as a function of other random variables, an alternative way of defining  $\{X_m\}$  is introducing the fluctuation in either the mean or variance of such underlying variables.

In this thesis, the above technique is used to provide very general expressions to approximate the distribution of any positive real random variable from its MGF. The approach, which is given below, is presented in

[46] P. Ramírez-Espinosa, D. Morales-Jimenez, J. A. Cortés, J. F. París, and E. Martos-Naya, "New approximation to distribution of positive RVs applied to Gaussian quadratic forms", *IEEE Signal Process. Lett.*, vol. 26, no. 6, pp. 923–927, Jun. 2019,

attached in Appendix A.1.

Consider a random variable  $X \in \mathbb{R}^+$  with continuous distribution, and assume that the MGF of  $X$  is given by  $M_X(s)$ . In order to approximate its CDF, and according to the proposed method, we define the auxiliary sequence of random variables  $\{X_m : m \in \mathbb{N}^+\}$  with

$$X_m \triangleq X/\xi_m, \quad (3.1)$$

where  $\xi_m$  is a random variable, independent of  $X$ , which follows a gamma distribution with shape parameter  $m$  and scale parameter  $1/(m-1)$ , i.e.,  $\xi_m \sim \Gamma(m, 1/(m-1))$ . The PDF of  $\xi_m$  is therefore given by (2.16)

$$f_{\xi_m}(u) = \frac{(m-1)^m}{\Gamma(m)} u^{m-1} e^{-(m-1)u}. \quad (3.2)$$

That is, we generate  $X_m$  by introducing a random fluctuation in  $X$ , whose severity decreases as  $m$  increases. As proved in Section 2.2.4, the sequence  $\{\xi_m : m \in \mathbb{N}^+\}$  converges in distribution to the constant  $C = \mathbb{E}[\xi_m]$ , which is calculated according to (2.20), obtaining  $\mathbb{E}[\xi_m] = 1$ . Therefore, we have that  $\{\xi_m\} \Rightarrow 1$  and, from Slutsky's theorem [93, sec. 3.6][55, sec. 1.2], that  $\{X_m\} \Rightarrow X$ .

Hence, the above result allows us to approximate the CDF of  $X$  by that of  $X_m$  with sufficiently large  $m$ , as stated in the following lemma.

**Lemma 3.1** *Let  $X$  be a positive random variable with continuous distribution and MGF given by  $M_X(s)$ , and  $X_m$  as in (3.1). Then, the CDF of  $X$  satisfies*

$$F_X(x) = \lim_{m \rightarrow \infty} F_{X_m}(x) = \lim_{m \rightarrow \infty} \sum_{k=0}^{m-1} \frac{(m-1)^k}{x^k k!} \left. \frac{d^k}{ds^k} M_X(s) \right|_{s=(1-m)/x}. \quad (3.3)$$

The conditions for which convergence in distribution also implies convergence of PDFs are stated in Section 2.2.1. In our case, these conditions are met if the PDF of  $X$ , namely  $f_X(x)$ , is uniformly continuous, i.e., for all  $x_1, x_2 \in [0, \infty)$  exists  $\delta > 0$  and  $\epsilon > 0$  such that  $|x_1 - x_2| < \delta$  implies  $|f_X(x_1) - f_X(x_2)| < \epsilon$ . Therefore, if  $f_X(x)$  is uniformly continuous, we can also approximate it by the PDF of  $X_m$ . This is stated in the following corollary.

**Corollary 3.2** *Let  $X$  be a positive random variable with MGF  $M_X(s)$  and uniformly continuous PDF, and  $X_m$  as in (3.1). Then, the PDF of  $X$  satisfies*

$$f_X(x) = \lim_{m \rightarrow \infty} f_{X_m}(x) = \lim_{m \rightarrow \infty} \frac{(m-1)^m}{x^{m+1} \Gamma(m)} \left. \frac{d^m}{ds^m} M_X(s) \right|_{s=(1-m)/x}. \quad (3.4)$$

Lemma 3.1 and Corollary 3.2 provide a general result to approximate the distribution of a positive random variable in terms of the derivatives of its MGF. As already highlighted, the main benefit of this method is that, since we approximate the distribution of

a  $X$  by that of another variable  $X_m$ , the approximation (for any  $m$ ) always represents a valid distribution.

We also aimed that any level of accuracy could be reached independently of the target variable under analysis. This is ensured by the weak convergence of  $\{X_m\}$  to  $X$ , i.e., increasing the value of  $m$  always leads to a more accurate approximation. In fact, the normalized mean squared error (MSE) between the target variable and  $X_m$ , which is a good indicator of the similarity between both random variables, is a monotonic decreasing function that does not depend on  $X$ , as given in the following lemma.

**Lemma 3.3** *Let  $X$  be a positive random variable, and  $X_m$  as in (3.1). For  $m > 2$ , the normalized MSE admits the following compact expression:*

$$\overline{\epsilon^2} = \mathbb{E}[(X - X_m)^2] / \mathbb{E}[X^2] = (m - 2)^{-1}. \quad (3.5)$$

From (3.5), it is clear that  $\lim_{m \rightarrow \infty} \overline{\epsilon^2} = 0$ , and thus we can achieve any target accuracy in the approximation by choosing  $m$  large enough. Note however that, although informative on the closeness between  $X_m$  and  $X$ , the normalized MSE does not directly translate into the error between the approximated CDF and the true one. An expression for the error in probability is unfortunately difficult to obtain due to the generality of the problem.

We consider appropriate to name this method of approximating the distribution of random variables as *analysis through confluence*, since the target variable is perturbed in order to generate an auxiliary sequence that facilitates the analysis and converge to the original variable in the limit, achieving that confluence. Therefore, for coherence, we denoted the auxiliary variables,  $X_m$ , as *confluent variables*.

As with most of the classical series expansions, where the moments are required, the calculation of (3.3) and (3.4) may be challenging if the derivatives of the MGF of  $X$  are difficult to compute or not expressible in closed form. Thus, large values of  $m$  imply the computation of high-order derivatives of  $M_X(s)$ , which may be tedious in some cases. For instance, if numerical integration (e.g., Cauchy integrals) are used, the computational cost can grow exponentially and round-off errors can lead to a total amount of error that increases with the order of differentiation [94].

However, there are cases where these derivatives can be readily obtained. That is, for instance, the case of those variables whose MGF is given as a product of elementary functions, since its derivatives can be calculated recursively from the derivatives of the logarithm of the MGF (the CGF).

Specifically, consider an arbitrary function  $f(s)$ . The  $k$ -th order derivative of  $f(s)$  can be calculated as [4, eq. (3.2b.3)]

$$\frac{d^k}{ds^k} f(s) = \left( \sum_{r_1=0}^{k-1} \binom{k-1}{r_1} g_{k-1-r_1}(s) \sum_{r_2=0}^{r_1-1} \binom{r_1-1}{r_2} g_{r_1-1-r_2}(s) \dots \right) f(s) \quad (3.6)$$

where

$$g_k(s) = \frac{d^k}{ds^k} g(s) = \frac{d^{k+1}}{ds^{k+1}} \ln f(s). \quad (3.7)$$

From (3.6), the derivatives of  $f(s)$  can be calculated recursively as

$$\frac{d^k}{ds^k} f(s) = f(s) D_k(s) \quad (3.8)$$

with  $D_0(s) = 1$  and, for  $k > 1$ ,

$$D_k(s) = \sum_{j=0}^{k-1} \frac{(k-1)!}{j!(k-j-1)!} g_{k-1-j}(s) D_j(s). \quad (3.9)$$

Thus, if the MGF of  $X$  is given as a product of elementary functions, then  $\ln M_X(s)$  is written in terms of a sum of such simple functions, and its derivatives could be easily written in closed form. This allows a straightforward calculation of the derivatives of  $M_X(s)$  from (3.7) and (3.9) by replacing  $f(s) = M_X(s)$ .

With that, we conclude the presentation of our new method to approximate the distribution of random variables. In next sections, we apply the proposed technique to both complex and real GQFs.

### 3.1.2 Application to non-central real Gaussian quadratic forms

In this section, the proposed approach is used to give a simple and efficient approximation for the distribution of non-central positive definite GQFs, i.e., we aim to provide approximated expressions for both the PDF and CDF of the quadratic form (2.46)

$$Q_R = (\mathbf{x} + \bar{\mathbf{x}})^T \mathbf{A} (\mathbf{x} + \bar{\mathbf{x}}) \quad (3.10)$$

where  $\bar{\mathbf{x}} \in \mathbb{R}^{n \times 1}$  is a constant vector,  $\mathbf{A} \in \mathbb{R}^{n \times n}$  is a *positive definite* symmetric matrix and  $\mathbf{x} \sim \mathcal{N}_n(\mathbf{0}_{n \times 1}, \mathbf{\Sigma})$ .

These results, along with the comparison with other classical approaches listed in Section 2.3.2, are given in

[46] P. Ramírez-Espinosa, D. Morales-Jimenez, J. A. Cortés, J. F. París, and E. Martos-Naya, "New approximation to distribution of positive RVs applied to Gaussian quadratic forms", *IEEE Signal Process. Lett.*, vol. 26, no. 6, pp. 923–927, Jun. 2019.

#### Distribution of $Q_R$

Since  $Q_R$  in (3.10) is a positive random variable, (3.3) and (3.4) can be directly used to approximate its chief statistics, namely PDF and CDF. The only remaining task is



calculating the derivatives of the MGF of  $Q_R$ , for which the approach in (3.7)-(3.9) is employed.

Thus, from (2.56), the CGF of  $Q_R$  is readily written as

$$\ln M_{Q_R}(s) = \sum_{i=1}^n \frac{b_i^2 \lambda_i s}{1 - 2\lambda_i s} - \frac{1}{2} \ln(1 - 2\lambda_i s) \quad (3.11)$$

and, straightforwardly, its derivatives are calculated in closed form as

$$g_k(s) = \frac{d^{k+1}}{ds^{k+1}} \ln M_{Q_R}(s) = 2^k k! \sum_{j=1}^n \frac{\lambda_j^{k+1} [(k+1)b_j^2 + 1 - 2\lambda_j s]}{(1 - 2\lambda_j s)^{k+2}}. \quad (3.12)$$

With the above results, approximated expressions for both the PDF and CDF of  $Q_R$  are given in the next corollary.

**Corollary 3.4** *Consider a positive definite real GQF as in (3.10). Then, its PDF and CDF can be approximated by*

$$f_{Q_R}(x) \approx \frac{(m-1)^m}{x^{m+1}\Gamma(m)} M_{Q_R} \left( \frac{1-m}{x} \right) D_m \left( \frac{1-m}{x} \right), \quad (3.13)$$

$$F_{Q_R}(x) \approx M_{Q_R} \left( \frac{1-m}{x} \right) \sum_{k=0}^{m-1} \frac{(m-1)^k}{x^k k!} D_k \left( \frac{1-m}{x} \right), \quad (3.14)$$

where  $M_{Q_R}(s)$  is given in (2.56) and  $D_k(s)$  in (3.9) with  $g_k(s)$  as in (3.12).

### Numerical results and discussion

We now compare the proposed approximation for real GQFs in Corollary 3.4 with the classical results in Section 2.3.2. Specifically, we consider the power series in (2.62) and the Laguerre and  $\chi^2$  expansions in (2.64) and (2.65), respectively. The other approaches proposed in the literature are disregarded due to the drawbacks listed in Section 2.3.2.

For the sake of simplicity, both  $\mathbf{A}$  and  $\mathbf{\Sigma}$  are considered exponential matrices, i.e.,  $(\mathbf{A})_{i,j} = \alpha^{|i-j|}$  and  $(\mathbf{\Sigma})_{i,j} = \rho^{|i-j|}$  with  $0 < \alpha, \rho < 1$ . With this assumption, which does not imply any loss of generality in the obtained results, our proposal is compared with the above-mentioned techniques in Figs. 3.1-3.4.

We first consider the comparison with the power series showed in Fig. 3.1. It can be observed that the power series renders a valid approximation only up to a certain point in  $x$ , remarkably failing thereafter; the value of  $x$  from which the series diverges depends on the parameters of the quadratic form. As illustrated, increasing the number of terms in the series from  $N = 100$  to  $N = 150$  does not seem to solve the problem. In contrast, our proposed solution shows an excellent agreement with simulations for all parameter choices and all  $x$ .

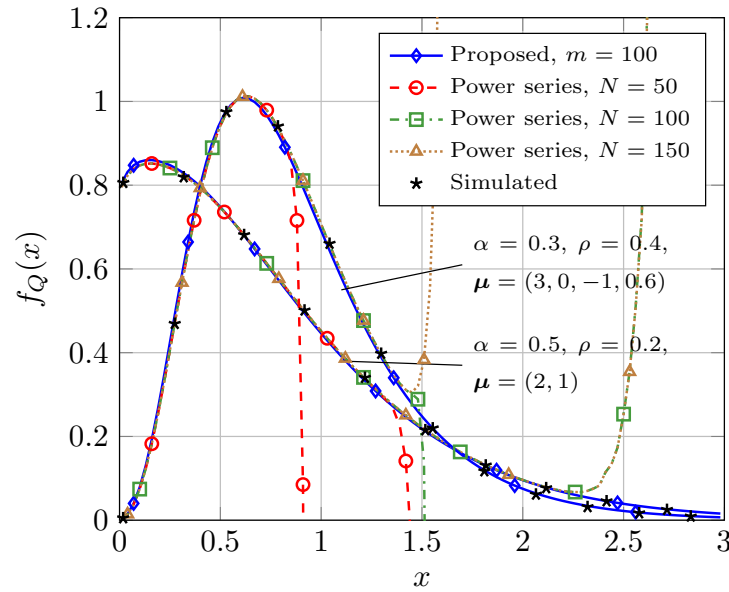


FIGURE 3.1: PDF of  $Q_R$  for different values of  $\alpha$ ,  $\rho$  and  $\bar{x}$ . The proposed approximation in (3.13) is compared with the power series expansion in and with Monte Carlo simulations.  $N$  denotes the number of terms calculated in the power series.

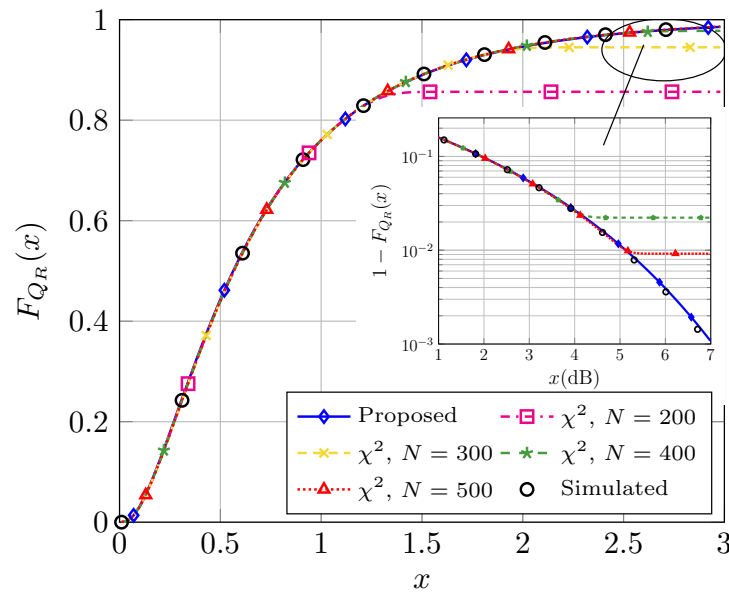


FIGURE 3.2: CDF of  $Q_R$  for  $\alpha=0.7$ ,  $\rho = 0.5$  and  $\bar{x} = (2, 1, -1, 0.6, -0.9)$ . Our proposed method in (3.14) with  $m = 100$  is compared with the  $\chi^2$  expansion in (2.65) and with Monte Carlo simulations.  $N$  denotes the number of terms calculated in the  $\chi^2$  series expansion.

Fig. 3.2 compares our results with the  $\chi^2$  densities expansion in (2.65) by plotting in this case the CDF of  $Q_R$  (similar trends are observed for the PDF). As pointed out in Section 2.3.2, the  $\chi^2$  approximation artificially introduces an additional parameter  $0 < \beta_\chi < \min_j \{\lambda_j\}$  that controls the series convergence. Since a higher value of  $\beta_\chi$  in this interval seems to accelerate the series convergence, i.e., smaller values of  $\beta_\chi$  requires a larger  $N$  to achieve the same accuracy, a value  $\beta_\chi = 0.9 \min_j \{\lambda_j\}$  has been chosen. Regarding Fig. 3.2, it is observed that the number of terms required for the  $\chi^2$  expansion,  $N$ ,

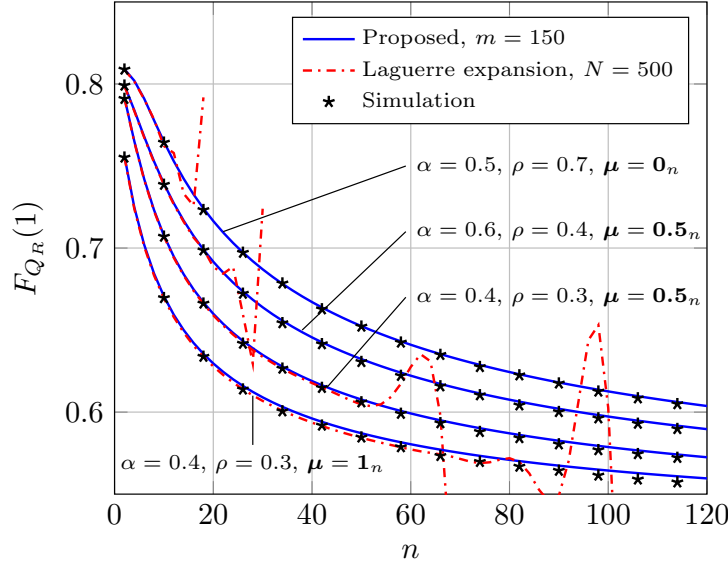


FIGURE 3.3: CDF of  $Q_R$  at  $x = 1$  for distinct quadratic form order,  $n$ . Our proposed expression in (3.14) is compared with the Laplace approximation in (2.64) with  $\beta_L = 10$  and with Monte Carlo simulations.

is much larger than in our method (the value of  $m$ ) to accurately approximate the distribution of the quadratic form. Furthermore, it is important to note that the  $\chi^2$  expansion does not yield a valid CDF, as observed in the right-hand tail, where the approximated CDF does not reach to one if  $N$  is not sufficiently large.

A comparison between (3.14) and the Laguerre series expansion in (2.64) is shown in Fig. 3.3, where  $F_{Q_R}(x)$  at  $x = 1$  is depicted for distinct quadratic form orders,  $n$ . Although useful in many situations, this approximation has two clear drawbacks. The first one is that, as the previous approximations, the resulting function is not a proper CDF if the number of terms computed,  $N$ , is not large enough (in fact, the resulting CDF presents an oscillatory behavior). The second one is the uncertainty in the actual value of the parameter  $\beta_L$ , introduced to control the series convergence, that yields the best approximation. As stated in Section 2.3.2, the convergence is mathematically ensured for all  $x$  only if  $\beta_l > \max_j \{\lambda_j\}/2$ . Specifically, a value of  $\beta_l > (\max_j \{\lambda_j\} + \min_j \{\lambda_j\})/2$  is recommended in order to minimize the approximation error. However, we noticed that, in some cases, this choice renders considerable numerical errors that prevent the series convergence. In fact, increasing the value of  $N$  in those cases makes the approximation even less accurate, probably due to the total increased amount of error, while maintaining the same  $N$  and changing the value of  $\beta_L$  lead to a tight approximation. Hence, finding the value of  $\beta_L$  that yields the best approximation in each case is a difficult task. For the calculation in Fig. 3.3, a value of  $\beta_L = 10$  has been chosen, which seems to minimize such numerical issues.

As shown in this figure, the series diverges when the order of  $Q_R$  increases, with independence of the quadratic form parameters. Note that the considered values of  $n$  are not particularly extreme, but rather moderate, particularly in applications such as signal

detection where large numbers of samples are typically employed.

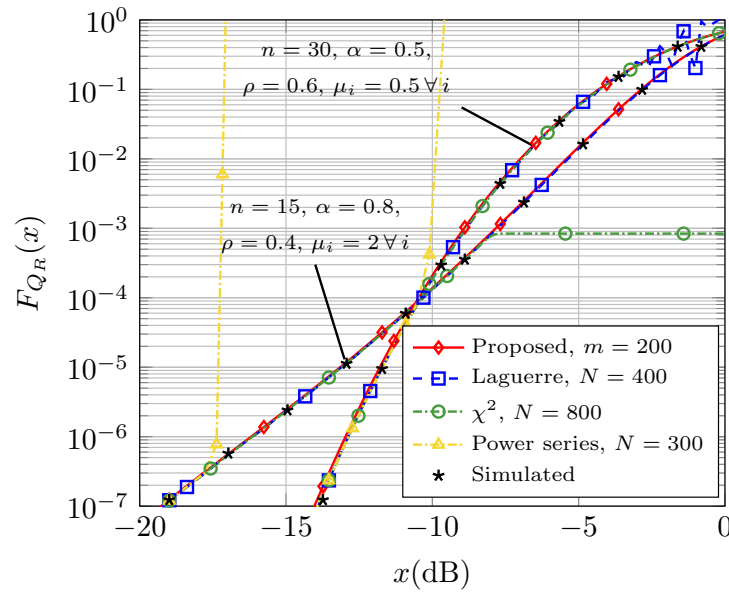


FIGURE 3.4: CDF of  $Q_R$  for different values of  $n$ ,  $\alpha$ ,  $\rho$  and  $\bar{x}$ . The proposed method is compared with the power series in (2.62), the Laguerre expansion in (2.64) and the  $\chi^2$  expansion in (2.65) and contrasted with Monte Carlo simulations. Parameters:  $\beta_L = 9$  for  $n = 15$  and  $\beta_L = 12$  for  $n = 30$ .

The last comparison is shown in Fig. 3.4, where the CDF of  $Q_R$  is plotted in logarithmic scale in order to analyze the accuracy of the distinct approaches to approximate the left tail of the distribution. As observed, the aforementioned drawbacks of the alternative methods are also relevant when focusing on the left tail of the distribution. In turn, our proposed technique renders again an excellent approximation with independence of the parameters of  $Q_R$ .

Overall, obtained results show that the analysis through confluence is a good alternative to classical approaches to approximate not only the left tail, but also the complete range of the distribution. Moreover, it has a distinctive feature over the classical ones: the robustness. Hence, it provides accurate results with independence of the parameters of the quadratic form, also ensuring that the resulting functions properly represent a valid distribution independently of the number of terms ( $m$ ) that are computed. Furthermore, the goodness of the approximation does not depend on arbitrary constants as in the  $\chi^2$  and the Laguerre series expansions.

### 3.1.3 Application to non-central complex Gaussian quadratic forms

The proposed technique is now employed to characterize non-central complex GQFs, i.e., we seek an approximation for the PDF and CDF of the quadratic form (2.52)

$$Q_C = (\mathbf{v} + \bar{\mathbf{v}})^\dagger \mathbf{A}(\mathbf{v} + \bar{\mathbf{v}}) \quad (3.15)$$

where  $\mathbf{A} \in \mathbb{C}^{n \times n}$  is an Hermitian matrix and  $\mathbf{v} \sim \mathcal{CN}_n(\mathbf{0}_{n \times 1}, \Sigma)$ .

Since it has been proved that a complex GQF is equivalent to a real one with the eigenvalues given in pairs (see Section 2.3.1), (3.13) and (3.14) could be directly used to approximate the distribution of  $Q_C$  in the positive definite case. However, we can exploit the particularities of the complex case and go one step further, obtaining an alternative approximation with two additional advantages. The first one is that it is valid not only for positive definite complex GQFs but also in the indefinite case, providing more generality. The second one is that the resulting expressions are more suitable for further analytical purposes. The recursion in (3.13) and (3.14) involving the independent variable  $x$  may pose a challenge to that end, and therefore circumventing this recursion is an additional value due to the importance of complex GQFs in performance analysis of communications systems and signal processing applications (e.g., signal detection). These alternative approximation is achieved by defining the sequence  $\{X_m : m \in \mathbb{N}^+\}$  in a different way as in (3.1).

The analysis of  $Q_C$  with the proposed technique, its comparison with other approaches given in 2.3.2 and its application to the analysis of MRC systems is presented in

[47] P. Ramírez-Espinosa, L. Moreno-Pozas, J. F. París, J. A. Cortés, and E. Martos-Naya, "A new approach to the statistical analysis of non-central complex Gaussian quadratic forms with applications", *IEEE Trans. Veh. Technol.*, vol. 68, no. 7, pp. 6734–6746, Jul. 2019,

attached in Appendix A.2, and summarized below.

### Distribution of $Q_C$

As introduced before, in order to characterize  $Q_C$ , an alternative auxiliary sequence of variables is used. Thus, instead of defining  $X_m$  by directly perturbing the quadratic form as in the real case, we here introduce the random fluctuation in the mean of the underlying Gaussian variables of  $Q_C$ . To that end, we consider the formulation in (2.53)

$$Q_C = (\mathbf{s} + \bar{\mathbf{h}})^\dagger \mathbf{\Lambda} (\mathbf{s} + \bar{\mathbf{h}}) \quad (3.16)$$

where the distinct parameters are properly defined in Section 2.3.1. From (3.16), we define the sequence  $\{Q_m : m \in \mathbb{N}^+\}$  such that

$$Q_m = (\mathbf{s} + \mathbf{D}_\xi \bar{\mathbf{h}})^\dagger \mathbf{\Lambda} (\mathbf{s} + \mathbf{D}_\xi \bar{\mathbf{h}}), \quad (3.17)$$

with  $\mathbf{D}_\xi \in \mathbb{R}^{n \times n}$  a diagonal matrix whose entries,  $\xi_{m,i}$  for  $i = 1, \dots, n$ , are independent and identically distributed (i.i.d.) random variables such that  $\xi_{m,i}^2$  are gamma distributed with shape parameter  $m$  and  $\mathbb{E}[\xi_{m,i}^2] = 1$ , i.e.,  $\xi_{m,i}^2 \sim \Gamma(m, 1/m)$ .

As proved in Section 2.2.4,  $\xi_{m,i}^2 \Rightarrow \mathbb{E}[\xi_{m,i}^2] = 1$  for all  $i$  and, from the relationship between the CDF of  $\xi_{m,i}^2$  and that of  $\xi_{m,i}$ , it can also be proved that  $\xi_{m,i} \Rightarrow 1$ . Therefore,  $\mathbf{D}_\xi$  becomes the identity matrix when  $m \rightarrow \infty$  and, intuitively, it can be observed that  $\{Q_m\}$  converges to  $Q_C$  in the limit. Note also that, in the central case, i.e.,  $\bar{\mathbf{h}} = \mathbf{0}_{n \times 1}$ ,  $Q_m = Q_C$  for any value of  $m$ .

However, this convergence needs to be formally proved before approximating the distribution of  $Q_C$  by that of  $Q_m$ . In order to do so, we first calculate the MGF of  $Q_m$  by conditioning  $M_Q(s)$  on  $\mathbf{D}_\xi$  and averaging over all its possible values.

**Lemma 3.5** Consider  $Q_m$  as in (3.17). Then, its MGF is given by

$$M_{Q_m}(s) = \prod_{i=1}^n \frac{\left(1 - \frac{\lambda_i \mu_i s}{m(1 - \lambda_i s)}\right)^{-m}}{1 - \lambda_i s}, \quad \operatorname{Re}\{s\} \lambda_i (1 + \mu_i/m) < 1 \quad \forall i, \quad (3.18)$$

where  $\mu_i = \|h_i\|^2$ .

From (3.18), and taking into account that

$$\lim_{m \rightarrow \infty} \left(1 - \frac{\lambda_i \mu_i s}{m(1 - \lambda_i s)}\right)^{-m} = \exp\left(\frac{\lambda_i \mu_i s}{1 - \lambda_i s}\right), \quad (3.19)$$

it is clear that  $\lim_{m \rightarrow \infty} M_{Q_m}(s) = M_{Q_C}(s)$  for any  $s = jt$  with  $t \in \mathbb{R}$ . Therefore, from Lévy's continuity theorem, we have that  $\{Q_m\} \Rightarrow Q_C$  [52, chap. 18].

An important remark is that  $M_{Q_m}(s)$  does not have the exponential term present in (2.66). This considerably eases the mathematical analysis by allowing to write (3.18) as a rational function of the form

$$M_{Q_m}(s) = B \prod_{i=1}^n \frac{(s - 1/\lambda_i)^{m-1}}{(s - \beta_i)^m} \quad (3.20)$$

where  $\beta_i = [\lambda_i(1 + \mu_i/m)]^{-1}$  and

$$B = \prod_{k=1}^n \left[ -\lambda_k \left(1 + \frac{\mu_k}{m}\right)^m \right]^{-1}. \quad (3.21)$$

Assuming there can be repeated zeroes ( $1/\lambda_i$ ) and poles ( $\beta_i$ ), and taking into consideration that, if  $\mu_i = 0$  for a certain  $i$  then  $\beta_i = 1/\lambda_i$ , the rational function in (3.20) can be simplified. Thus, denoting as  $\tilde{\beta}_i$  and  $1/\tilde{\lambda}_j$  for  $i = 1, \dots, n_\beta$  and  $j = 1, \dots, n_\lambda$  the distinct poles and zeroes resulting from this simplification with multiplicities  $p_i$  and  $q_i$ , respectively, the MGF of  $Q_m$  is finally expressed as

$$M_{Q_m}(s) = B \frac{\prod_{j=1}^{n_\lambda} (s - 1/\tilde{\lambda}_j)^{q_j}}{\prod_{i=1}^{n_\beta} (s - \tilde{\beta}_i)^{p_i}}. \quad (3.22)$$

Observe that, in contrast to the MGF of the original quadratic form  $Q_C$  in (2.66), the expression of  $M_{Q_m}$  in (3.22) allows an straightforward inversion, i.e., we can directly obtain the PDF and CDF of  $Q_m$  by performing an inverse Laplace transformation as

$$f_{Q_m}(s) = \mathcal{L}^{-1} \{M_{Q_m}(-s)\}, \quad F_{Q_m}(s) = \mathcal{L}^{-1} \left\{ \frac{1}{s} M_{Q_m}(-s) \right\} \quad (3.23)$$

and then approximating the PDF and CDF of  $Q_C$  by leveraging the convergence between both variables, as stated in the following lemma.

**Lemma 3.6** *Consider an indefinite non-central complex GQF as in (3.16). Then, its PDF and CDF can be approximated by those of  $Q_m$  as*

$$f_{Q_C}(x) \approx f_{Q_m}(x) = \sum_{i=1}^{n_\beta} \sum_{j=1}^{p_i} \alpha_{i,j} e^{-\tilde{\beta}_i x} x^{j-1} u(\tilde{\beta}_i x) \operatorname{sgn}(x), \quad (3.24)$$

$$F_{Q_C}(x) \approx F_{Q_m}(x) = u(x) + \sum_{i=1}^{n_\beta} \sum_{j=1}^{p_i} \omega_{i,j} e^{-\tilde{\beta}_i x} x^{j-1} u(\tilde{\beta}_i x) \operatorname{sgn}(x), \quad (3.25)$$

where  $u(\cdot)$  is the unit step function,  $\operatorname{sgn}(\cdot)$  is the sign function and

$$\alpha_{i,j} = \frac{(-1)^n}{(j-1)!} B A_{i,j}, \quad \omega_{i,j} = \frac{(-1)^n}{(j-1)!} B C_{i,j}, \quad (3.26)$$

with  $A_{i,j}$  and  $C_{i,j}$  the residues arising from performing a partial fraction decomposition in (3.22) after evaluating  $M_{Q_m}(-s)$  and  $M_{Q_m}(-s)/s$ , respectively.

Note that, although  $m$  does not appear explicitly in (3.24) and (3.25), both the poles  $\tilde{\beta}_i$  and their multiplicities  $p_i$  depends on  $m$ , as well as zeroes multiplicities  $q_i$ . Moreover, in the central case, *exact* expressions for both  $f_{Q_C}(x)$  and  $F_{Q_C}(x)$  can be obtained from (3.24) and (3.25) for any value of  $m$ , e.g.,  $m = 1$ .

As for the calculation of the residues  $A_{i,j}$  and  $C_{i,j}$ , although they admit a closed formulation, their computation is impractical for very large  $m$  due to the resulting combinatorial expressions. A more suitable approach is the algorithm proposed in [95], which provides recursive expressions for the partial fraction residues of both proper and improper rational functions. The recursion starts from the higher order residues, i.e.,  $A_{i,p_i}$  and  $C_{i,p_i}$ , which can be directly calculated from the definition in [96, eq. (A.36)], and computes the other residues recursively according to [95, eqs. (11a) and (11b)].

Finally, to complete the statistical analysis of  $Q_C$ , we aim to characterize somehow the approximation error. As in the real case, a closed form expression for the error between  $F_{Q_m}(x)$  and  $F_{Q_C}(x)$  would be desirable. However, it is difficult to obtain an useful expression for such error. Therefore, since we are not truncating any series expansion but instead approximating the distribution of a target variable from that of another, we resort again on the normalized MSE as an informative measurement of the closeness between  $Q_C$  and  $Q_m$ .



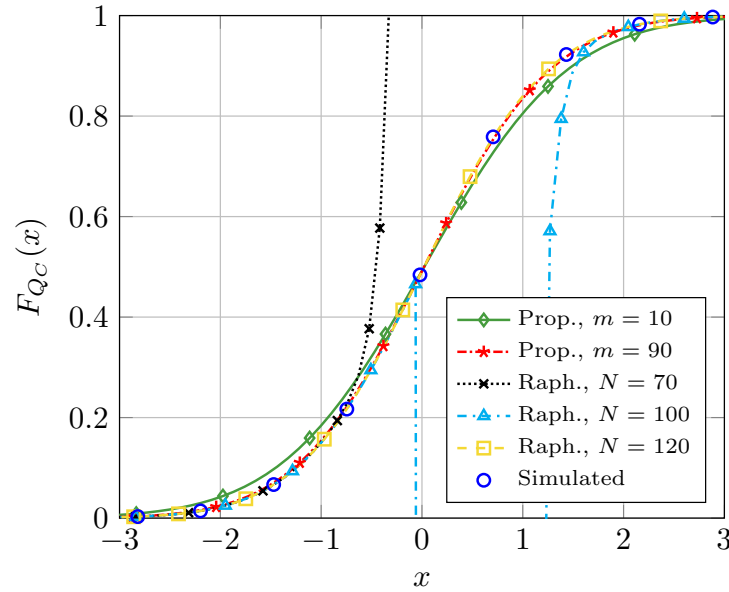


FIGURE 3.5: CDF of  $Q_C$  for  $n = 6$ ,  $\lambda = (-3, -1.8, -1, 1, 2.1, 3)$  and  $\mu = (8.5, 7.4, 4, 5, 6.8, 7.9)$ . Exact (simulated) CDF is compared with the proposed approximation in (3.25) and Raphaeli's approach in (2.70) with  $N$  terms computed.

**Lemma 3.7** Consider  $Q$  and  $Q_m$  as in (3.16) and (3.17), respectively. Then, the normalized MSE between  $Q$  and  $Q_m$  is given by

$$\bar{\epsilon}^2 \triangleq \frac{\mathbb{E}[(Q_m - Q)^2]}{\mathbb{E}[Q^2]} = \frac{\sum_{i=1}^n \lambda_i^2 \mu_i \left[ 4 \left( 1 - \frac{\Gamma(m+1/2)}{m^{1/2} \Gamma(m)} \right) + \frac{\mu_i}{m} \right]}{\sum_{j=1}^n \left( \lambda_j^2 (1 + 2\mu_j) \right) + \left( \sum_{j=1}^n \lambda_j (1 + \mu_j) \right)^2}. \quad (3.27)$$

Regarding (3.27) we observe that, when  $\mu_i = \|h_i\|^2 = 0$  for  $i = 1, \dots, n$ , then  $\bar{\epsilon}^2 = 0$  for any value of  $m$ . This is coherent with the fact that setting  $\mu_i = 0 \forall i$  implies having a central quadratic form and, therefore,  $\mathbf{D}_\xi$  vanishes in (3.17). Additionally, it is easy to prove that the error also goes to zero when  $m \rightarrow \infty$  by taking the limit in (3.27) and using [50, eq. (6.1.39)].

### Comparison with other approaches

The proposed results are now compared to other approximations given in the literature. Specifically, Raphaeli's approach in (2.70) and the saddle-point approximation in (2.78) are considered. Compared to these results, our proposed method provides a twofold benefit. The first one is that approximations in (3.4) and (3.25) are useful for further analytic purposes (e.g., calculation of expectations over  $Q_C$ ) since they are given in terms of elementary functions. The second one is that our approach always renders a valid distribution (for any  $m$ ), in contrast to the other methods. This is shown in Figs. 3.5 and 3.6, where the CDF of  $Q_C$ , calculated using the different techniques, is depicted.



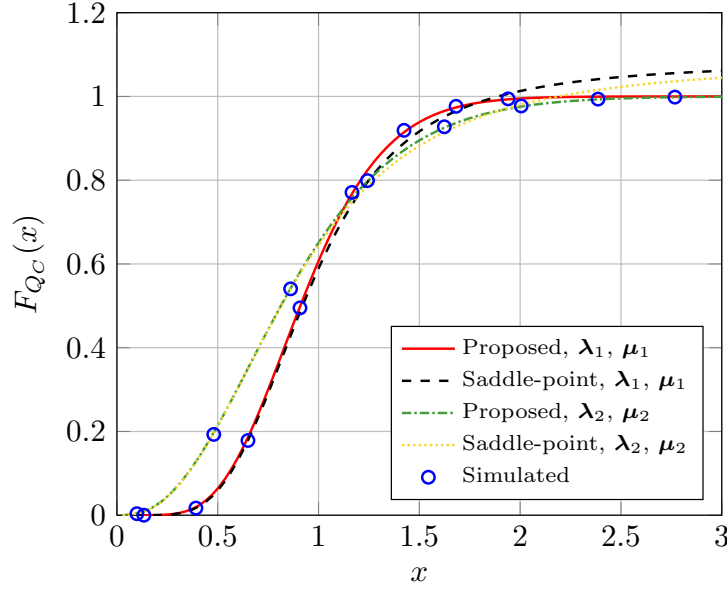


FIGURE 3.6: CDF of  $Q_C$  for different parameters. Exact (simulated) CDF is compared with the proposed approximation in (3.25) with  $m = 50$  and the saddle-point approach in (2.78). Data:  $\lambda_1 = [0.2, 1, 1.4, 3, 5]$ ,  $\lambda_2 = [0.1, 0.6, 1]$ ,  $\mu_1 = [0.6, 7.4, 3, 2.6, 5.5]$  and  $\mu_2 = [1, 0.8, 3.4]$ .

For simplicity, the vector containing the  $n$  eigenvalues  $\lambda_i$  is denoted by  $\lambda$  and, analogously, the vector  $\mu$  is defined such that  $\mu = (\mu_1, \dots, \mu_n)$ . The theoretical calculations are validated through Monte Carlo simulations of  $Q_C$ .

Thus, Fig. 3.5 focuses on the comparison with Raphaëli's method in (2.70). It is clear that this approximation produces invalid CDF values for certain  $x$  if the number of terms computed,  $N$ , is not large enough. Not until a value of  $N = 120$  is reached that the CDF converges for all  $x$ . Moreover, we have observed that the number of terms required strongly depends on the eigenvalues  $\lambda_i$ . That is, the smaller the difference between the eigenvalues the larger the value of  $N$  needed. In turn, our approach renders a valid distribution with independence of  $m$ .

On the other hand, Fig. 3.6 compares the proposed method with the saddle-point approach in (2.78). Although the latter arises as a very efficient approximation, it suffers from the same drawbacks as the previous one. As observed, it gives probabilities greater than one in the right tail. In addition, it is not suitable for further analytic purposes.

### Practical example: MRC systems over correlated Rice fading channels

The usefulness of the proposed method is now exemplified through the performance analysis of MRC systems over correlated Rice channels. To the best of the authors' knowledge, only asymptotic expressions have been given in the literature for the bit error rate (BER) and the outage probability ( $P_{\text{out}}$ ) for arbitrary number of branches and correlation between them [97], [98] and infinite series representations when the number of

branches is limited to  $P = 2$  [99], [100]. Taking advantage of the mathematical tractability of our derived results, we here provide expressions for these metrics.

Considering perfect synchronization and channel estimation, the SNR at the output of the receiver when applying MRC can be written as

$$\gamma = \bar{\gamma} \mathbf{g}^\dagger \mathbf{g} \quad (3.28)$$

where  $\bar{\gamma}$  is the average SNR at each branch and  $\mathbf{g} \in \mathbb{C}^{P \times 1}$  is the channel gain vector. Since the fading at each branch is assumed to be Rice distributed with  $K_i$  factor for  $i = 1, \dots, P$ ,  $\mathbf{g}$  is a complex Gaussian vector such that  $\mathbf{g} \sim \mathcal{CN}_P(\bar{\mathbf{g}}, \mathbf{\Sigma})$ , with  $\bar{\mathbf{g}} = \mathbb{E}[\mathbf{g}]$  and  $\mathbf{\Sigma} = \mathbb{E}[(\mathbf{g} - \bar{\mathbf{g}})(\mathbf{g} - \bar{\mathbf{g}})^\dagger]$  the covariance matrix. The entries of both the mean vector and the covariance matrix can be expressed in terms of the Rice factor as<sup>1</sup>

$$\bar{g}_i = \sqrt{\frac{K_i}{K_i + 1}}, \quad (\mathbf{\Sigma})_{i,j} = \sqrt{\frac{1}{(1 + K_i)(1 + K_j)}} (\mathbf{R})_{i,j} \quad (3.29)$$

with  $(\mathbf{R})_{i,j}$  for  $i, j = 1, \dots, P$  the entries of the correlation matrix  $\mathbf{R}$  of  $\mathbf{g}$ . Note that each element of  $\mathbf{g}$  has unit power, i.e.,  $\mathbb{E}[|g_i|^2] = 1$ , so we consider normalized fading channels.

It is observed that  $\gamma$  in (3.28) is a particular case of the quadratic form in (3.15) with  $\mathbf{A} = \mathbf{I}_P$ , and, therefore, we can use the proposed method to analyze the performance of the system. To that end, the sequence  $\{\gamma_m : m \in \mathbb{N}^+\}$  is defined with  $\gamma_m$  directly obtained by particularizing (3.17). Hence, we can approximate both  $P_{\text{out}}$  and the BER from the statistical analysis of  $\gamma_m$  when  $m$  takes appropriate large values:

- **Outage probability.** Defining  $\gamma_{\text{th}}$  as the minimum SNR required for a reliable communication, the outage probability is given by [101, eq. (6.46)]

$$P_{\text{out}}(\gamma_{\text{th}}) = P(\gamma < \gamma_{\text{th}}) \approx P(\gamma_m < \gamma_{\text{th}}) = \int_0^{\gamma_{\text{th}}} f_{\gamma_m}(\gamma_m) d\gamma_m, \quad (3.30)$$

which corresponds to the CDF of  $\gamma_m$ . Then, from (3.25), we straightforwardly have

$$P_{\text{out}}(\gamma_{\text{th}}) \approx 1 + \sum_{i=1}^{n_\beta} \sum_{j=1}^{p_i} \omega_{i,j} e^{-\tilde{\beta}_i \gamma_{\text{th}} / \bar{\gamma}} \left( \frac{\bar{\gamma}}{\gamma_{\text{th}}} \right)^{-j+1} \quad (3.31)$$

where  $\omega_{i,j}$ ,  $\tilde{\beta}_i$ ,  $n_\beta$  and  $p_i$  are obtained by identification with (3.25).

- **BER.** Since the BER is a continuous and bounded function, Helly-Bray theorem allows to approximate the BER over the SNR variable  $\gamma$  through the analysis of  $\gamma_m$ , as stated in Section 2.2.1. The probability error for an arbitrary modulation can be obtained by averaging the BER in additive white Gaussian noise (AWGN) channels, which is denoted by  $P_0(\cdot)$ , over the distribution of the fading, which in our case is

<sup>1</sup>There is a typo in [47, eq. (34)] which has been corrected in this thesis.

represented by  $\gamma_m$ , as [18, eq. (8.102)]

$$P_b(\bar{\gamma}) \approx \int_0^\infty P_0(\gamma_m) f_{\gamma_m}(\gamma_m) d\gamma_m \quad (3.32)$$

where  $f_{\gamma_m}(\gamma_m)$  is readily obtained from (3.24).

Assuming a Gray coded constellation,  $P_0(\gamma_m)$  for an arbitrary  $M$ -ary square quadrature amplitude modulation (QAM) is given by [102], finally obtaining

$$P_b(\bar{\gamma}) \approx \sqrt{M} \sum_{i=1}^{n_\beta} \sum_{j=1}^{p_i} \sum_{k=1}^{\sqrt{M}-1} \omega(k) \alpha_{i,j} \left[ \frac{\Gamma(j)}{2\tilde{\beta}_i^j} - \frac{\delta_k \Gamma(j + \frac{1}{2})}{\tilde{\beta}_i^{j+1/2}} \right] \times \sqrt{\frac{\bar{\gamma}}{2\pi}} {}_2F_1\left(\frac{1}{2}, j + \frac{1}{2}; \frac{3}{2}; \frac{-\delta_k^2 \bar{\gamma}}{2\tilde{\beta}_i}\right) \quad (3.33)$$

where  $\delta_k = (2k-1)\sqrt{3/(M-1)}$ , constants  $\omega(k)$  are given in [102, eqs. (6), (14) and (21)] and  ${}_2F_1(\cdot)$  is the Gauss hypergeometric function [50, eq. (15.1.1)].

## Numerical results

In the following, the influence of the channel parameters and the number of branches of the receiver in the outage probability and the BER is assessed using (3.31) and (3.33) and contrasted through Monte Carlo simulations. For simplicity, the vector containing the  $P$  Rice  $K$  factors is denoted as  $\mathbf{k} = (K_1, \dots, K_P)$  and the correlation matrix  $\mathbf{R}$  is assumed to be exponential, i.e.,  $(\mathbf{R})_{i,j} = \rho^{|i-j|}$  with  $\|\rho\| < 1$  [103], [104]. The results are plotted in Figs. 3.7-3.9, showing a perfect match between the analytic and the simulated values in all cases.

First, the impact of the correlation matrix and the Rice  $K$  factors in the outage probability is studied both in the low-SNR and high-SNR regime. Since  $P_{\text{out}}$  exhibits complementary behaviors in both regimes, a different representation is employed in each case. Thus, Fig. 3.7 depicts the complementary outage probability  $(1 - P_{\text{out}})$  for  $P = 2$  when the SNR takes low values compared to the threshold, whereas Fig. 3.8 show the values of  $P_{\text{out}}$  in the high-SNR regime and for a larger number of branches ( $P = 4$ ) in order to enrich the system.

Regarding both Figs. 3.7 and 3.8, we observe that the strength of the LoS has an opposite effect in the low- and high-SNR regimes. Hence, while in the former a weak direct component (low values for  $K_i$ ) seems to be beneficial, a strong LoS achieves in general a better performance in the latter. This behavior can be justified as follows. A strong LoS component implies less random fluctuation in the received signal, i.e., the scattering is less relevant. In the high SNR regime, where the mean of the instantaneous SNR is large enough, this fluctuation represented by the scattering may occasionally lead to deep fading that makes the instantaneous SNR drops below the threshold. Therefore, increasing

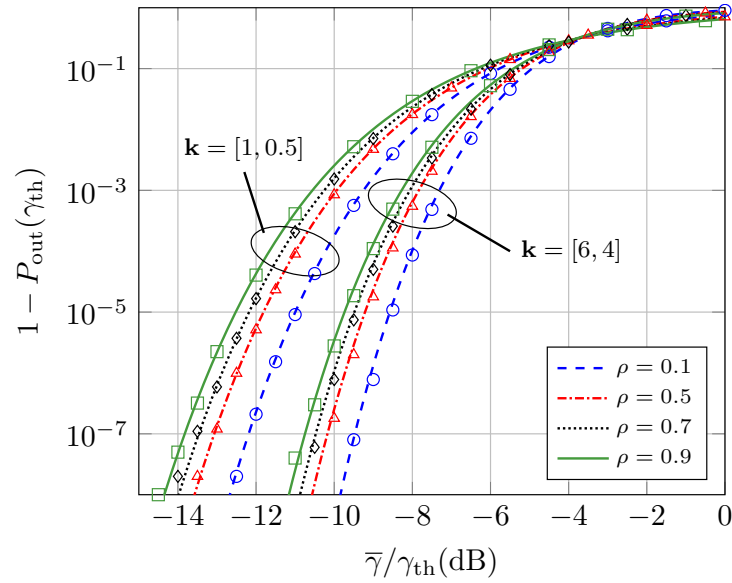


FIGURE 3.7: Complementary  $P_{\text{out}}$  vs.  $\bar{\gamma}/\gamma_{\text{th}}$  for  $P = 2$ , different values of  $\rho$  and different values of  $K$  at each path. Solid lines correspond to theoretical calculation with  $m = 40$  for  $\mathbf{k} = (1, 0.5)$  and  $m = 100$  for  $\mathbf{k} = (6, 4)$ , while markers correspond to Monte Carlo simulations.

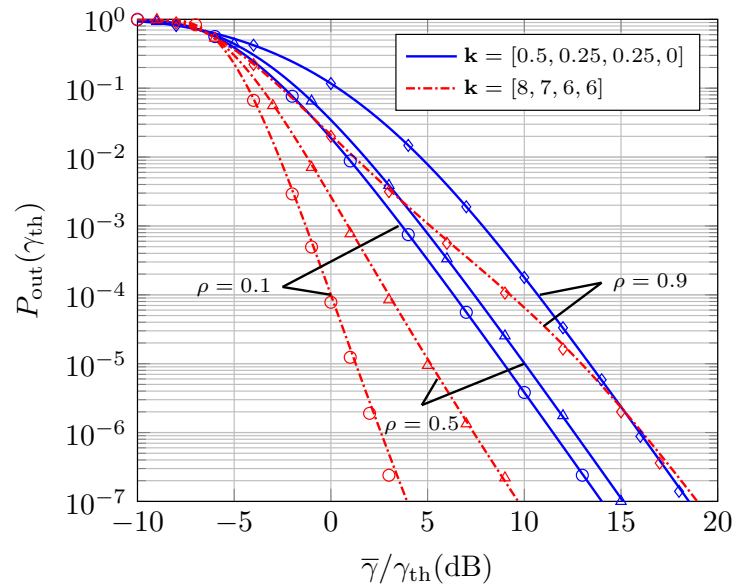


FIGURE 3.8:  $P_{\text{out}}$  vs.  $\bar{\gamma}/\gamma_{\text{th}}$  for  $P = 4$ , different values of  $\rho$  and different values of  $K$  at each path. Solid lines correspond to theoretical calculation while markers correspond to Monte Carlo simulations. For theoretical calculation,  $m = 40$  for  $\mathbf{k} = (0.5, 0.25, 0.25, 0)$  and  $m = 200$  for  $\mathbf{k} = (8, 7, 6, 6)$ .

the  $K$  factor (the power of the LoS) when the mean SNR takes large values is beneficial since it reduces such probability. In turn, in the low-SNR regime, the fluctuation in the received signal may have the opposite effect, punctually rendering values for the instantaneous SNR much larger than the mean value. In that case, increasing the  $K$  factor will reduce the probability of getting SNR values that are greater than the threshold.

Similarly, a high correlation factor gives a better performance for low values of  $\bar{\gamma}$ ,

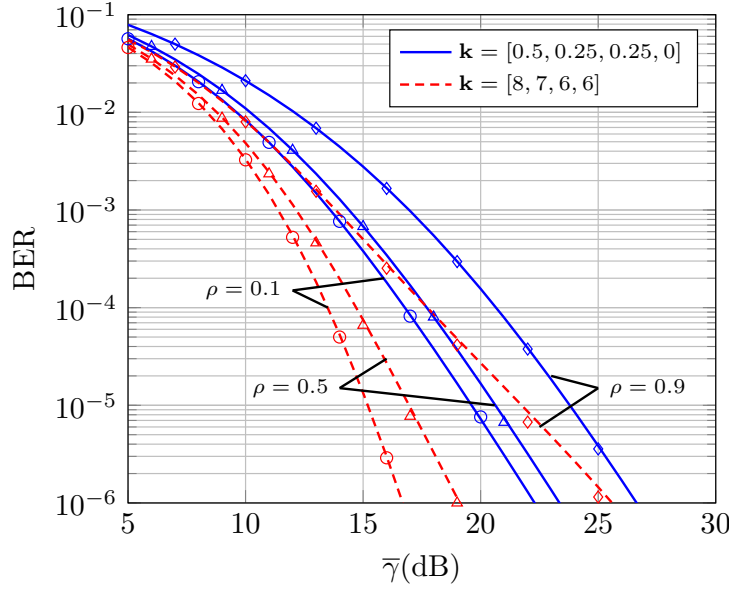


FIGURE 3.9: BER vs.  $\bar{\gamma}$  for 16-QAM,  $P = 4$  and different values of  $\rho$  and  $\mathbf{k}$ . Solid lines correspond to theoretical calculation with  $m = 40$  for  $\mathbf{k} = (0.5, 0.25, 0.25, 0)$  and  $m = 150$  for  $\mathbf{k} = (8, 7, 6, 6)$ , while markers correspond to Monte Carlo simulations.

while the opposite behavior is observed in the high-SNR regime. Similar conclusions are drawn in [99], [100] for large  $\bar{\gamma}$ , but none of these works pay attention to the behavior of  $P_{\text{out}}$  in the low SNR regime.

An interesting behavior is noticed in the case of strongly correlated branches and large  $\bar{\gamma}$ . Regarding Fig. 3.8, we can observe that for  $\rho = 0.9$  a strong LoS implies a considerable degradation of the system performance, being the outage probability asymptotically higher for large values of  $K$ . However, this effect is not observed for lower values of  $\rho$ , i.e., less correlated branches. This behavior is deeply analyzed in [105], where it is shown that, in multiple-input multiple-output (MIMO)-MRC systems, increasing the distinct  $K_i$  factors have a negative impact on the system performance until a certain value,  $K_{\text{th}}$ , is reached, from which  $P_{\text{out}}$  starts to decrease as  $K_i$  increase. In fact, expressions for this threshold are provided in [105, sec. IV-B] under the assumption of identically distributed Rice channels, observing that  $K_{\text{th}}$  depends on the correlation matrix. However, despite this assumption, it is difficult to determine how an arbitrary correlation between branches would impact this turning value of  $K$ .

Finally, the impact of the correlation and of the strength of the LoS in the BER is evaluated in Fig. 3.9, where  $P_b(\bar{\gamma})$  is depicted for 16-QAM and different values of  $\rho$  and  $\mathbf{k}$ . Same conclusions as with the outage probability can be given: negative effect of correlated branches and better performance in general as Rice  $K$  factors increase. However, for values of  $\rho$  close to one, we observe again that increasing the LoS power does not always render a clear benefit. Similar results are observed for distinct values of  $M$ .

## 3.2 Generalizations of the $\kappa$ - $\mu$ shadowed distribution

The auxiliary (confluent) random variables defined in the previous section were used just as simple tools to facilitate the analysis of the original random variable from which they emerge, i.e., we were interested only in the limit behavior of their distributions.

However, these auxiliary random variables can also be interesting by themselves. For instance, in channel modeling, the addition of a random fluctuation to a variable representing the fading can be used to characterize shadowing at the same time. In fact, this is the same idea from which some generalized fading model arise, e.g., the Rician shadowed and the  $\kappa$ - $\mu$  shadowed models: introducing a random fluctuation in the LoS component in order to better characterize the fluctuations produced by shadowing. To that end, the perturbation is chosen to be gamma distributed because of two main reasons: *i*) its mathematical tractability and *ii*) it has been proved that gamma distribution can be as accurate as lognormal distribution when characterizing shadowing [87], [106].

Although both the Rician shadowed and the  $\kappa$ - $\mu$  shadowed models are in fact generalizations of the classical ones (Rayleigh, Rice), in the context of the analysis through confluence, a  $\kappa$ - $\mu$  shadowed random variable can be seen as the confluent version of a  $\kappa$ - $\mu$  one and the same relationship can be established between the Rician shadowed model and the Rice distribution, though in these cases there is no interest in using the confluence approach since closed-form expressions are known for the distribution of the original variables.

With this idea, two new fading models are proposed in this thesis. The first one, namely the fluctuating Beckmann (FB) distribution, arises as an extension of both the  $\kappa$ - $\mu$  shadowed and the Beckmann distributions. From the point of view of the analysis through confluence, the FB distribution can be seen as the auxiliary variable used to characterize the classical Beckmann model, simplifying its analysis and allowing the derivation of closed-form expressions for its PDF and CDF. Compared to the  $\kappa$ - $\mu$  shadowed model, the FB distribution is a natural generalization by considering the effect of power imbalance in both LoS and non-line-of-sight (NLoS) components, as the Beckmann model does.

The second model here introduced takes advantage of the partial results obtained through the analysis of complex GQFs, generalizing the  $\kappa$ - $\mu$  shadowed distribution by accounting for the impact of the correlation between the contributions of each cluster.

### 3.2.1 The fluctuating Beckmann fading model

This section introduces the very general FB fading model, providing its first and second order statistics as well as discussing the impact of the distinct model parameters on its distribution. A more detailed analysis of this fading model can be found in

[48] P. Ramírez-Espinosa, F. J. López-Martínez, J. F. París, M. D. Yacoub, and E. Martos-Naya, “An extension of the  $\kappa$ - $\mu$  shadowed fading model: Statistical characterization and applications”, *IEEE Trans. Veh. Technol.*, vol. 67, no. 5, pp. 3826–3837, May 2018,

attached in Appendix A.3.

### Physical model

As stated before, the physical model of the FB distribution arises as a generalization of both the  $\kappa$ - $\mu$  shadowed and the Beckmann distribution. Thus, it inherits the clustering structure, i.e., the model is built out of the sum of the square modulus of independent random variables, together with the fluctuating LoS component already present in the physical model of the  $\kappa$ - $\mu$  shadowed distribution. In addition, the FB model also takes into account the effect of the in-phase and quadrature power imbalance in the LoS and NLoS components. Therefore, the received signal amplitude is expressed as

$$R = \left( \sum_{i=1}^{\mu} \|\sigma_x X_i + j\sigma_y Y_i + \xi(p_i + jq_i)\|^2 \right)^{1/2} \quad (3.34)$$

where  $\mu \in \mathbb{N}^+$ ,  $\sigma_x, \sigma_y \in \mathbb{R}^+$  and  $p_i, q_i \in \mathbb{R}$  are constants;  $X_i, Y_i$  for all  $i$  are i.i.d. standard Gaussian random variables, i.e.,  $X_i, Y_i \sim \mathcal{N}(0, 1)$ , and  $\xi$  is a random variable, independent of  $X_i$  and  $Y_i$ , such that  $\xi^2$  is gamma distributed<sup>2</sup> with shape parameter  $m$  and  $\mathbb{E}[\xi^2] = 1$ , i.e.,  $\xi^2 \sim \Gamma(m, 1/m)$ .

As in other generalized fading models,  $\xi$  in (3.34) accounts for the fluctuation of the LoS component, being controlled by the parameter  $m$ . Thus, this fluctuation is less severe as  $m$  increases. On the other hand, as opposed to the  $\kappa$ - $\mu$  shadowed model, the FB model considers that the in-phase and quadrature components ( $X_i$  and  $Y_i$ ) can have different variances, namely  $\sigma_x^2$  and  $\sigma_y^2$ . This allows to characterize the effect of power imbalance in the diffuse components associated to NLoS propagation. Similarly, it can also be considered that the power of the LoS components can be imbalanced. Hence, the physical model in (3.34) can be also regarded as a generalization of the Beckmann fading model through the consideration of clustering and LoS fluctuation.

Due to its generality, the FB distribution inherits the parametrization from both the Beckmann model and the  $\kappa$ - $\mu$  shadowed model, being completely described by parameters  $m, \mu$  and

$$\kappa = \frac{\sum_{i=1}^{\mu} p_i^2 + q_i^2}{\mu(\sigma_x^2 + \sigma_y^2)}, \quad \eta = \frac{\sigma_x^2}{\sigma_y^2}, \quad \varrho^2 = \frac{\sum_{i=1}^{\mu} p_i^2}{\sum_{j=1}^{\mu} q_j^2}. \quad (3.35)$$

<sup>2</sup>or, equivalently,  $\xi$  is Nakagami- $m$  distributed with  $\mathbb{E}[\xi^2] = 1$ .



TABLE 3.1: Connections between the FB fading model and other models in the literature. In order to avoid confusion, FB parameters are underlined. Note that setting  $\kappa = 0$  implies that  $m$  and  $\varrho$  vanish.

Channels	Fluctuating Beckmann Fading Parameters
Rayleigh	$\underline{\kappa} = 0, \underline{\mu} = 1, \underline{\eta} = 1$
Rice	$\underline{\kappa} = K, \underline{\mu} = 1, \underline{m} \rightarrow \infty, \underline{\eta} = 1, \forall \varrho$
Nakagami- $m$	$\underline{\kappa} = 0, \underline{\mu} = m, \underline{\eta} = 1$
Hoyt	$\underline{\kappa} = 0, \underline{\mu} = 1, \underline{\eta} = \eta$
$\eta$ - $\mu$	$\underline{\kappa} = 0, \underline{\mu} = \mu, \underline{\eta} = \eta$
Beckmann	$\underline{\kappa} = K, \underline{\mu} = 1, \underline{m} \rightarrow \infty, \underline{\eta} = \eta, \underline{\varrho} = \varrho$
$\kappa$ - $\mu$	$\underline{\kappa} = \kappa, \underline{\mu} = \mu, \underline{m} \rightarrow \infty, \underline{\eta} = 1, \forall \varrho$
Rician Shadowed	$\underline{\kappa} = \kappa, \underline{\mu} = 1, \underline{m} = m, \underline{\eta} = 1, \forall \varrho$
$\kappa$ - $\mu$ shadowed	$\underline{\kappa} = \kappa, \underline{\mu} = \mu, \underline{m} = m, \underline{\eta} = 1, \forall \varrho$

Parameters  $\kappa$ ,  $\mu$  and  $m$  are analogous to those in the  $\kappa$ - $\mu$  shadowed model, and  $\eta$  and  $\varrho$  are defined as in the Beckmann distribution in order to account for the power imbalance in NLoS and LoS components, respectively. Thus, the FB distribution provides the unification of a large number of important fading distributions. These connections are summarized in Table 3.1, on which the parameters corresponding to the FB distribution are underlined in order to avoid confusion with the parameters of any of the distributions included as special cases.

### First order statistics

A first order characterization of the FB distribution is now provided in terms of its chief probability functions, namely MGF, PDF and CDF. Since fading distributions are usually analyzed in terms of the SNR [18], hereinafter we will consider the random variable

$$\gamma \triangleq \bar{\gamma} \frac{R^2}{\mathbb{E}[R^2]}, \quad (3.36)$$

where  $\mathbb{E}[R^2] = \mu(\sigma_x^2 + \sigma_y^2) + \sum_{i=1}^{\mu} (p_i^2 + q_i^2)$  and  $\bar{\gamma} \triangleq \mathbb{E}[\gamma]$  is the average SNR, representing the instantaneous SNR at the receiver side. Then,  $\gamma$  follows a FB distribution with parameters  $\kappa$ ,  $\mu$ ,  $m$ ,  $\eta$  and  $\varrho$ , and for convenience we denoted it as  $\gamma \sim \mathcal{FB}(\bar{\gamma}; \kappa, \mu, m, \eta, \varrho)$ .

The MGF of the FB fading model can be obtain by conditioning the MGF of the Beckmann distribution [18, eq. (2.38)] on  $\xi$ , after introducing the clustering, and averaging over all the possible values of  $\xi$ , as stated in the following lemma.



**Lemma 3.8** Let  $\gamma \sim \mathcal{FB}(\bar{\gamma}; \kappa, \mu, m, \eta, \varrho)$ . Then, the MGF of  $\gamma$  is given by

$$M_\gamma(s) = \frac{(-1)^\mu \alpha_2^{m-\mu/2}}{s^\mu \bar{\gamma}^\mu \alpha_1^m} \left(1 - \frac{\mu(1+\eta)(1+\kappa)}{2\eta\bar{\gamma}s}\right)^{m-\frac{\mu}{2}} \times \left(1 - \frac{\mu(1+\eta)(1+\kappa)}{2\bar{\gamma}s}\right)^{m-\frac{\mu}{2}} \left(1 - \frac{c_1}{\bar{\gamma}s}\right)^{-m} \left(1 - \frac{c_2}{\bar{\gamma}s}\right)^{-m}, \quad (3.37)$$

where  $c_{1,2}$  are the roots of  $\alpha_1 s^2 + \beta s + 1$  with

$$\alpha_1 = \frac{4\eta}{\mu^2(1+\eta)^2(1+\kappa)^2} + \frac{2\kappa(\varrho^2 + \eta)}{m(1+\varrho^2)\mu(1+\eta)(1+\kappa)^2}, \quad (3.38)$$

$$\beta = \frac{-1}{1+\kappa} \left[ \frac{2}{\mu} + \frac{\kappa}{m} \right], \quad (3.39)$$

and  $\alpha_2$  is calculated as

$$\alpha_2 = \frac{4\eta}{\mu^2(1+\eta)^2(1+\kappa)^2}. \quad (3.40)$$

Analytic expressions are attainable for the PDF and CDF of  $\gamma$  by performing the inverse Laplace transformation to (3.37), as stated in (3.23), and given below.

**Lemma 3.9** Let  $\gamma \sim \mathcal{FB}(\bar{\gamma}; \kappa, \mu, m, \eta, \varrho)$ . Then, the PDF and CDF of  $\gamma$  are given by

$$f_\gamma(\gamma) = \frac{\alpha_2^{m-\mu/2} \gamma^{\mu-1}}{\bar{\gamma}^\mu \Gamma(\mu) \alpha_1^m} \Phi_2^{(4)} \left( \frac{\mu}{2} - m, \frac{\mu}{2} - m, m, m; \mu; \frac{-\gamma}{\bar{\gamma}\sqrt{\eta\alpha_2}}, \frac{-\gamma\sqrt{\eta}}{\bar{\gamma}\sqrt{\alpha_2}}, \frac{-\gamma c_1}{\bar{\gamma}}, \frac{-\gamma c_2}{\bar{\gamma}} \right), \quad (3.41)$$

$$F_\gamma(\gamma) = \frac{\alpha_2^{m-\mu/2} \gamma^\mu}{\bar{\gamma}^\mu \Gamma(\mu+1) \alpha_1^m} \Phi_2^{(4)} \left( \frac{\mu}{2} - m, \frac{\mu}{2} - m, m, m; \mu+1; \frac{-\gamma}{\bar{\gamma}\sqrt{\eta\alpha_2}}, \frac{-\gamma\sqrt{\eta}}{\bar{\gamma}\sqrt{\alpha_2}}, \frac{-\gamma c_1}{\bar{\gamma}}, \frac{-\gamma c_2}{\bar{\gamma}} \right), \quad (3.42)$$

where  $\Phi_2^{(n)}$  is the confluent form of the generalized Lauricella series defined in [107, p. 34].

As observed, the PDF and CDF of the FB distribution are given in terms of the multivariate  $\Phi_2^{(n)}$  function, which also appears in other fading distributions in the literature [29], [31], [108]. Apparently, and because it is defined as an  $n$ -fold infinite summation, its numerical evaluation may pose some challenges from a computational point of view. However, the Laplace transform of the  $\Phi_2^{(n)}$  function has a comparatively simpler form in terms of a finite product of elementary functions, which becomes evident by inspecting the expression of the MGF in (3.37). Therefore, the  $\Phi_2^{(n)}$  function can be evaluated by means of a numerical inverse Laplace transform [109], [110].

Remarkably, as with the  $\kappa$ - $\mu$  and  $\eta$ - $\mu$  models, the statistics of the FB are also valid for  $\mu \in \mathbb{R}^+$ , although the underlying model of random variables in (3.34) loses its meaning. Moreover, when  $\eta = 1$  the effect of the parameter  $\varrho$  vanishes, as can be observed from (3.38); conversely, when setting  $\varrho = 1$  the effect of  $\eta$  is still relevant.

Simple and more tractable expressions can be obtained for the PDF and CDF of the FB distribution under certain conditions. Specifically, if  $m$  and  $\mu$  are assumed to be an integer number and an even number, respectively, (3.37) can be expressed in an alternative form thanks to partial fraction expansion, allowing the derivation of PDF and CDF in terms of elementary functions (i.e., exponentials and powers), as stated next.

**Corollary 3.10** *Let  $\gamma \sim \mathcal{FB}(\bar{\gamma}; \kappa, \mu, m, \eta, \varrho)$  with  $m$  being an integer number and  $\mu$  an even number. Then, the PDF and CDF of  $\gamma$  are given by*

$$f_{\gamma}(\gamma) = \frac{\alpha_2^{m-\frac{\mu}{2}}}{\alpha_1^m \bar{\gamma}^{\mu}} \sum_{i=1}^{N(m,\mu)} e^{-\tau_i \gamma / \bar{\gamma}} \sum_{j=1}^{|\omega_i|} \frac{A_{i,j} \gamma^{j-1}}{(j-1)!}, \quad (3.43)$$

$$F_{\gamma}(\gamma) = 1 + \frac{\alpha_2^{m-\frac{\mu}{2}}}{\alpha_1^m \bar{\gamma}^{\mu}} \sum_{i=1}^{N(m,\mu)} e^{-\tau_i \gamma / \bar{\gamma}} \sum_{j=1}^{|\omega_i|} \frac{B_{i,j} \gamma^{j-1}}{(j-1)!}, \quad (3.44)$$

where  $A_{i,j}$  and  $B_{i,j}$  are the residues arising from performing a partial fraction decomposition in (3.37) after evaluating  $M_{\gamma}(-s)$  and  $M_{\gamma}(-s)/s$ , respectively;  $N(m, \mu) = 2[1 + u(\mu/2 - m)]$  and  $\omega_i$  and  $\tau_i$  are the elements of vectors  $\boldsymbol{\omega}$  and  $\boldsymbol{\tau}$ , defined as

$$\boldsymbol{\omega} = \left[ m, m, \frac{\mu}{2} - m, \frac{\mu}{2} - m \right], \quad (3.45)$$

$$\boldsymbol{\tau} = \left[ c_1, c_2, \frac{\mu(1+\eta)(1+\kappa)}{2\eta}, \frac{\mu(1+\eta)(1+\kappa)}{2} \right]. \quad (3.46)$$

### Second order statistics

First-order statistics (e.g., PDF and CDF) provide valuable information about the statistical behavior of the amplitude (or, equivalently, power) of the received signal affected by fading. However, they do not incorporate information related to the dynamic behavior of the fading process, which is of paramount relevance in the context of wireless communications because of the relative motion of transmitter, receivers and scatterers due to mobility. In the literature, two metrics are used to capture the dynamics of a general random process: *i*) the level crossing rate (LCR), which measures how often the amplitude of the received signal crosses a given threshold value, and *ii*) the average fade duration (AFD), which measures how long the amplitude of the received signal remains below this threshold.

In the calculation of both statistics (LCR and AFD), we assume that the fluctuations in the diffuse part (i.e., NLoS) occur at a smaller scale compared to those of the LoS component. This is the case, e.g., where such LoS fluctuation (represented by the random variable  $\xi$ ) is associated to shadowing, which is classically considered to occur at a larger scale than fading.

The LCR of the received signal amplitude  $R$  can be computed using Rice's formula [111] as

$$N_R(u) = \int_0^\infty \dot{r} f_{R,\dot{R}}(u, \dot{r}) d\dot{r}, \quad (3.47)$$

where  $\dot{R}$  denotes the time derivative of the signal envelope and  $f_{R,\dot{R}}(r, \dot{r})$  is the joint PDF of the received signal amplitude and its time derivative. Although an analytic expression for  $N_R(u)$  have been obtained, it is given in terms of a two-fold integral which considerably reduces its usefulness.

It is possible to arrive at a more tractable expression for a simpler yet general case by considering the scenario in which in-phase and quadrature components are independent. Independence between in-phase and quadrature components can be achieved by assuming  $q_i = 0$  and  $p_i \neq 0$  or vice-versa in (3.34), leading to a simpler underlying model that eases the analysis. Note, however, that such a scenario is still a FB fading model, and does not bear any similarity with other previous models published in the literature. Therefore, assuming the case  $q_i = 0 \forall i$  (a similar expression is obtained for  $p_i = 0 \forall i$ ), the physical model in (3.34) can be decomposed as

$$R^2 = \sum_{i=1}^{\mu} (\sigma_x X_i + \xi p_i)^2 + \sum_{k=1}^{\mu} \sigma_y^2 Y_i^2, \quad (3.48)$$

facilitating the calculation of the LCR, which is ultimately given by

$$\begin{aligned} N_R(u) &= \frac{m^m [\mu(1+\eta)(1+\kappa)]^{\mu-1/2} \sqrt{-\ddot{\rho}(0)}}{2^{\mu-1} \Gamma^2(\mu/2) \eta^{\mu/2} (\frac{\mu\kappa(1+\eta)}{2\eta} + m)^m \sqrt{2\pi}} \cdot u^{(2\mu-1)} \exp\left(-\frac{\mu}{2}(1+\eta)(1+\kappa)u^2\right) \\ &\times \int_0^1 [1 + (\eta-1)x]^{\frac{1}{2}} (1-x)^{\mu/2-1} x^{\mu/2-1} \exp\left(-\frac{\mu(1-\eta^2)(1+\kappa)}{2\eta} u^2 x\right) \\ &\times {}_1F_1\left(m, \mu/2; \frac{\frac{\kappa\mu^2(1+\eta)^2(1+\kappa)}{4\eta^2}}{\frac{\mu\kappa(1+\eta)}{2\eta} + m} u^2 x\right) dx \end{aligned} \quad (3.49)$$

where  $\Omega = \mathbb{E}[R^2]$  and  $\ddot{\rho}(0)$  is the second derivative of the temporal autocorrelation function evaluated at 0.

Note that, although (3.49) is also in integral form, it can be easily computed due to the bounded integral limits and the integrand behavior. Moreover, despite the assumption  $q_i = 0$ , (3.49) is also valid for  $p_i = 0 \forall i$  and  $q_i \neq 0$  by just setting  $\eta \rightarrow 1/\eta$ , since both cases are equivalent as can be observed from (3.34).

Finally, with the knowledge of the LCR, the AFD is straightforwardly calculated as

$$T_R(u) = \frac{F_R(u)}{N_R(u)} \quad (3.50)$$

where  $F_R(u)$  is the CDF of the received signal amplitude, which can be derived from (3.42) after a simple change of variables.

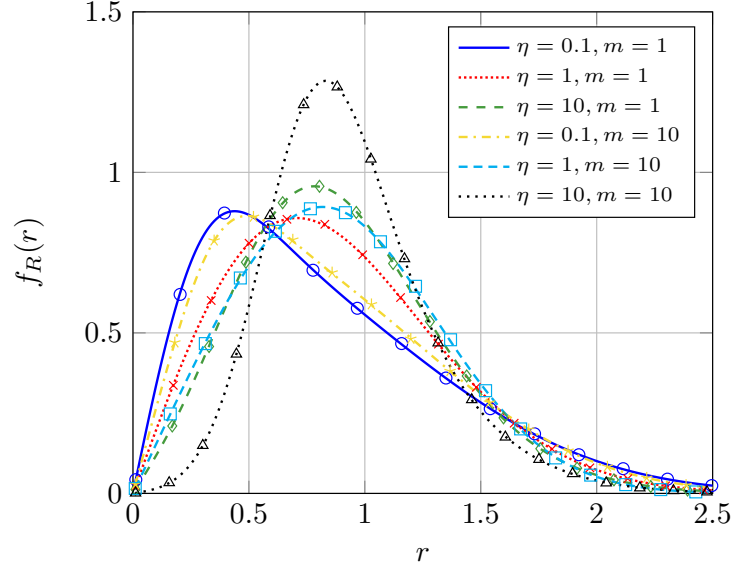


FIGURE 3.10: FB signal envelope distribution for different values of  $\eta$  and  $m$  in weak LoS scenario ( $\kappa = 1$ ) with  $\varrho = 0.1$ ,  $\mu = 1$  and  $\Omega = \mathbb{E}[R^2] = 1$ . Solid lines correspond to the exact PDF, while markers correspond to Monte Carlo simulations.

### Numerical results and discussion

After attaining a full statistical characterization of the newly proposed distribution, we now exemplify the influence of the distinct parameters of the FB model over the distribution of the received signal amplitude,  $R$ , in Figs. 3.10-3.12 and over the second order statistics in Figs. 3.13-3.14. Note that the PDF of  $R$  can be directly obtained from (3.41) as  $f_R(r) = 2r\frac{\bar{\gamma}}{\Omega}f_{\gamma}(\bar{\gamma}r^2/\Omega)$ . In addition, in order to double-check the validity of the theoretical expressions, Monte Carlo simulations are also provided.

We will focus on understanding the effect of the power imbalance in the LoS and NLoS components (i.e., the effect of  $\varrho$  and  $\eta$ ), since these are the two parameters that effectively extend the original  $\kappa$ - $\mu$  shadowed fading model to a more general case. To that end, Fig. 3.10 represents the PDF of  $R$  for different values of  $\eta$  with mild and strong LoS fluctuation ( $m = 10$  and  $m = 1$ , respectively) and  $\mu = 1$ . The parameter  $\varrho$  is set to  $\varrho^2 = 0.1$ , indicating a moderately large LoS power imbalance. In fact,  $\varrho^2 = 0.1$  specifies that the in-phase component of the LoS is 10 times more powerful than the quadrature one.

With this parameters choice, it can be observed from Fig. 3.10 that the effect of increasing  $\eta$  causes the amplitude values to be more concentrated around its mean value. Besides, compared to the case of  $\eta = 1$  (i.e., the  $\kappa$ - $\mu$  shadowed fading distribution), the effect of having a power imbalance in the NLoS component clearly has an impact on the distribution of the signal envelope. Interestingly, in contrast to the  $\eta$ - $\mu$  fading model, the behavior of the distribution with respect to  $\eta$  is no longer symmetrical between  $\eta \in [0, 1]$  and  $\eta \in [1, \infty)$  for a fixed  $\varrho^2 \neq 1$ . In fact, one interesting effect comes from the observation of the effect of increasing  $\eta$ : both setting  $\eta = 0.1$  or  $\eta = 10$  implies that the NLoS

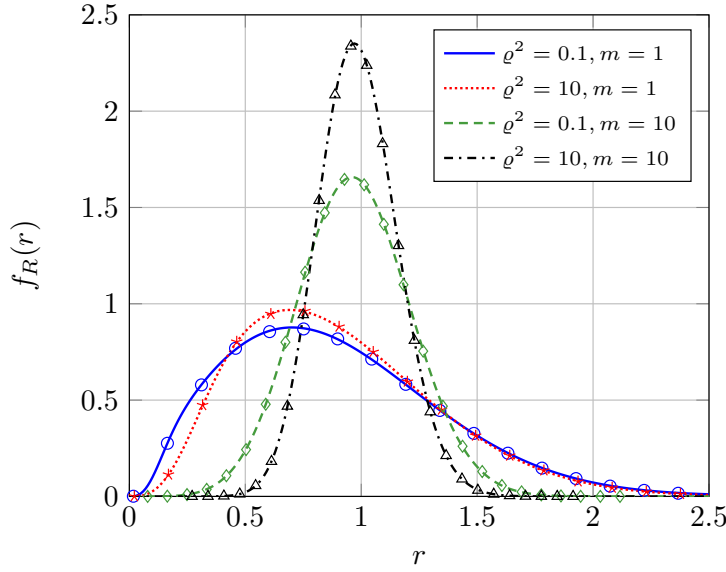


FIGURE 3.11: FB signal envelope distribution for different values of  $\varrho$  and  $m$  in strong LoS scenario ( $\kappa = 10$ ) with  $\eta = 0.1$ ,  $\mu = 2$  and  $\Omega = \mathbb{E}[R^2] = 1$ . Solid lines correspond to the exact PDF, while markers correspond to Monte Carlo simulations.

power is imbalanced by a factor of 10. However, it is evident that if this NLoS imbalance goes to the component associated with a larger LoS imbalance ( $\eta = 0.1$  since  $\varrho^2 = 0.1$ ), this is much more detrimental for the received signal envelope than having the NLoS imbalance in the other component.

Fig. 3.11 focuses now on the impact of the LoS power imbalance, depicting the PDF of the received signal amplitude for different values of  $\varrho$  and  $m$  with  $\kappa = 10$  (i.e., strong LoS scenario),  $\mu = 2$  and  $\eta = 0.1$ . Because the LoS component is now much more relevant, the effect of changing  $m$  is more noticeable. It is noticed that low values of  $\varrho$  and  $m$  cause the amplitude values being more sparse. Also, the same behavior as with  $\eta$  is observed for varying  $\varrho$ , i.e., having the LoS imbalance in the opposite component as in the NLoS (in this case, since  $\eta = 0.1$ , it is obtained for  $\varrho^2 = 10$ ) makes the amplitude values being more concentrated around its mean value than in the case where the imbalance of both LoS and NLoS is in the same component, i.e.,  $\eta = 0.1$  and  $\varrho^2 = 0.1$ .

Remarkably, a bimodal behavior is observed as the imbalance is reduced through  $\varrho$  or  $\eta$ , as observed in Fig. 3.12. When both  $\varrho$  and  $\eta$  decrease, the in-phase components have considerably less power than the quadrature components. Because  $\kappa$  is sufficiently large, the distribution will mostly fluctuate close to the LoS part of the quadrature component due to the low value  $m$ , and the first maximum on the PDF in the low-amplitude region appears as the highly imbalanced in-phase component only is able to contribute in this region. We must note that this bimodal behavior does not appear in the original  $\kappa$ - $\mu$  shadowed or Beckmann distributions from which the FB distribution originates. Nevertheless, such bimodality indeed appears in other fading models [31], [112].

Finally, the effect of the FB parameters in the second order statistics (LCR and AFD)

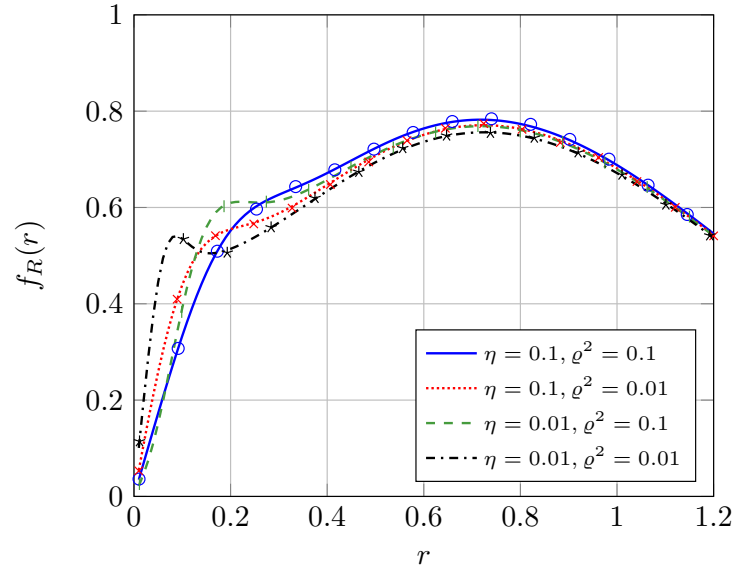


FIGURE 3.12: FB signal envelope distribution for different values of  $\varrho$  and  $\eta$  in strong LoS scenario ( $\kappa = 10$ ) with  $m = 1$ ,  $\mu = 1$  and  $\Omega = \mathbb{E}[R^2] = 1$ . Solid lines correspond to the exact PDF, while markers correspond to Monte Carlo simulations.

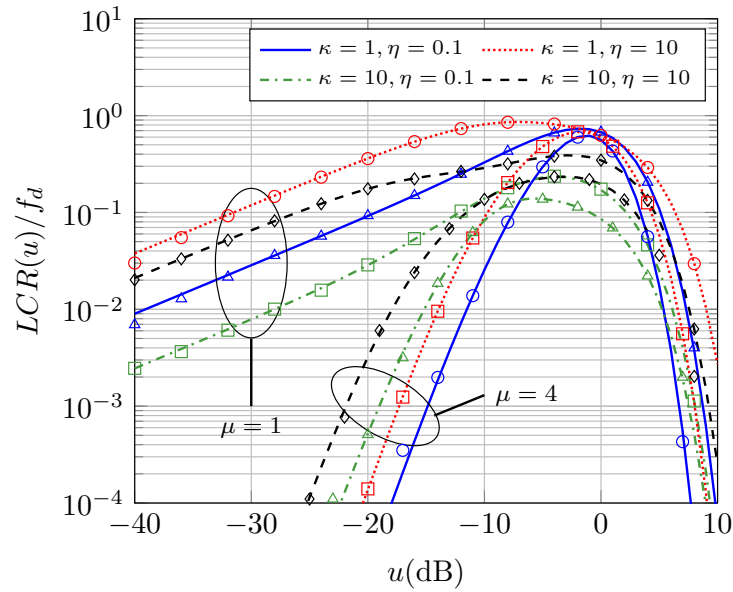


FIGURE 3.13: Normalized LCR vs threshold value  $u$ (dB) for different values of  $\kappa$ ,  $\eta$  and  $\mu$ , with  $m = 1$ ,  $\varrho \rightarrow \infty$  and  $\Omega = \mathbb{E}[R^2] = 1$ . Solid lines correspond to theoretical calculations, while markers correspond to Monte Carlo simulations.

is investigated in Figs. 3.13-3.14. We assume a time variation of the diffuse component according to Clarke's correlation model [17, sec. 2.1.1] with maximum Doppler shift  $f_d$ , implying that  $\sqrt{-\ddot{\rho}(0)} = \sqrt{2}f_d\pi$  [113, eq. (34)]. We also consider that  $\varrho^2 \rightarrow \infty$ , so the LCR and AFD are calculated as in (3.49) and (3.50). Also, a sampling period  $T_s \gg f_d$  is assumed in Monte Carlo simulations in order to avoid missing level crossings at very low threshold values.

Thus, Fig. 3.13 represents the LCR vs the normalized threshold,  $u$ , for different values

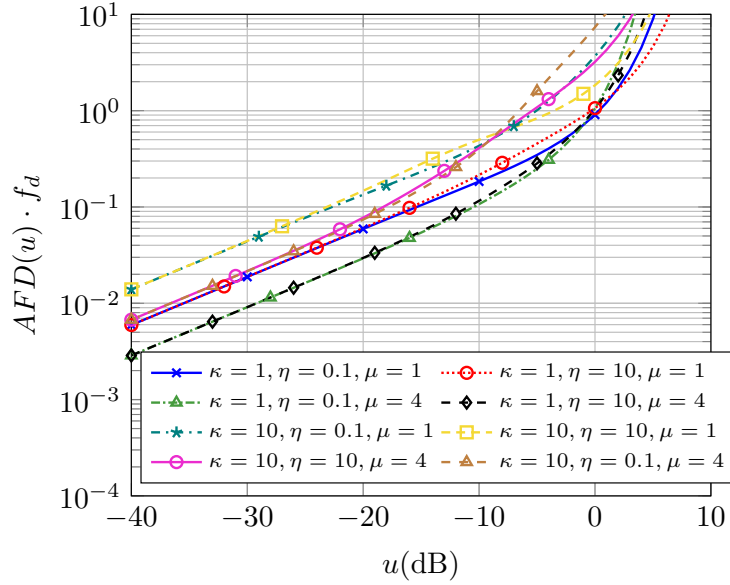


FIGURE 3.14: Normalized AFD vs threshold value  $u(\text{dB})$  for different values of  $\kappa$ ,  $\eta$  and  $\mu$ , with  $m = 1$ ,  $\varrho \rightarrow \infty$  and  $\Omega = \mathbb{E}[R^2] = 1$ . Solid lines correspond to theoretical calculations, while markers correspond to Monte Carlo simulations.

of the FB model parameters. Interestingly, when increasing  $\mu$ , the number of crossings at very low threshold values is drastically reduced. Similarly, the number of crossings in this region grows when reducing  $\kappa$  or increasing  $\eta$ . This latter effect is coherent with the fact that  $\varrho \rightarrow \infty$  in this case, so that having a value of  $\eta < 1$  reduces the fading severity.

The beneficial impact of increasing  $\mu$  is also observed in Fig. 3.14, in which lower values of  $\mu$  render a larger duration of deep fades. Remarkably, for very low  $u$ , the AFD seems to be independent of the values of  $\eta$ .

### 3.2.2 The $\kappa$ - $\mu$ shadowed fading model with intercluster correlation

This section introduces the second generalization of the  $\kappa$ - $\mu$  shadowed fading model proposed in this thesis, showing that this new distribution is closely related to the auxiliary random variables in (3.17) we used to analyze complex GQFs. The physical model of the distribution is given, along with simple closed-form expressions for its first order statistics, namely PDF, CDF and MGF.

The results provided in the following are a summary of those given in

[49] P. Ramírez-Espinosa, J. F. París, J. A. Cortés, and E. Martos-Naya, “The  $\kappa$ - $\mu$  shadowed fading model with arbitrary intercluster correlation”, in *2018 15th Int. Symp. Wireless Commun. Syst. (ISWCS)*, Aug. 2018, pp. 1–5,

attached in Appendix A.4.



### Physical model

The physical model of this new fading distribution arises as a generalization of the physical model of the original  $\kappa$ - $\mu$  shadowed distribution in (2.99). Thus, the received signal power is modeled as the sum of the squared modulus of  $\mu$  Gaussian random variables (clustering structure) whose means randomly fluctuates. The power of each variable is assumed to be the same. However, as opposed to the original model, we here assume that these diffuse waves, i.e., the underlying Gaussian variables, are correlated, introducing an arbitrary correlation factor for the intercluster components. Hence, while the FB model extends the  $\kappa$ - $\mu$  shadowed distribution by considering the power imbalance in the LoS and NLoS, this newly proposed model maintains the restriction of equal powers for the in-phase and quadrature components but takes into account the possibility of the distinct contributions of each cluster to be correlated. Therefore, we consider appropriate to name this extension as correlated  $\kappa$ - $\mu$  shadowed fading model.

The received signal amplitude under correlated  $\kappa$ - $\mu$  shadowed fading can then be written as

$$R = \left( \sum_{i=1}^{\mu} \|Z_i + \xi p_i\|^2 \right)^{1/2}, \quad (3.51)$$

where  $\mu \in \mathbb{N}^+$  is the same parameter as in previous models,  $p_i$  for  $i = 1, \dots, \mu$  is a complex number representing the LoS contribution and  $Z_i$  are complex Gaussian random variables such that  $Z_i \sim \mathcal{CN}(0, \sigma^2)$ . As in the  $\kappa$ - $\mu$  shadowed and the FB distributions,  $\xi$  is a random variable, independent of  $Z_i$ , such that  $\xi^2 \sim \Gamma(m, 1/m)$  with  $\mathbb{E}[\xi^2] = 1$ , which accounts for the random fluctuations of the LoS component due to shadowing. The novelty is that the distinct  $Z_i$  can be correlated with correlation coefficient  $\text{corr}(Z_i, Z_j) = \rho_{i,j}$  for  $i, j = 1, \dots, \mu$  with

$$\rho_{i,j} = \frac{\mathbb{E}[Z_i Z_j^\dagger]}{\sigma^2}. \quad (3.52)$$

Note that, if  $\rho_{i,j} = 0 \ \forall i \neq j$ , then (3.51) becomes the original  $\kappa$ - $\mu$  shadowed physical model. Equivalently, if we consider the vector  $\mathbf{z} \in \mathbb{C}^{\mu \times 1}$  with entries  $Z_i$ , then  $\mathbf{z} \sim \mathcal{CN}_\mu(\mathbf{0}_{\mu \times 1}, \sigma^2 \mathbf{R})$  with  $\mathbf{R}$  the correlation matrix, i.e.,  $(\mathbf{R})_{i,j} = \rho_{i,j}$ .

Regarding (3.51), it can be observed that, when conditioned on  $\xi$ ,  $R^2$  is a particular case of the complex quadratic form in (2.52) in which  $\mathbf{A} = \mathbf{I}_\mu$ . Therefore, applying the same procedure as described in Section 2.3.1 for complex GQFs,  $R$  is rewritten as

$$R = \left( \sum_{i=1}^{\mu} \left\| \sqrt{\lambda_i} \sigma \tilde{Z}_i + \xi \sqrt{\lambda_i} \tilde{p}_i \right\|^2 \right)^{1/2}, \quad (3.53)$$

where  $\tilde{Z}_i \sim \mathcal{CN}(0, 1)$ ,  $\tilde{p}_i$  are the entries of the vector  $\tilde{\mathbf{p}} = \mathbf{U}^\dagger \mathbf{C}^{-1} \mathbf{p}$  with  $\mathbf{p} = (p_1, \dots, p_\mu)^T$ ,  $\lambda_i$  are the eigenvalues of  $\mathbf{C}^\dagger \mathbf{C}$  (i.e., those of  $\mathbf{R}$ ) and  $\mathbf{U}$  is a unitary matrix whose  $i$ -th column is the eigenvector of  $\mathbf{C}^\dagger \mathbf{C}$  associated with  $\lambda_i$ .



### Statistical characterization

As with the FB distribution, we provide the statistical characterization of the correlated  $\kappa$ - $\mu$  shadowed fading model based on the instantaneous SNR random variable  $\gamma = \bar{\gamma}R^2/\mathbb{E}[R^2]$ , with  $\bar{\gamma}$  denoting the average SNR at the receiver side and  $\mathbb{E}[R^2] = \mu\sigma^2 + \sum_{i=1}^{\mu} \|p_i\|^2$ . Therefore, we say that  $\gamma$  follows a correlated  $\kappa$ - $\mu$  shadowed distribution with parameters  $\kappa = \sum_{i=1}^{\mu} \|p_i\|^2/(\mu\sigma^2)$ ,  $\mu$ ,  $m$  and  $\mathbf{R}$ , i.e.,  $\gamma \sim \mathcal{CS}_{\kappa\mu}(\bar{\gamma}; \kappa, \mu, m, \mathbf{R})$ . Moreover, aiming to relay the mathematical complexity of the newly proposed fading model, we assume that both  $m$  and  $\mu$  are positive integer numbers, i.e., the proposed model inherits the formulation given in [30].

We will focus first on the MGF of  $\gamma$ . Since, conditioned on  $\xi$ ,  $R^2$  is a specific complex GQF, the conditioned MGF is straightforwardly obtained from (2.66). Then, the unconditional MGF is derived by averaging over  $\xi$ , as given next.

**Lemma 3.11** *Let  $\gamma \sim \mathcal{CS}_{\kappa\mu}(\bar{\gamma}; \kappa, \mu, m, \mathbf{R})$ . Then, its MGF reads as*

$$M_{\gamma}(s) = \frac{\mu^{\mu}(\kappa+1)^{\mu}}{\prod_{i=1}^{\mu} (\mu(\kappa+1) - s\lambda_i\bar{\gamma})} \left( 1 - \frac{1}{m} \sum_{j=1}^{\mu} \frac{d_j \lambda_j s \bar{\gamma}}{\mu(\kappa+1) - s\lambda_j\bar{\gamma}} \right)^{-m} \quad (3.54)$$

where  $d_i = \|\tilde{p}_i\|^2/\sigma^2$ .

It is easy to prove that, when no correlation is applied ( $\mathbf{R} = \mathbf{I}_{\mu}$ ), then  $\lambda_i = 1$  for  $i = 1, \dots, \mu$ , so (3.54) becomes the MGF of the original  $\kappa$ - $\mu$  shadowed distribution in [29, eq. (5)].

We observe that (3.54) has a very similar form to the MGF of the auxiliary variables that were used to analyze complex GQFs in (3.18). In fact, (3.54) also admits a formulation in terms of a rational function as

$$M_{\gamma}(s) = \frac{\mu^{\mu}(\kappa+1)^{\mu}}{(-\bar{\gamma})^{\mu} \left( 1 + \sum_{k=1}^{\mu} d_k/m \right)^m} \frac{\prod_{j=1}^{\mu} \left( s - \frac{\mu(\kappa+1)}{\lambda_j\bar{\gamma}} \right)^{m-1}}{\prod_{l=1}^{\mu} \lambda_l \prod_{i=1}^{n_{\beta}} (s - \beta_i)^{q_i m}}. \quad (3.55)$$

where  $\beta_i$  for  $i = 1, \dots, n_{\beta}$  are the distinct roots, with multiplicities  $q_i$ , of the  $\mu$ -th order polynomial given by

$$P(s) = m \prod_{i=1}^{\mu} \left( 1 - \frac{\lambda_i \bar{\gamma}}{\mu(\kappa+1)} s \right) - \sum_{j=1}^{\mu} \frac{d_j \lambda_j \bar{\gamma}}{\mu(\kappa+1)} s \prod_{\substack{k=1 \\ k \neq j}}^{\mu} \left( 1 - \frac{\lambda_k \bar{\gamma}}{\mu(\kappa+1)} s \right). \quad (3.56)$$

Thus, from (3.55), both the PDF and CDF of  $\gamma$  can be obtained by following the same steps as in previous sections, i.e., performing a partial fraction expansion and using the Laplace transform pairs in (3.23). The results are stated in the following lemma.

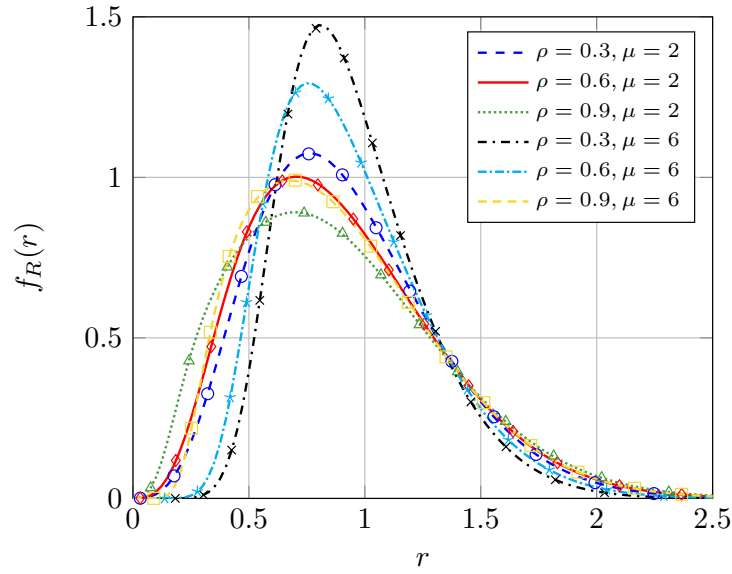


FIGURE 3.15: Signal envelope distribution for different values of  $\mu$  and  $\rho$  with  $\kappa = 1$ ,  $m = 1$  and  $\mathbb{E}[R^2] = 1$ . Solid lines correspond to the exact PDF while markers correspond to Monte Carlo simulations.

**Lemma 3.12** Let  $\gamma \sim \mathcal{CS}_{\kappa\mu}(\bar{\gamma}; \kappa, \mu, m, \mathbf{R})$ . Then, its PDF and CDF are given by

$$f_{\gamma}(\gamma) = \alpha \sum_{i=1}^{n_{\beta}} \sum_{j=1}^{q_i m} A_{i,j} \gamma^{j-1} e^{-\beta_i \gamma}, \quad (3.57)$$

$$F_{\gamma}(\gamma) = 1 + \alpha \sum_{i=1}^{n_{\beta}} \sum_{j=1}^{q_i m} C_{i,j} \gamma^{j-1} e^{-\beta_i \gamma}, \quad (3.58)$$

with

$$\alpha = \frac{\mu^{\mu}(\kappa + 1)^{\mu}}{\bar{\gamma}^{\mu} \Gamma(j)} \left( 1 + \sum_{j=1}^{\mu} \frac{d_j}{m} \right)^{-m} \prod_{l=1}^{\mu} \lambda_l^{-1} \quad (3.59)$$

and  $A_{i,j}$  and  $C_{i,j}$  the residues arising from performing a partial fraction expansion in (3.55) after evaluating  $M_{\gamma}(-s)$  and  $M_{\gamma}(-s)/s$ , respectively.

As can be observed, very simple expressions for the statistics of the newly proposed model are given, being suitable for the further analytic purposes when analyzing systems performance. Remarkably, (3.57) and (3.58) have a similar form to those presented in [30] for the original  $\kappa$ - $\mu$  shadowed distribution, and hence the larger generality introduced does not come at the price of an increased mathematical complexity.

## Numerical Results

We aim now to exemplify the impact of the intercluster correlation matrix in the distribution of the received signal amplitude since it is the parameter that effectively extends the original  $\kappa$ - $\mu$  shadowed model. Note that, as with the FB distribution, the PDF of  $R$  is easily obtained from (3.57) by applying a simple change of variables. As usually

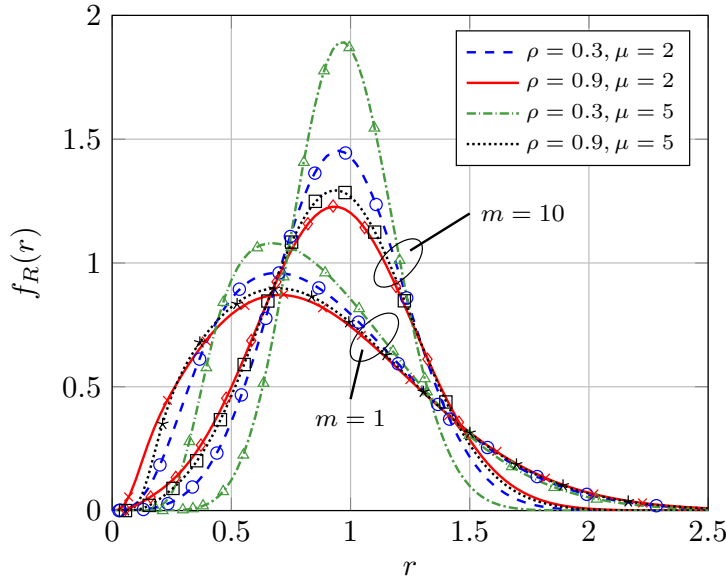


FIGURE 3.16: Signal envelope distribution for different values of  $\mu$ ,  $\rho$  and  $m$  with  $\kappa = 4$  and  $\mathbb{E}[R^2] = 1$ . Solid lines correspond to the exact PDF while markers correspond to Monte Carlo simulations.

done throughout this thesis, we again assume that the correlation matrix  $\mathbf{R}$  is exponential in order to simplify the presentation of the results, i.e.,  $(\mathbf{R})_{i,j} = \rho^{|i-j|}$  with  $0 \leq \|\rho\| < 1$ . With this consideration, Figs. 3.15-3.16 depict the distribution of the received signal amplitude for different values of the model parameters.

Thus, Fig. 3.15 shows the PDF of  $R$  for distinct values of  $\mu$  and  $\rho$  in a weak LoS scenario ( $\kappa = 1$ ) with heavily fluctuating dominant component ( $m = 1$ ). It is observed that large values of  $\rho$ , i.e., more correlation between the components of each cluster, always render more sparse values of the signal amplitude, with independence of the value of  $\mu$ .

A stronger LoS component is considered in Fig. 3.16, where the impact of  $m$  is also taken into account. It can be noticed that the impact of  $\rho$  is slightly less relevant in this case, which is a coherent result since the correlation only affects to the scattering according to the physical model in (3.51). Moreover, the impact of  $\rho$  in the received signal amplitude distribution seems to be independent of the value of  $m$ . However, a severe fluctuation of the dominant component (corresponding to lower values of  $m$ ) is more detrimental for the signal envelope, as we already saw in the original model [29], [30].

## Chapter 4

# Conclusions and future work

In this final chapter, the main conclusions that arise from the contributions of this thesis are outlined. Also, some future lines and possible applications of the obtained results are suggested.

### 4.1 Conclusions

A twofold objective has been achieved in this thesis. On the one hand, it has provided simpler approximated expressions than those given in the literature for the distribution of both real and complex GQFs. To that end, a general method to approximate the PDF and CDF of random variables haven been derived, which has been named *analysis through confluence*.

More specifically, the proposed technique allows us to obtain approximating expressions for the first order statistics of a target variable,  $X$ , through the analysis of a suitably defined sequence of variables,  $\{X_m\}$ . This sequence is obtained from  $X$  by perturbing it somehow, i.e., introducing a random fluctuation in the mean or variance of the original variable. The main advantages of this method compared to other solutions available in the literature are: *i)* the resulting expressions *always* represent a valid distribution, and *ii)* any target level of accuracy can be reached with independence of the parametrization of the random variable under analysis.

Before directly apply the analysis through confluence to GQFs, it has been used to provide very general expressions for the PDF and CDF of an arbitrary positive variable in terms of the derivatives of its MGF. Also, it has been shown that these derivatives can be recursively obtained from the derivatives of the CGF. This technique is specially useful when the target MGF is given in terms of the product of easily differentiable functions. In the context of the analysis of GQFs, the following results have been obtained:

- The general expressions for the statistics of positive variables have been particularized to the case of positive definite non-central real GQFs, obtaining simple recursive approximations for the PDF and CDF which outperform the classical solutions.

- Simple closed-form approximants for the statistics of non-central indefinite complex GQFs have been derived, rendering expressions in terms of elementary functions that are suitable for further analytic purposes. Besides, this approximation inherits the properties of the confluence method presented in the thesis.
- To the best of the author's knowledge, very tight approximated expressions for the BER and the outage probability in MRC systems over correlated non-identically distributed Rice fading have been provided for the first time. The results are valid for any number of antennas and for arbitrary correlation between branches.

On the other hand, seeking to unifying the wide variety of existing fading models, two new distributions haven been provided. Both the novel technique to analyze random variables and these two general fading distributions, albeit apparently unconnected, arise in fact from the same underlying methodology. In the context of channel modeling, the contributions are summarized below:

- The versatile Fluctuating Beckmann distribution has been introduced as a generalization of both the  $\kappa$ - $\mu$  shadowed and the Beckmann models. It accounts for the clustering of waves and the fluctuation of the LoS component as the  $\kappa$ - $\mu$  shadowed model and also for the power imbalance between the in-phase and quadrature components, as the Beckmann distribution does. Expressions of its first and second order statistics have been provided, although its PDF and CDF remains in terms of a generalized hypergeometric function. To circumvent this issue, simple expressions are also provided in terms of elementary functions under certain conditions.
- An alternative extension of the  $\kappa$ - $\mu$  shadowed model have been provided, named correlated  $\kappa$ - $\mu$  shadowed fading model since it allows the distinct components arising from each cluster to be arbitrary correlated. Exact closed-form expressions of its first order statistics have been derived, proving that the proposed model is as tractable as Nakagami- $m$  distribution, but much more general.

## 4.2 Future work

As highlighted through this thesis, the proposed method to analyze random variables renders simple and useful approximations when it is suitably applied. Therefore, its usefulness exceeds the analysis of GQFs. In fact, the derived approximants for the statistics of an arbitrary positive random variable could be potentially applied to a considerable number of applications.

Besides, an important future line of work can be the extension of the method to the analysis of more intricate random variables, such as those arising from the sum or product of several variables. In these cases, obtaining expressions for the resulting distribution usually poses a challenge, and the proposed method may simplify the analysis.

Also, due to the fact that most of the involved variables in communications and signal processing are complex, the derived expressions for the PDF and CDF of complex GQFs can be used to analyze multiple systems, e.g. systems with reception diversity, performance analysis of ML estimators or signal detection. The tractability of the proposed expressions can undoubtedly simplify the characterization of these systems, allowing to obtain closed-form expressions for important metrics such as BER and probabilities of detection and false alarm, to mention but a couple of relevant examples.

In the context of diversity systems, a possible future line of work is the extension of the presented analysis to the case of quadratic forms in Gaussian matrices, which naturally arises when multiple antennas are used both at the transmitter and the receiver [105].

Focusing on channel modeling, the analysis through confluence can be applied to the analysis of more general fading models that take into account the multiplicative shadowing, usually referred to as composite models. The analysis of these distributions is usually more difficult, and a general framework to study such a versatile models can simplify the characterization of the joint impact of shadowing and fading. Some preliminary results can already be found in [114].

Finally, the generalized fading models derived in this thesis could lead to systems performance analyses which are valid in a wide variety of propagation conditions, instead of requiring particular expressions for each scenario. Therefore, the scientific community seems to be interested in these type of general models and some results in this context have already been provided [115], [116].



UNIVERSIDAD  
DE MÁLAGA

## Appendix A

# Publications

### A.1 New approximation to distribution of positive random variables applied to Gaussian quadratic forms

[46] P. Ramírez-Espinosa, D. Morales-Jimenez, J. A. Cortés, J. F. París, and E. Martos-Naya, “New approximation to distribution of positive RVs applied to Gaussian quadratic forms”, *IEEE Signal Process. Lett.*, vol. 26, no. 6, pp. 923–927, Jun. 2019.

DOI: 10.1109/LSP.2019.2912295.

#### Abstract

This letter introduces a new approach to the problem of approximating the probability density function (PDF) and the cumulative distribution function (CDF) of a positive random variable. The novel approximation strategy is based on the analysis of a suitably defined sequence of auxiliary variables which converges in distribution to the target variable. By leveraging such convergence, simple approximations for both the CDF and PDF of the target variable are given in terms of the derivatives of its moment generating function (MGF). In contrast to classical approximation methods based on truncated series of moments or cumulants, our approximations always represent a valid distribution and the relative error between variables is independent of the variable under analysis. The derived results are then used to approximate the statistics of positive-definite real Gaussian quadratic forms, comparing our proposed approach with other existing approximations in the literature.





UNIVERSIDAD  
DE MÁLAGA

## A.2 A new approach to the statistical analysis of non-central complex Gaussian quadratic forms with applications

[47] P. Ramírez-Espinosa, L. Moreno-Pozas, J. F. París, J. A. Cortés, and E. Martos-Naya, “A new approach to the statistical analysis of non-central complex Gaussian quadratic forms with applications”, *IEEE Trans. Veh. Technol.*, vol. 68, no. 7, pp. 6734–6746, Jul. 2019. DOI: 10.1109/TVT.2019.2916725.

### Abstract

This paper proposes a novel approach to the statistical characterization of non-central complex Gaussian quadratic forms (CGQFs). Its key strategy is the generation of an auxiliary random variable that replaces the original CGQF and converges in distribution to it. This technique is valid for both definite and indefinite CGQFs and yields simple expressions of the probability density function (PDF) and the cumulative distribution function (CDF) that only involve elementary functions. This overcomes a major limitation of previous approaches, where the complexity of the resulting PDF and CDF does not allow for further analytical derivations. Additionally, the mean square error between the original-CGQF and the auxiliary one is provided in a simple closed-form formulation. These new results are then leveraged to analyze the outage probability and the average bit error rate of maximal ratio combining systems over correlated Rician channels.



UNIVERSIDAD  
DE MÁLAGA

### A.3 An extension of the $\kappa$ - $\mu$ shadowed fading model: statistical characterization and applications

[48] P. Ramírez-Espinosa, F. J. López-Martínez, J. F. París, M. D. Yacoub, and E. Martos-Naya, “An extension of the  $\kappa$ - $\mu$  shadowed fading model: Statistical characterization and applications”, *IEEE Trans. Veh. Technol.*, vol. 67, no. 5, pp. 3826–3837, May 2018.

DOI: 10.1109/TVT.2017.2787204.

#### Abstract

We here introduce an extension and natural generalization of both the  $\kappa$ - $\mu$  shadowed and the classical Beckmann fading models: the Fluctuating Beckmann (FB) fading model. This new model considers the clustering of multipath waves on which the line-of-sight (LoS) components randomly fluctuate, together with the effect of in-phase/quadrature power imbalance in the LoS and non-LoS components. Thus, it unifies a variety of important fading distributions as the one-sided Gaussian, Rayleigh, Nakagami- $m$ , Rician,  $\kappa$ - $\mu$ ,  $\eta$ - $\mu$ ,  $\eta$ - $\kappa$ , Beckmann, Rician shadowed, and the  $\kappa$ - $\mu$  shadowed distribution. The chief probability functions of the FB model, namely probability density function, cumulative distribution function, and moment generating function are derived. The second-order statistics such as the level crossing rate and the average fade duration are also analyzed. These results can be used to derive some performance metrics of interest of wireless communication systems operating over FB fading channels.



UNIVERSIDAD  
DE MÁLAGA

## A.4 The $\kappa$ - $\mu$ shadowed fading model with arbitrary intercluster correlation

[49] P. Ramírez-Espinosa, J. F. París, J. A. Cortés, and E. Martos-Naya, “The  $\kappa$ - $\mu$  shadowed fading model with arbitrary intercluster correlation”, in *2018 15th Int. Symp. Wireless Commun. Syst. (ISWCS)*, Aug. 2018, pp. 1–5.

DOI: 10.1109/ISWCS.2018.8491099.

### Abstract

In this paper, we propose a generalization of the well-known  $\kappa$ - $\mu$  shadowed fading model. Based on the clustering of multipath waves as the baseline model, the novelty of this new distribution is the addition of an arbitrary correlation for the scattered components within each cluster. It also inherits the random fluctuation of the dominant component, which is assumed to be the same for all clusters. Thus, it unifies a wide variety of models: Rayleigh, Rician, Rician shadowed, Nakagami- $m$ ,  $\kappa$ - $\mu$  and  $\kappa$ - $\mu$  shadowed as well as multivariate Rayleigh, Rician and Rician shadowed. The main statistics of the newly proposed model, i.e. moment generating function, probability density function and cumulative density function, are given in terms of exponentials and powers, and some numerical results are provided in order to analyze the impact of the arbitrary intercluster correlation.



UNIVERSIDAD  
DE MÁLAGA

## Appendix B

# Resumen en Castellano

Según el reglamento de doctorado de la Universidad de Málaga, si la memoria de tesis se redacta al completo en inglés, se requiere incluir un breve resumen en castellano donde se reflejen las principales contribuciones de la misma. Nótese, sin embargo, que este anexo no es el propio manuscrito de la tesis sino un sólo resumen para mostrar los resultados más relevantes.

### B.1 Introducción y motivación

El análisis de FCG, o combinaciones lineales de variables gaussianas al cuadrado, es de gran interés en el ámbito de las comunicaciones y el procesamiento de señal debido al incontable número de aplicaciones de este tipo de variables no sólo en dichos campos sino en estadística en general. Por ejemplo, las FCG aparecen en problemas de detección [2], [3], pruebas  $\chi^2$  [4], análisis de filtros adaptativos [6] y problemas de estimación [8].

Las FCG también juegan un papel fundamental en comunicaciones, surgiendo de manera natural en el estudio de distintos esquemas de modulación [9], [10] así como en el análisis de sistemas con diversidad [11]–[14], debido a que la relación señal a ruido (SNR, *signal-to-noise ratio*) a la salida de estos sistemas viene dada por una FCG cuando se asumen ganancias gaussianas en los distintos canales. De hecho, la mayoría de modelos de canal empleados actualmente pueden verse como casos particulares de una forma cuadrática más general, incluyendo tanto los modelos clásicos que surgen de la aplicación del teorema central del límite [17]–[19] como nuevas distribuciones presentadas en los últimos años con el fin de otorgar mayor flexibilidad y un mejor ajuste en escenarios emergentes [28]–[31]. Por tanto, el análisis de las FCG aparece como una solución para el estudio unificado de la mayoría de modelos de canal existentes.

Desafortunadamente, a pesar de su gran número de aplicaciones, no se conocen expresiones cerradas para la distribución de las FCG en el caso general. Es por ello que a lo largo de los años se han ido desarrollando distintas aproximaciones para la función densidad de probabilidad (PDF, *probability density function*) y la función de distribución (CDF, *cumulative distribution function*) de este tipo de variables [4], [5], [11], [69]–[79]. Sin



embargo, todas estas aproximaciones tienen la misma desventaja presente en la mayoría de técnicas clásicas para aproximar la distribución de variables aleatorias: las funciones resultantes no representan una *distribución válida*, i.e., la PDF aproximada puede no tener área unidad y se pueden obtener probabilidades mayores a uno e incluso negativas.

En este contexto, esta tesis tiene un doble objetivo. En primer lugar, se pretende obtener un nuevo método para el análisis de FCG, con el propósito de derivar aproximaciones simples y cerradas para sus estadísticos de primer orden que no presenten el principal inconveniente de los métodos clásicos anteriormente citados. Igualmente, sacando partido de la relación entre los distintos modelos de desvanecimiento y este tipo de variables, se buscan nuevos modelos de canal que generalicen y unifiquen la gran variedad de distribuciones presentes en la literatura.

## B.2 Análisis de variables aleatorias por confluencia

En esta sección se presenta el nuevo método para análisis de variables aleatorias y su aplicación a las variables de interés en esta tesis: las FCG tanto reales como complejas.

### B.2.1 Método propuesto

La mayoría de métodos clásicos para aproximar la distribución de variables aleatorias, entre los que se incluyen la técnica del *saddle-point* [32]–[35], las series de Edgeworth [35]–[38] o las expansiones en términos de polinomios ortogonales [39], presentan el problema anteriormente comentado: no se garantiza que las expresiones obtenidas representen distribuciones válidas. Otras técnicas, como las aproximaciones basadas en mixturas [40]–[45] solventan ese inconveniente, pero la falta de un método general y la complejidad de su aplicación limitan su utilidad.

La técnica aquí propuesta busca, en vez de aproximar los estadísticos de la variable en cuestión por expansiones en series, analizar una secuencia de variables auxiliares que converjan a la variable objetivo en el límite. De esta forma, se garantiza que las funciones obtenidas para cualquier grado de precisión representen distribuciones válidas. Específicamente, dada una variable  $X$ , se busca una secuencia  $\{X_m : m \in \mathbb{N}^+\}$  tal que  $\{X_m\} \Rightarrow X$ , donde  $X_m$  se obtiene introduciendo alguna perturbación aleatoria en  $X$  de modo que se simplifique su análisis.

Como primer ejemplo, se aplicará el método propuesto a la caracterización estadística de variables positivas. Considérese por tanto una variable aleatoria  $X \in \mathbb{R}^+$  con distribución continua y función generadora de momentos (MGF, *moment generating function*)  $M_X(s)$ . Con el fin de aproximar su CDF, se define la secuencia  $\{X_m : m \in \mathbb{N}^+\}$  tal que

$$X_m \triangleq X/\xi_m, \quad (\text{B.1})$$

donde  $\xi_m$  es una variable aleatoria independiente de  $X$  siguiendo una distribución gamma con parámetros  $m$  y  $1/(m-1)$ , i.e.  $\xi_m \sim \Gamma(m, 1/(m-1))$ . Es sencillo comprobar que  $\{\xi_m : m \in \mathbb{N}^+\} \Rightarrow 1$  y por tanto, aplicando el teorema de Slutsky [93, sec. 3.6][55, sec. 1.2], se tiene que  $\{X_m\} \Rightarrow X$ . Es decir, es posible aproximar la CDF de  $X$  por la de  $X_m$

$$F_X(x) = \lim_{m \rightarrow \infty} F_{X_m}(x) = \lim_{m \rightarrow \infty} \sum_{k=0}^{m-1} \frac{(m-1)^k}{x^k k!} \frac{d^k}{ds^k} M_X(s) \Big|_{s=(1-m)/x}. \quad (\text{B.2})$$

En general, la convergencia en CDF no implica el mismo comportamiento para la PDF. Sin embargo, bajo ciertas condiciones [53], la convergencia en distribución también garantiza que las funciones de densidad converjan. En el caso bajo consideración, puede comprobarse como dichas condiciones son válidas, pudiendo por tanto extender el método para aproximar también la PDF de  $X$  como

$$f_X(x) = \lim_{m \rightarrow \infty} f_{X_m}(x) = \lim_{m \rightarrow \infty} \frac{(m-1)^m}{x^{m+1} \Gamma(m)} \frac{d^m}{ds^m} M_X(s) \Big|_{s=(1-m)/x}. \quad (\text{B.3})$$

Finalmente, el error cuadrático medio (MSE, *mean squared error*) normalizado entre  $X$  y la variable auxiliar viene dado por

$$\overline{\epsilon^2} = \mathbb{E}[(X - X_m)^2] / \mathbb{E}[X^2] = (m-2)^{-1}, \quad (\text{B.4})$$

viéndose claro que  $\lim_{m \rightarrow \infty} \overline{\epsilon^2} = 0$ . Nótese, sin embargo, que el MSE no equivale directamente a una medida del error cometido al aproximar la CDF o la PDF, aunque no obstante da información de la similitud entre la variable objetivo y la auxiliar. Por ende, una reducción en el MSE también conlleva una disminución del error cometido al aproximar los estadísticos de  $X$ .

Este método general de análisis de variables basado en secuencias auxiliares obtenidas introduciendo un perturbación en la variable original ha sido denominado como *análisis por confluencia*, ya que se lleva al límite la secuencia auxiliar de variables (nombradas *confluentes*) para converger o *confluir* a la variable original.

La principal dificultad para aplicar esta nueva técnica vendría dada por la complejidad en el cálculo de las derivadas de la MGF. Sin embargo, hay situaciones donde estas derivadas pueden obtenerse de manera sencilla, como es el caso donde  $M_X(s)$  venga dada por el producto de funciones elementales. Bajo estas condiciones, las derivadas de la MGF pueden calcularse recursivamente a partir de las derivadas de su logaritmo como

$$\frac{d^k}{ds^k} M_X(s) = M_X(s) D_k(s) \quad (\text{B.5})$$

con  $D_0(s) = 1$  y

$$D_k(s) = \sum_{j=0}^{k-1} \frac{(k-1)!}{j!(k-j-1)!} g_{k-1-j}(s) D_j(s), \quad k > 1, \quad (\text{B.6})$$

$$g_k(s) = \frac{d^k}{ds^k} g(s) = \frac{d^{k+1}}{ds^{k+1}} \ln M_X(s). \quad (\text{B.7})$$

### B.2.2 Aplicación a FCG reales no centrales

Una vez presentando el método de análisis por confluencia, se va a proceder a su aplicación para el estudio de las FCG, comenzando por el caso de formas reales definidas positivas. Es decir, se buscan expresiones aproximadas para la PDF y CDF de la forma cuadrática

$$Q_R = (\mathbf{x} + \bar{\mathbf{x}})^T \mathbf{A} (\mathbf{x} + \bar{\mathbf{x}}) \quad (\text{B.8})$$

donde  $\bar{\mathbf{x}} \in \mathbb{R}^{n \times 1}$  es un vector constante,  $\mathbf{A} \in \mathbb{R}^{n \times n}$  es una matriz simétrica y *definida positiva* y  $\mathbf{x} \sim \mathcal{N}_n(\mathbf{0}_{n \times 1}, \mathbf{\Sigma})$ .

Dado que  $Q_R$  es definida positiva, es posible aplicar directamente (B.2) y (B.3) para aproximar sus estadísticos, obteniéndose

$$f_{Q_R}(x) \approx \frac{(m-1)^m}{x^{m+1} \Gamma(m)} M_{Q_R} \left( \frac{1-m}{x} \right) D_m \left( \frac{1-m}{x} \right), \quad (\text{B.9})$$

$$F_{Q_R}(x) \approx M_{Q_R} \left( \frac{1-m}{x} \right) \sum_{k=0}^{m-1} \frac{(m-1)^k}{x^k k!} D_k \left( \frac{1-m}{x} \right), \quad (\text{B.10})$$

donde

$$M_{Q_R}(s) = \prod_{i=1}^n \exp \left( \frac{b_i^2 \lambda_i s}{1 - 2\lambda_i s} \right) (1 - 2\lambda_i s)^{-1/2}, \quad \lambda_i \operatorname{Re}\{s\} < 1/2 \quad \forall i, \quad (\text{B.11})$$

$$g_k(s) = \frac{d^{k+1}}{ds^{k+1}} \ln M_{Q_R}(s) = 2^k k! \sum_{j=1}^n \frac{\lambda_j^{k+1} \left[ (k+1)b_j^2 + 1 - 2\lambda_j s \right]}{(1 - 2\lambda_j s)^{k+2}}. \quad (\text{B.12})$$

con  $\lambda_i$  para  $i = 1, \dots, n$  los autovalores de la matrix  $\tilde{\mathbf{A}} = \mathbf{C}^T \mathbf{A} \mathbf{C}$  y  $b_i$  los elementos del vector  $\mathbf{b} = \mathbf{U}^T \mathbf{C}^{-1} \bar{\mathbf{x}}$ , donde  $\mathbf{U}$  es la matriz ortogonal resultante de la diagonalización de  $\tilde{\mathbf{A}}$ .

Con el fin de resaltar las ventajas de las aproximaciones propuestas en (B.9) y (B.10), éstas se van a comparar con otros métodos disponibles en la literatura. En concreto, se consideran las aproximaciones en términos de series infinitas de potencias, de polinomios de Laguerre y de funciones de densidad  $\chi^2$  [4], [70], [71]. Por simplicidad en la presentación de los resultados, se asume que tanto  $\mathbf{A}$  como  $\mathbf{\Sigma}$  son matrices exponenciales, i.e.,  $(\mathbf{A})_{i,j} = \alpha^{|i-j|}$  y  $(\mathbf{\Sigma})_{i,j} = \rho^{|i-j|}$  con  $0 < \alpha, \rho < 1$ .

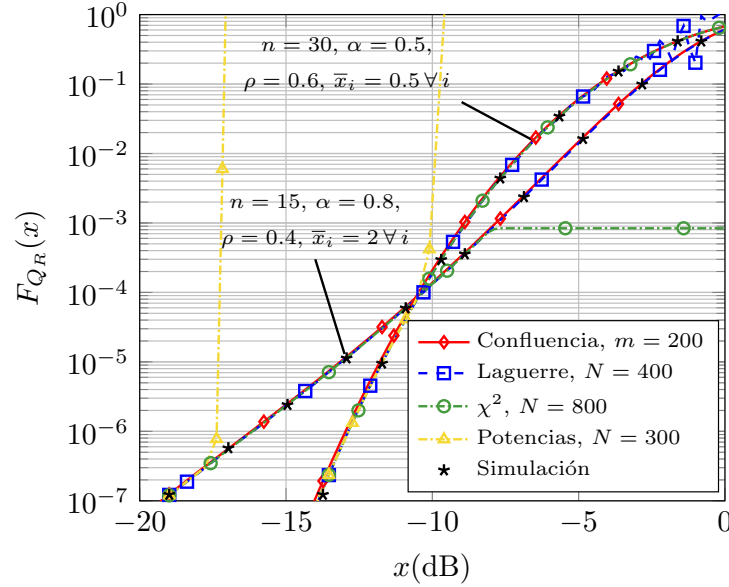


FIGURA B.1: PDF de  $Q_R$  para distintos valores de  $\alpha$ ,  $\rho$  y  $\bar{x}$ . El método propuesto se compara con distintas técnicas alternativas y con simulaciones de Monte Carlo.  $N$  denota el número de términos computados en cada una de las aproximaciones.

Como se observa en la Fig. B.1, las aproximaciones clásicas divergen a partir de determinados valores de  $x$ , obteniendo resultados que claramente no son una CDF válida. Específicamente, las series de potencias tienden a infinito a partir de cierto valor, mientras que la expansión en  $\chi^2$  satura en un determinado valor de probabilidad distinto de uno y la serie en polinomios de Laguerre presenta un carácter oscilatorio para valores de probabilidad cercanos a la unidad. En cambio, la aproximación propuesta en esta tesis se muestra suficientemente precisa con independencia de los valores de los parámetros de la forma cuadrática y del punto donde evaluemos su CDF.

Los comportamientos anteriormente descritos para las aproximaciones clásicas siguen siendo visibles aún aumentando el número de términos de las series, y mostrando una fuerte dependencia con la parametrización de la variable bajo análisis. A ello, se suma la presencia de ciertos parámetros artificiales en las expansiones en términos de  $\chi^2$  y Laguerre que son introducidos para controlar la convergencia de las series, y cuyo valor óptimo se ha comprobado difícil de elegir y dependiente una vez más de los parámetros de la forma cuadrática.

En conclusión, la técnica aquí propuesta se muestra como una opción más robusta que los distintos métodos disponibles en la literatura, permitiendo aproximaciones precisas y garantizando que los resultados obtenidos representan distribuciones válidas.

### B.2.3 Aplicación a FCG complejas no centrales

En esta sección, nuestro método va a aplicarse al análisis de FCG complejas indefinidas y no centrales, i.e. se buscan expresiones para la PDF y CDF de

$$Q_C = (\mathbf{v} + \bar{\mathbf{v}})^\dagger \mathbf{A} (\mathbf{v} + \bar{\mathbf{v}}) \quad (\text{B.13})$$

donde  $\bar{\mathbf{v}} \in \mathbb{C}^{n \times 1}$  es un vector constante,  $\mathbf{A} \in \mathbb{C}^{n \times n}$  es una matriz hermítica y  $\mathbf{v} \sim \mathcal{CN}_n(\mathbf{0}_{n \times 1}, \mathbf{\Sigma})$ .

#### Distribución de $Q_C$

Sacando partido de las particularidades del caso de formas complejas frente a las reales, se va a aplicar el método de análisis por confluencia de una forma ligeramente distinta, de modo que las expresiones resultantes no sean recursivas y sean válidas más allá del caso definido positivo, a diferencia de (B.9) y (B.10).

Con este fin, se adopta una formulación distinta de  $Q_C$ , la cual se obtiene aplicando transformaciones algebraicas a (B.13), resultando

$$Q_C = (\mathbf{s} + \bar{\mathbf{h}})^\dagger \mathbf{\Lambda} (\mathbf{s} + \bar{\mathbf{h}}), \quad (\text{B.14})$$

donde  $\mathbf{s} \sim \mathcal{CN}_n(\mathbf{0}_{n \times 1}, \mathbf{I}_n)$ ,  $\bar{\mathbf{h}} = \mathbf{U}^\dagger \mathbf{C}^{-1} \bar{\mathbf{v}}$  con  $\mathbf{C} \mathbf{C}^\dagger = \mathbf{\Sigma}$  y  $\mathbf{U}, \mathbf{\Lambda}$  son las matrices resultantes de la diagonalización de  $\mathbf{C}^\dagger \mathbf{A} \mathbf{C}$ .

A partir de (B.14), se define la secuencia de variables auxiliares (confluentes) introduciendo la perturbación aleatoria en la media de las gaussianas subyacentes, en lugar de introducirlas en la varianza como en el caso de las formas cuadráticas reales. Así pues, se define  $\{Q_m : m \in \mathbb{N}^+\}$  con

$$Q_m = (\mathbf{s} + \mathbf{D}_\xi \bar{\mathbf{h}})^\dagger \mathbf{\Lambda} (\mathbf{s} + \mathbf{D}_\xi \bar{\mathbf{h}}), \quad (\text{B.15})$$

donde  $\mathbf{D}_\xi \in \mathbb{R}^{n \times n}$  es una matriz diagonal cuyos elementos,  $\xi_{m,i}$  para  $i = 1, \dots, n$ , son variables aleatorias independientes e idénticamente distribuidas tal que  $\xi_{m,i}^2 \sim \Gamma(m, 1/m)$ .

A partir de la MGF de  $Q_m$ , es posible demostrar que  $\{Q_m\} \Rightarrow Q_C$ , pudiendo aproximar nuevamente los estadísticos de  $Q_C$  por los de sus variables confluentes, con la ventaja adicional de que  $Q_m$  admite expresiones cerradas para su PDF y CDF. Con el fin de derivar dichas expresiones, la MGF de  $Q_m$  necesita ser formulada en términos de una función racional, obteniendo

$$M_{Q_m}(s) = B \prod_{i=1}^n \frac{(s - 1/\lambda_i)^{m-1}}{(s - \beta_i)^m} \quad (\text{B.16})$$

con  $\beta_i = [\lambda_i(1 + \mu_i/m)]^{-1}$  y

$$B = \prod_{k=1}^n \left[ -\lambda_k \left( 1 + \frac{\mu_k}{m} \right)^m \right]^{-1}, \quad (\text{B.17})$$

donde  $\lambda_i$  para  $i = 1, \dots, n$  son los elementos de  $\Lambda$  y  $\mu_i = \|\bar{h}_i\|^2$ .

Simplificando la función racional de (B.16) y denotando por  $\tilde{\beta}_i$  y  $1/\tilde{\lambda}_j$  para  $i = 1, \dots, n_\beta$  y  $j = 1, \dots, n_\lambda$  a los distintos polos y ceros resultantes de dicha simplificación, la PDF y la CDF de  $Q_m$  se obtienen directamente aplicando la transformada inversa de Laplace a  $M_{Q_m}(-s)$  y  $M_{Q_m}(-s)/s$ , respectivamente, llegando a

$$f_{Q_C}(x) \approx f_{Q_m}(x) = \sum_{i=1}^{n_\beta} \sum_{j=1}^{p_i} \alpha_{i,j} e^{-\tilde{\beta}_i x} x^{j-1} u(\tilde{\beta}_i x) \operatorname{sgn}(x), \quad (\text{B.18})$$

$$F_{Q_C}(x) \approx F_{Q_m}(x) = u(x) + \sum_{i=1}^{n_\beta} \sum_{j=1}^{p_i} \omega_{i,j} e^{-\tilde{\beta}_i x} x^{j-1} u(\tilde{\beta}_i x) \operatorname{sgn}(x). \quad (\text{B.19})$$

En dichas expresiones,  $u(\cdot)$  representa la función escalón unitario,  $\operatorname{sgn}(\cdot)$  denota la función signo y

$$\alpha_{i,j} = \frac{(-1)^n}{(j-1)!} B A_{i,j}, \quad \omega_{i,j} = \frac{(-1)^n}{(j-1)!} B C_{i,j}, \quad (\text{B.20})$$

con  $A_{i,j}$  y  $C_{i,j}$  los residuos resultantes de descomponer en fracciones simples la función racional en (B.16), una vez evaluada la MGF en los puntos anteriormente indicados.

Para finalizar la caracterización estadística de las FCG complejas no centrales, al igual que se hizo en el caso de variables reales, se proporciona una métrica para el error cometido en la aproximación. En este caso, dado la dificultad de extraer expresiones y cotas útiles para el error cometido entre la CDF real y la aproximada, se proporciona nuevamente el MSE normalizado como medida de la similitud entre la variable original y las confluentes, el cual viene dado por

$$\bar{\epsilon}^2 \triangleq \frac{\mathbb{E}[(Q_m - Q)^2]}{\mathbb{E}[Q^2]} = \frac{\sum_{i=1}^n \lambda_i^2 \mu_i \left[ 4 \left( 1 - \frac{\Gamma(m+1/2)}{m^{1/2} \Gamma(m)} \right) + \frac{\mu_i}{m} \right]}{\sum_{j=1}^n \left( \lambda_j^2 (1 + 2\mu_j) \right) + \left( \sum_{j=1}^n \lambda_j (1 + \mu_j) \right)^2}. \quad (\text{B.21})$$

### Aplicación a sistemas MRC sobre canales Rice correlados

La utilidad de los resultados derivados en la sección anterior se va a ejemplificar a través de su aplicación para el análisis de sistemas MRC (*maximal ratio combining*) sobre canales Rice correlados, obteniendo precisas aproximaciones para la probabilidad de *outage* y la probabilidad de error (BER, *bit error rate*). Bajo estas condiciones, sólo se conocen

resultados asintóticos [97], [98] o resultados parciales limitados a un número de antenas  $P = 2$  [99], [100].

Asumiendo que tanto la sincronización como la estimación del canal son ideales, la SNR a la salida del receptor tras aplicar MRC viene dada por

$$\gamma = \bar{\gamma} \mathbf{g}^\dagger \mathbf{g}, \quad (\text{B.22})$$

donde  $\bar{\gamma}$  es la SNR media en cada rama y  $\mathbf{g} \in \mathbb{C}^{P \times 1}$  es el vector de ganancias del canal. Dado que los desvanecimientos en cada rama siguen una distribución Rice con parámetro  $K_i$  para  $i = 1, \dots, P$ , entonces  $\mathbf{g} \sim \mathcal{CN}_P(\bar{\mathbf{g}}, \mathbf{\Sigma})$ . Los elementos del vector de medias y de la matriz de covarianzas pueden obtenerse a partir de las relaciones

$$\bar{g}_i = \sqrt{\frac{K_i}{K_i + 1}}, \quad (\mathbf{\Sigma})_{i,j} = \sqrt{\frac{1}{(1 + K_i)(1 + K_j)}} (\mathbf{R})_{i,j} \quad (\text{B.23})$$

con  $\mathbf{R}$  la matriz de coeficientes de correlación entre las distintas antenas. Nótese que se están considerando canales normalizados, i.e.  $\mathbb{E}[\|\mathbf{g}_i\|^2] = 1$ .

Como puede observarse, (B.22) es un caso particular de la forma cuadrática en (B.13), y por tanto podemos aplicar los resultados anteriormente derivados para caracterizar  $\gamma$ . Por consiguiente, definiendo  $\gamma_{\text{th}}$  como la SNR mínima requerida para una comunicación fiable, la probabilidad de *outage* puede aproximarse por

$$P_{\text{out}}(\gamma_{\text{th}}) \approx 1 + \sum_{i=1}^{n_\beta} \sum_{j=1}^{p_i} \omega_{i,j} e^{-\tilde{\beta}_i \gamma_{\text{th}} / \bar{\gamma}} \left( \frac{\bar{\gamma}}{\gamma_{\text{th}}} \right)^{-j+1} \quad (\text{B.24})$$

donde  $\omega_{i,j}$ ,  $\tilde{\beta}_i$ ,  $n_\beta$  y  $p_i$  se obtienen por identificación con (B.19).

Igualmente, dado que la BER es una función continua y acotada, se puede explotar la convergencia en distribución entre  $\gamma$  y la variable confluyente empleada para su análisis y obtener una expresión para la BER gracias al teorema de Helly-Bray [55, sec. 1.3], la cual viene dada por

$$\begin{aligned} P_b(\bar{\gamma}) \approx & \sqrt{M} \sum_{i=1}^{n_\beta} \sum_{j=1}^{p_i} \sum_{k=1}^{\sqrt{M}-1} \omega(k) \alpha_{i,j} \left[ \frac{\Gamma(j)}{2\tilde{\beta}_i^j} - \frac{\delta_k \Gamma(j + \frac{1}{2})}{\tilde{\beta}_i^{j+1/2}} \right. \\ & \times \left. \sqrt{\frac{\bar{\gamma}}{2\pi}} {}_2F_1\left(\frac{1}{2}, j + \frac{1}{2}; \frac{3}{2}; \frac{-\delta_k^2}{2\tilde{\beta}_i \bar{\gamma}}\right) \right], \end{aligned} \quad (\text{B.25})$$

donde  $\delta_k = (2k - 1)\sqrt{3/(M - 1)}$ , las constantes  $\omega(k)$  vienen dadas en [102, eqs. (6), (14) and (21)] y  ${}_2F_1(\cdot)$  es la función hipergeométrica de Gauss [50, eq. (15.1.1)].

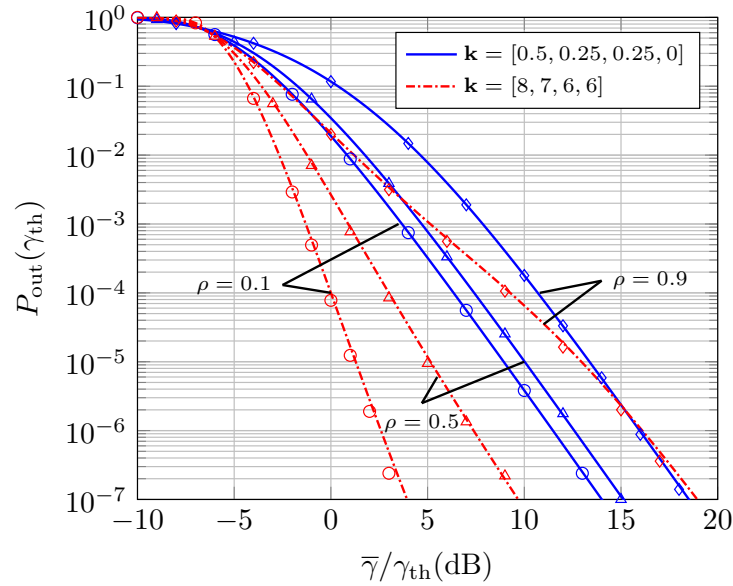


FIGURA B.2:  $P_{\text{out}}$  en función de  $\bar{\gamma}/\gamma_{\text{th}}$  para  $P = 4$  y distintos valores de  $\rho$  y  $K_i$ . Las líneas sólidas corresponden con los resultados teóricos mientras que los marcadores representan los resultados simulados. Para los cálculos teóricos se ha empleado un valor de  $m = 40$  para  $\mathbf{k} = (0.5, 0.25, 0.25, 0)$  y de  $m = 200$  para  $\mathbf{k} = (8, 7, 6, 6)$ .

### Resultados numéricos

A continuación, se va a estudiar el impacto del parámetro Rice en cada rama y de la matriz de coeficientes de correlación en ambas métricas (probabilidad de *outage* y BER). Para comprobar la precisión de los resultados teóricos, éstos se comparan nuevamente con el resultado de las simulaciones. Por simplicidad, se denota como  $\mathbf{k} = (K_1, \dots, K_P)$  al vector que contiene los  $P$  parámetros Rice,  $K$ , e igualmente se asume que la matriz de coeficientes de correlación  $\mathbf{R}$  es exponencial, i.e.  $(\mathbf{R})_{i,j} = \rho^{|i-j|}$  con  $|\rho| < 1$  [103], [104].

En primer lugar, en la Fig. B.2 se estudia el efecto de los parámetros del canal en la probabilidad de *outage*. Fijándonos en primer lugar en el efecto de los parámetros  $K$  (equivalentemente, la potencia de la componente directa), se observa cómo generalmente un incremento en estos parámetros conlleva una mejora de prestaciones del sistema. Sin embargo, para valores muy elevados de  $\rho$  (correlación muy alta entre antenas), vemos que el comportamiento del sistema es opuesto; un aumento de la potencia de la línea de visión directa conlleva a una mayor probabilidad de *outage* para valores altos de  $\bar{\gamma}$ . Este mismo efecto es analizado con más detalle en [105].

Finalmente, en la Fig. B.3 se evalúa el impacto de la correlación y la potencia de la componente directa en la BER, extrayéndose las mismas conclusiones que para la probabilidad de *outage*: efecto negativo de la correlación y mejor rendimiento en general para valores de  $K$  elevados.



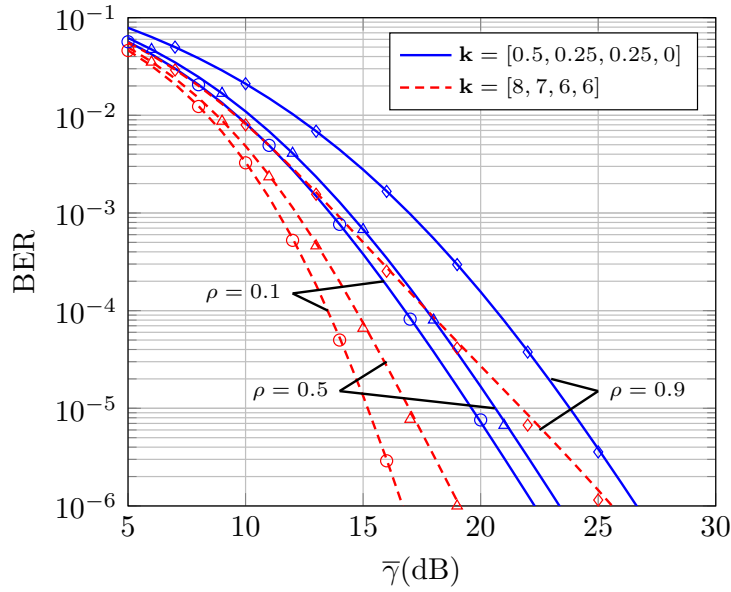


FIGURA B.3: BER para una constelación 16-QAM para  $P = 4$  y distintos valores de  $\rho$  y  $K_i$ . Las líneas sólidas corresponden con los resultados teóricos mientras que los marcadores representan los resultados simulados. Para los cálculos teóricos se ha empleado un valor de  $m = 40$  para  $\mathbf{k} = (0.5, 0.25, 0.25, 0)$  y de  $m = 150$  para  $\mathbf{k} = (8, 7, 6, 6)$ .

### B.3 Generalizaciones del modelo de desvanecimientos $\kappa$ - $\mu$ *shadowed*

Las variables aleatorias confluentes definidas en secciones anteriores han sido usadas simplemente como herramientas matemáticas para estudiar otras variables cuyo análisis es complejo. Es decir, el interés recaía únicamente en el comportamiento límite de su distribución.

Sin embargo, estas variables pueden tener utilidad por sí mismas. Un ejemplo de ello es el caso del modelado de canal, donde la introducción de una fluctuación aleatoria en la variable original puede usarse para caracterizar el *shadowing*. De hecho, esta es la misma idea de la que surgen distintos modelos de canal generalizados, tales como el Rician *shadowed* [86], [87] y el  $\kappa$ - $\mu$  *shadowed* [29].

Aunque estas distribuciones son generalizaciones de los modelos clásicos, desde el punto de vista del análisis por confluencia una variable Rician *shadowed* puede verse como la versión confluyente de una variable Rice, y la misma relación puede establecerse entre los modelos  $\kappa$ - $\mu$  [28], [88] y  $\kappa$ - $\mu$  *shadowed*.

Con esta idea, y sacando partido del análisis de las FCG, en esta tesis se presentan dos nuevos modelos de canal, los cuales buscan unificar a la mayoría de distribuciones de desvanecimientos existentes en la literatura.

### B.3.1 El modelo Beckmann fluctuante

El primero modelo aquí presentado es el Beckmann fluctuante (BF), el cual es una generalización tanto de la distribución Beckmann [85] como de la  $\kappa$ - $\mu$  *shadowed*. En el contexto del análisis por confluencias, el modelo BF puede verse como la variable auxiliar para analizar la distribución Beckmann. Si se compara con el  $\kappa$ - $\mu$  *shadowed*, el modelo BF es su extensión natural considerando el efecto del desequilibrio de potencia entre las componentes en fase y cuadratura.

#### Modelo físico

De acuerdo con el modelo BF, la amplitud de la señal recibida se expresa como

$$R = \left( \sum_{i=1}^{\mu} |\sigma_x X_i + j\sigma_y Y_i + \xi(p_i + jq_i)|^2 \right)^{1/2} \quad (\text{B.26})$$

donde  $\mu \in \mathbb{N}^+$ ,  $\sigma_x, \sigma_y \in \mathbb{R}^+$  y  $p_i, q_i \in \mathbb{R}$  son constantes;  $X_i, Y_i$  para todo  $i$  son variables gaussianas estándar independientes e idénticamente distribuidas, i.e.  $X_i, Y_i \sim \mathcal{N}(0, 1)$ , y  $\xi$  es una variable aleatoria, independiente de  $X_i$  y  $Y_i$ , tal que  $\xi^2 \sim \Gamma(m, 1/m)$ .

Este nuevo modelo queda totalmente caracterizado por los parámetros  $m, \mu$  y

$$\kappa = \frac{\sum_{i=1}^{\mu} p_i^2 + q_i^2}{\mu(\sigma_x^2 + \sigma_y^2)}, \quad \eta = \frac{\sigma_x^2}{\sigma_y^2}, \quad \varrho^2 = \frac{\sum_{i=1}^{\mu} p_i^2}{\sum_{i=1}^{\mu} q_i^2}. \quad (\text{B.27})$$

Debido a su generalidad y flexibilidad, la mayoría de distribuciones de desvanecimientos presentes en la literatura quedan recogidas como casos particulares del modelo BF, tal y como se indica en la Tabla B.1.

#### Caracterización estadística

Una vez presentado el modelo físico de la nueva distribución, se procede a la caracterización estadística de primer orden, i.e. la obtención de expresiones para su PDF, CDF y MGF. Dado que es habitual analizar los modelos de desvanecimientos en términos de la SNR [18], de aquí en adelante se considera la variable aleatoria

$$\gamma \triangleq \bar{\gamma} \frac{R^2}{\mathbb{E}[R^2]}, \quad (\text{B.28})$$

donde  $\mathbb{E}[R^2] = \mu(\sigma_x^2 + \sigma_y^2) + \sum_{i=1}^{\mu} (p_i^2 + q_i^2)$  y  $\bar{\gamma} \triangleq \mathbb{E}[\gamma]$  es la SNR media. Por tanto,  $\gamma$  representa la SNR instantánea en el receptor, la cual sigue una distribución BF, i.e.  $\gamma \sim \mathcal{FB}(\bar{\gamma}; \kappa, \mu, m, \eta, \varrho)$ .

TABLE B.1: Relación entre el modelo BF y distintas distribuciones de desvanecimientos dadas en la literatura. Para evitar confusión, los parámetros del BF están subrayados. Nótese que  $\kappa = 0$  implica que  $m$  y  $\varrho$  desaparecen.

Modelo de canal	Parámetros del modelo Beckmann fluctuante
Rayleigh	$\underline{\kappa} = 0, \underline{\mu} = 1, \underline{\eta} = 1$
Rice	$\underline{\kappa} = K, \underline{\mu} = 1, \underline{m} \rightarrow \infty, \underline{\eta} = 1, \forall \varrho$
Nakagami- $m$	$\underline{\kappa} = 0, \underline{\mu} = m, \underline{\eta} = 1$
Hoyt	$\underline{\kappa} = 0, \underline{\mu} = 1, \underline{\eta} = \eta$
$\eta$ - $\mu$	$\underline{\kappa} = 0, \underline{\mu} = \mu, \underline{\eta} = \eta$
Beckmann	$\underline{\kappa} = K, \underline{\mu} = 1, \underline{m} \rightarrow \infty, \underline{\eta} = \eta, \underline{\varrho} = \varrho$
$\kappa$ - $\mu$	$\underline{\kappa} = \kappa, \underline{\mu} = \mu, \underline{m} \rightarrow \infty, \underline{\eta} = 1, \forall \varrho$
Rician Shadowed	$\underline{\kappa} = \kappa, \underline{\mu} = 1, \underline{m} = m, \underline{\eta} = 1, \forall \varrho$
$\kappa$ - $\mu$ shadowed	$\underline{\kappa} = \kappa, \underline{\mu} = \mu, \underline{m} = m, \underline{\eta} = 1, \forall \varrho$

La MGF del modelo propuesto puede obtenerse condicionando a  $\xi$  la MGF de la distribución Beckmann [18, eq. (2.38)] y posteriormente promediando sobre todos sus posibles valores, llegando a

$$M_\gamma(s) = \frac{(-1)^\mu \alpha_2^{m-\mu/2}}{s^\mu \bar{\gamma}^\mu \alpha_1^m} \left( 1 - \frac{\mu(1+\eta)(1+\kappa)}{2\eta\bar{\gamma}s} \right)^{m-\frac{\mu}{2}} \times \left( 1 - \frac{\mu(1+\eta)(1+\kappa)}{2\bar{\gamma}s} \right)^{m-\frac{\mu}{2}} \left( 1 - \frac{c_1}{\bar{\gamma}s} \right)^{-m} \left( 1 - \frac{c_2}{\bar{\gamma}s} \right)^{-m}, \quad (\text{B.29})$$

donde  $c_{1,2}$  y  $\alpha_{1,2}$  son constantes que dependen de los parámetros de la distribución.

La PDF y la CDF de  $\gamma$  se obtienen aplicando la transformada inversa de Laplace a (B.29), de forma análoga a como se hizo en el análisis de las FCGs complejas, resultando

$$f_\gamma(\gamma) = \frac{\alpha_2^{m-\mu/2} \gamma^{\mu-1}}{\bar{\gamma}^\mu \Gamma(\mu) \alpha_1^m} \Phi_2^{(4)} \left( \frac{\mu}{2} - m, \frac{\mu}{2} - m, m, m; \mu; \frac{-\gamma}{\bar{\gamma}\sqrt{\eta\alpha_2}}, \frac{-\gamma\sqrt{\eta}}{\bar{\gamma}\sqrt{\alpha_2}}, \frac{-\gamma c_1}{\bar{\gamma}}, \frac{-\gamma c_2}{\bar{\gamma}} \right), \quad (\text{B.30})$$

$$F_\gamma(\gamma) = \frac{\alpha_2^{m-\mu/2} \gamma^\mu}{\bar{\gamma}^\mu \Gamma(\mu+1) \alpha_1^m} \Phi_2^{(4)} \left( \frac{\mu}{2} - m, \frac{\mu}{2} - m, m, m; \mu+1; \frac{-\gamma}{\bar{\gamma}\sqrt{\eta\alpha_2}}, \frac{-\gamma\sqrt{\eta}}{\bar{\gamma}\sqrt{\alpha_2}}, \frac{-\gamma c_1}{\bar{\gamma}}, \frac{-\gamma c_2}{\bar{\gamma}} \right), \quad (\text{B.31})$$

donde  $\Phi_2^{(n)}$  es la serie confluyente de Lauricella [107, p. 34], la cual aparece también en otros modelos presentes en la literatura [29], [31], [108] y puede calcularse fácilmente de forma numérica a través de una transformada inversa de Laplace [109], [110].

Bajo ciertas condiciones, la PDF y la CDF del modelo FB se simplifican, obteniéndose expresiones más sencillas y matemáticamente tratables. Específicamente, si  $m$  toma valores enteros y  $\mu$  es par, entonces (B.29) permite una descomposición en fracciones

simples, y (B.30) y (B.31) pueden expresarse en términos de funciones elementales (exponenciales y potencias).

Dado que la PDF y la CDF de una distribución, no reflejan el comportamiento dinámico de la misma, se proporcionan dos métricas adicionales para reflejar este comportamiento: *i)* el *level crossing rate* (LCR), que mide la frecuencia con que la amplitud recibida cruza un determinado umbral, y *ii)* el *average fade duration* (AFD), que caracteriza cuánto tiempo permanece dicha amplitud bajo el umbral.

El LCR de la señal recibida según el modelo BF puede calcularse mediante la fórmula de Rice [111]. No obstante, a pesar de que se ha obtenido una expresión analítica para  $N_R(u)$ , ésta viene dada en términos de una integral doble que limita su practicidad. Sin embargo, bajo la suposición de  $q_i = 0$  y  $p_i \neq 0$  o viceversa en (B.26), es posible llegar a una expresión más sencilla. Así pues, asumiendo  $q_i = 0 \forall i$  (la expresión resultante es válida para  $p_i = 0 \forall i$  simplemente realizando el cambio  $\eta \rightarrow 1/\eta$ ), el LCR viene dado por

$$\begin{aligned}
 N_R(u) = & \frac{m^m [\mu(1+\eta)(1+\kappa)]^{\mu-1/2} \sqrt{-\ddot{\rho}(0)}}{2^{\mu-1} \Gamma^2(\mu/2) \eta^{\mu/2} (\frac{\mu\kappa(1+\eta)}{2\eta} + m) m \sqrt{2\pi}} \cdot u^{(2\mu-1)} \exp\left(-\frac{\mu}{2}(1+\eta)(1+\kappa)u^2\right) \\
 & \times \int_0^1 [1 + (\eta-1)x]^{\frac{1}{2}} (1-x)^{\mu/2-1} x^{\mu/2-1} \exp\left(-\frac{\mu(1-\eta^2)(1+\kappa)}{2\eta} u^2 x\right) \\
 & \times {}_1F_1\left(m, \mu/2; \frac{\frac{\kappa\mu^2(1+\eta)^2(1+\kappa)}{4\eta^2}}{\frac{\mu\kappa(1+\eta)}{2\eta} + m} u^2 x\right) dx
 \end{aligned} \tag{B.32}$$

donde  $\Omega = \mathbb{E}[R^2]$  y  $\ddot{\rho}(0)$  es la derivada segunda de la función de autocorrelación evaluada en 0.

Finalmente, el AFD se calcula de forma inmediata como

$$T_R(u) = \frac{F_R(u)}{N_R(u)}. \tag{B.33}$$

## Resultados numéricos

Una vez caracterizado el nuevo modelo, se va a ejemplificar la influencia de sus parámetros en la distribución de la amplitud de señal recibida, la cual puede obtenerse a partir de (B.29) mediante el cambio de variables  $f_R(r) = 2r \frac{\bar{\gamma}}{\Omega} f_\gamma(\bar{\gamma} r^2 / \Omega)$ .

Dado que el desequilibrio en potencia caracterizado por los parámetros  $\eta$  y  $\varrho^2$  representa la generalización del modelo propuesto respecto al  $\kappa$ - $\mu$  *shadowed*, nos vamos a centrar en el estudio del impacto producido por la variación de dichos parámetros. Para ello, en la Fig. B.4 se representa la PDF de  $R$  para distintos valores de  $\eta$  en un escenario con fluctuaciones medias y severas para la componente directa ( $m = 10$  y  $m = 1$ , respectivamente). En este caso,  $\varrho^2$  se fija a  $\varrho^2 = 0.1$ , i.e. la componente en fase de la línea de visión directa tiene diez veces más potencia que la componente en cuadratura. Con estos parámetros, se observa cómo, a diferencia del modelo  $\eta$ - $\mu$  *shadowed*, la distribución BF no

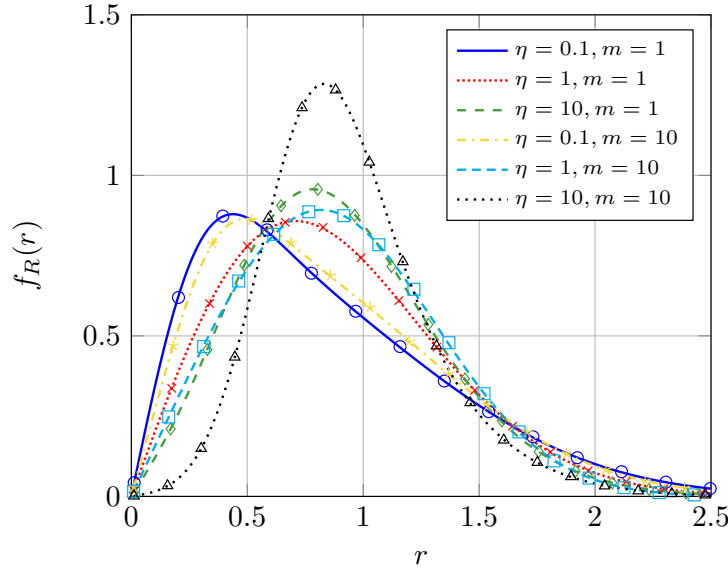


FIGURA B.4: Amplitud recibida según modelo BF para distintos valores de  $\eta$  y  $m$  con  $\kappa = 1$ ,  $\varrho = 0.1$ ,  $\mu = 1$  y  $\Omega = 1$ . Las líneas continuas corresponden con los valores teóricos, mientras que los marcadores corresponden a los resultados de la simulación.

es simétrica respecto a  $\eta \in [0, 1]$  y  $\eta \in [1, \infty)$  para un determinado  $\rho^2 \neq 1$ . De hecho, si el desequilibrio en potencia de la parte difusa se produce en favor de la misma componente que en la línea de visión de directa, el efecto es mucho más perjudicial que si se produjese hacia la componente contraria. Un comportamiento similar se reproduce para distintos valores de  $\varrho^2$  dado un  $\eta$  fijo.

Por último, se va a analizar el efecto de los parámetros de la distribución en el LCR. Para ello, se asume una variación de la componente difusa acorde al modelo de correlación de Clarke [17, sec. 2.1.1] con una frecuencia Doppler máxima  $f_d$ . Por tanto,  $\sqrt{-\ddot{\rho}(0)} = \sqrt{2}f_d\pi$  [113, eq. (34)]. Igualmente, se asume  $\varrho^2 \rightarrow \infty$  de modo que el LCR pueda calcularse como en (B.32).

Con dichas consideraciones, en la Fig. B.5 se representa el LCR en función del umbral,  $u$ , para distintos valores de los parámetros de la distribución BF. Curiosamente, al aumentar  $\mu$ , el número de cruces para umbrales bajos se reduce drásticamente, mientras que éstos aumentan al reducir  $\kappa$  o aumentar  $\eta$ .

### B.3.2 El modelo $\kappa$ - $\mu$ *shadowed* con correlación

#### Modelo físico

La segunda extensión del modelo  $\kappa$ - $\mu$  *shadowed* presentada en esta tesis recibe el nombre de  $\kappa$ - $\mu$  *shadowed* correlado. Según este nuevo modelo, la amplitud de señal recibida

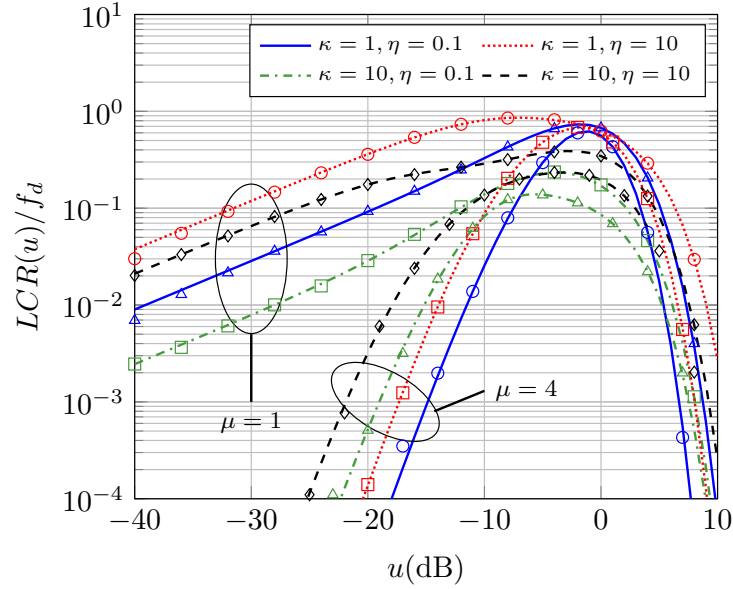


FIGURA B.5: LCR normalizado para distintos valores de  $\kappa, \eta$  y  $\mu$  con  $m = 1, \varrho \rightarrow \infty$  y  $\Omega = 1$ . Las líneas continuas corresponden con los valores teóricos, mientras que los marcadores corresponden a los resultados de la simulación.

viene dada por

$$R = \left( \sum_{i=1}^{\mu} |Z_i + \xi p_i|^2 \right)^{1/2}, \quad (\text{B.34})$$

donde  $\mu \in \mathbb{N}^+$ ,  $p_i$  para  $i = 1, \dots, \mu$  son números complejos representando la contribución de la componente directa y  $Z_i \sim \mathcal{CN}(0, \sigma^2)$ . La variable  $\xi$  representa las fluctuaciones debido al *shadowing*, al igual que en el modelo BF. La novedad aquí respecto al modelo original es que las variables  $Z_i$  pueden estar correladas con coeficiente de correlación  $\text{corr}(Z_i, Z_j) = \rho_{i,j}$  para  $i, j = 1, \dots, \mu$ , con

$$\rho_{i,j} = \frac{\mathbb{E}[Z_i Z_j^\dagger]}{\sigma^2}. \quad (\text{B.35})$$

Obsérvese que, condicionado a  $\xi$ ,  $R^2$  en (B.34) es un caso particular de la FCG compleja en (B.13), donde  $\mathbf{A} = \mathbf{I}_\mu$ . Por tanto, aplicando las mismas manipulaciones que para  $Q_C$ ,  $R$  puede escribirse como

$$R = \left( \sum_{i=1}^{\mu} \left| \sqrt{\lambda_i} \sigma \tilde{Z}_i + \xi \sqrt{\lambda_i} \tilde{p}_i \right|^2 \right)^{1/2}, \quad (\text{B.36})$$

donde  $\tilde{Z}_i \sim \mathcal{CN}(0, 1)$ ,  $\tilde{p}_i$  son los elementos del vector  $\tilde{\mathbf{p}} = \mathbf{U}^\dagger \mathbf{C}^{-1} \mathbf{p}$  con  $\mathbf{p} = (p_1, \dots, p_\mu)^T$ ,  $\lambda_i$  son los autovalores de  $\mathbf{C}^\dagger \mathbf{C}$  y  $\mathbf{U}$  es una matriz unitaria cuya columna  $i$ -ésima es el autovector de  $\mathbf{C}^\dagger \mathbf{C}$  asociado con  $\lambda_i$ .

### Caracterización estadística

Al igual que en la distribución BF, nos basaremos en el análisis estadístico de la SNR instantánea, definida como  $\gamma = \bar{\gamma}R^2/\mathbb{E}[R^2]$ , donde  $\bar{\gamma}$  denota la SNR media y  $\mathbb{E}[R^2] = \mu\sigma^2 + \sum_{i=1}^{\mu} \|p_i^2\|$ .

La MGF de  $\gamma$  viene dada por

$$M_{\gamma}(s) = \frac{\mu^{\mu}(\kappa+1)^{\mu}}{\prod_{i=1}^{\mu} (\mu(\kappa+1) - s\lambda_i\bar{\gamma})} \left( 1 - \frac{1}{m} \sum_{j=1}^{\mu} \frac{d_i\lambda_i s\bar{\gamma}}{\mu(\kappa+1) - s\lambda_i\bar{\gamma}} \right)^{-m}, \quad (\text{B.37})$$

con  $d_i = |\tilde{p}_i|^2 / \sigma^2$ .

A partir de (B.37), la PDF y la CDF de  $\gamma$  pueden obtenerse realizando una descomposición en fracciones simples y aplicando la transformada inversa de Laplace, resultando

$$f_{\gamma}(\gamma) = \alpha \sum_{i=1}^{n_{\beta}} \sum_{j=1}^{q_i m} A_{i,j} \gamma^{j-1} e^{-\beta_i \gamma}, \quad (\text{B.38})$$

$$F_{\gamma}(\gamma) = 1 + \alpha \sum_{i=1}^{n_{\beta}} \sum_{j=1}^{q_i m} C_{i,j} \gamma^{j-1} e^{-\beta_i \gamma}, \quad (\text{B.39})$$

donde  $\alpha$ ,  $A_{i,j}$  y  $C_{i,j}$  son constantes que dependen de los parámetros de la distribución.

### Resultados numéricos

Finalmente, se va a ejemplificar la influencia de la correlación en la distribución de la amplitud de señal recibida. Por simplicidad, asumimos que la correlación sigue un perfil exponencial, i.e.,  $\text{corr}(Z_i, Z_j) = \rho_{i,j} = \rho^{|i-j|}$  con  $0 \leq \rho < 1$ . Bajo esta suposición, en la Fig. B.6 se representa la PDF de la amplitud recibida para distintos valores de  $\rho$ ,  $\mu$  y  $m$  con  $\kappa = 4$ . Se observa que, independientemente del resto de parámetros, una correlación alta (valores de  $\rho$  próximos a la unidad) siempre producen valores de la señal más distribuidos, siendo prácticamente independiente de los valores de  $m$  empleados. Sin embargo, al aumentar  $\mu$ , este efecto de la correlación es aún más notorio.

## B.4 Conclusiones y líneas futuras

### Conclusiones

En esta tesis se ha conseguido un doble objetivo. Por un lado, se ha presentado un nuevo método de aproximar la distribución de variables aleatorias basado en el análisis de una secuencia de variables aleatorias auxiliares definidas a partir de la variable

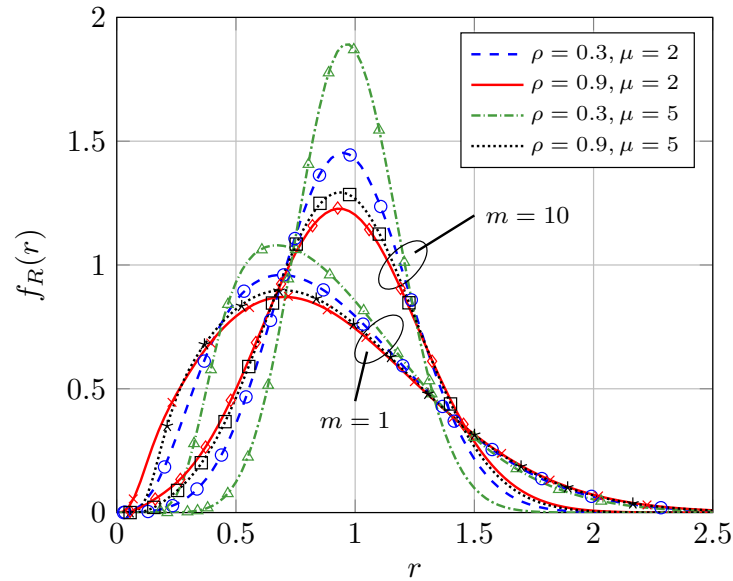


FIGURA B.6: Distribución de la amplitud recibida para distintos valores de  $\mu$ ,  $\rho$  y  $m$  para  $\kappa = 4$  y  $\mathbb{E}[R] = 1$ . Las líneas continuas corresponden a los cálculos teóricos mientras que los marcadores representan el valor de las simulaciones.

objetivo. La ventaja de este método respecto a otras soluciones disponibles en la literatura son: *i)* las expresiones obtenidas *siempre* representan una distribución válida y *ii)* puede obtenerse cualquier grado de precisión con independencia de los parámetros de la variable en cuestión.

Esta técnica de análisis se ha aplicado en el contexto de las FCG, dando lugar a las siguientes contribuciones:

- Se han proporcionado expresiones para la PDF y CDF de las FCG reales y definidas positivas que pueden computarse fácilmente de forma recursiva.
- Se han obtenido aproximaciones tratables matemáticamente en términos de funciones elementales para las FCG complejas.
- Se dan, por primera vez en la literatura, expresiones generales para la probabilidad de error y la probabilidad de *outage* en sistemas MRC sobre canales Rice correlados.

Por otro lado, la aplicación del método propuesto en el contexto de modelado de canal ha dado lugar a la presentación de dos modelos de canal generalizados que unifican a la mayoría de distribuciones de desvanecimientos más usadas. Específicamente, las contribuciones son:

- Presentación y análisis del modelo Beckmann fluctuante como generalización tanto de la distribución  $\kappa$ - $\mu$  *shadowed* como de la Beckmann, proporcionando expresiones para sus estadísticos de primer y segundo orden.
- Introducción del modelo  $\kappa$ - $\mu$  *shadowed* correlado, extendiendo la distribución original.



### Líneas futuras

En el contexto del análisis de variables aleatorias, una posible línea futura de investigación sería la aplicación del método general aquí propuesto a otros tipos de variables cuyo estudio es en general sumamente complejo, tales como aquellas variables que surgen de la suma o producto de otras.

Además, debido al número de aplicaciones de las FCG en procesado de señal y comunicaciones, y dada la relativa tratabilidad de las aproximaciones dadas en esta tesis, las expresiones aquí aportadas pueden ser útiles para el análisis de múltiples sistemas, e.g., sistemas con diversidad, detección de señales o análisis de prestaciones de estimadores.

Por otro lado, en lo referente a modelado de canal, el propio método aquí propuesto es interesante para el análisis de modelos *composite*, i.e., aquellos que contemplan a la vez el efecto de los desvanecimientos y un *shadowing* multiplicativo. En esta línea, algunos resultados preliminares pueden encontrarse ya en [114]. Finalmente, los dos modelos generalizados que se han introducido pueden ser de utilidad para el análisis de prestaciones de sistemas sobre una gran variedad de condiciones de propagación. Ejemplos del interés de la comunidad científica en estas distribuciones pueden encontrarse en [115], [116].

# Bibliography

- [1] P. Billingsley, *Probability and Measure*, ser. Wiley Series in Probability and Statistics. Wiley, 2012.
- [2] H. Van Trees, K. Bell, and Z. Tian, *Detection Estimation and Modulation Theory, Part I: Detection, Estimation, and Filtering Theory*, ser. Detection Estimation and Modulation Theory. Wiley, 2013.
- [3] V. K. Madisetti, *The Digital Signal Processing Handbook*, 2nd. CRC Press, 2009.
- [4] S. Provost and A. Mathai, *Quadratic Forms in Random Variables: Theory and Applications*, ser. Statistics : textbooks and monographs. Marcel Dekker, 1992.
- [5] G. E. P. Box, "Some theorems on quadratic forms applied in the study of analysis of variance problems, i. effect of inequality of variance in the one-way classification", *Ann. Math. Statist.*, vol. 25, no. 2, pp. 290–302, 1954.
- [6] T. Y. Al-Naffouri and M. Moinuddin, "Exact performance analysis of the  $\epsilon$ -NLMS algorithm for colored circular Gaussian inputs", *IEEE Trans. Signal Process.*, vol. 58, no. 10, pp. 5080–5090, 2010.
- [7] E. H. Gismalla and E. Alsusa, "Performance analysis of the periodogram-based energy detector in fading channels", *IEEE Trans. Signal Process.*, vol. 59, no. 8, pp. 3712–3721, 2011.
- [8] F. Athley, "Threshold region performance of maximum likelihood direction of arrival estimators", *IEEE Trans. Signal Process.*, vol. 53, no. 4, pp. 1359–1373, 2005.
- [9] Q. Zhao and H. Li, "Differential modulation for cooperative wireless systems", *IEEE Trans. Signal Process.*, vol. 55, no. 5, pp. 2273–2283, 2007.
- [10] D. Raphaeli, "Noncoherent coded modulation", *IEEE Trans. Commun.*, vol. 44, no. 2, pp. 172–183, Feb. 1996.
- [11] T. Y. Al-Naffouri, M. Moinuddin, N. Ajeeb, B. Hassibi, and A. L. Moustakas, "On the distribution of indefinite quadratic forms in Gaussian random variables", *IEEE Trans. Commun.*, vol. 64, no. 1, pp. 153–165, 2016.
- [12] B. D. Rao, M. Wengler, and B. Judson, "Performance analysis and comparison of MRC and optimal combining in antenna array systems", in *IEEE Int. Conf. Acoust. Speech Signal Process. Proceedings (Cat. No.01CH37221)*, vol. 5, 2001, pp. 2949–2952.
- [13] D. Lao and A. M. Haimovich, "Exact closed-form performance analysis of optimum combining with multiple cochannel interferers and Rayleigh fading", *IEEE Trans. Commun.*, vol. 51, no. 6, pp. 995–1003, Jun. 2003.

- [14] C. Kim, S. Lee, and J. Lee, "SINR and throughput analysis for random beamforming systems with adaptive modulation", *IEEE Trans. Wireless Commun.*, vol. 12, no. 4, pp. 1460–1471, Apr. 2013.
- [15] G. A. Ropokis, A. A. Rontogiannis, and P. T. Mathiopoulos, "Quadratic forms in normal RVs: Theory and applications to OSTBC over Hoyt fading channels", *IEEE Trans. Wireless Commun.*, vol. 7, no. 12, pp. 5009–5019, 2008.
- [16] V. Havary-Nassab, S. Shahbazpanahi, and A. Grami, "Optimal distributed beamforming for two-way relay networks", *IEEE Trans. Signal Process.*, vol. 58, no. 3, pp. 1238–1250, Mar. 2010.
- [17] G. L. Stuber, *"Principles of Mobile Communication"*, 2nd. Kluwer Academic Publishers, 2002.
- [18] M. K. Simon and M.-S. Alouini, *Digital communication over fading channels*. John Wiley & Sons, 2005, vol. 95.
- [19] J. Proakis and M. Salehi, *"Digital communications"*, McGraw-Hill Education, vol. 31, 2007.
- [20] M. Nakagami, "The  $m$ -distribution — a general formula of intensity distribution of rapid fading", in *Statistical Methods in Radio Wave Propagation*, W. Hoffman, Ed., Pergamon, 1960, pp. 3–36.
- [21] M. R. Akdeniz, Y. Liu, M. K. Samimi, S. Sun, S. Rangan, T. S. Rappaport, and E. Erkip, "Millimeter wave channel modeling and cellular capacity evaluation", *IEEE J. Sel. Areas Commun.*, vol. 32, no. 6, pp. 1164–1179, Jun. 2014.
- [22] T. S. Rappaport, G. R. MacCartney, M. K. Samimi, and S. Sun, "Wideband millimeter-wave propagation measurements and channel models for future wireless communication system design", *IEEE Trans. Commun.*, vol. 63, no. 9, pp. 3029–3056, Sep. 2015.
- [23] J. Medbo, K. Börner, K. Haneda, V. Hovinen, T. Imai, J. Järveläinen, T. Jämsä, A. Karttunen, K. Kusume, J. Kyröläinen, P. Kyösti, J. Meinilä, V. Nurmela, L. Raschkowski, A. Roivainen, and J. Ylitalo, "Channel modelling for the fifth generation mobile communications", in *Proc. 8th Eur. Conf. Antennas Propag. (EuCAP)*, Apr. 2014, pp. 219–223.
- [24] S. Hur, S. Baek, B. Kim, Y. Chang, A. F. Molisch, T. S. Rappaport, K. Haneda, and J. Park, "Proposal on millimeter-wave channel modeling for 5G cellular system", *IEEE J. Sel. Topics Signal Process.*, vol. 10, no. 3, pp. 454–469, Apr. 2016.
- [25] Q.-U.-A. Nadeem, A. Kammoun, A. Chaaban, M. Debbah, and M.-S. Alouini, "Large intelligent surface assisted MIMO communications", *arXiv preprint arXiv:1903.08127*, 2019.
- [26] A. Taha, M. Alrabeiah, and A. Alkhateeb, "Enabling large intelligent surfaces with compressive sensing and deep learning", *arXiv preprint arXiv:1904.10136*, 2019.
- [27] M. Stojanovic and J. Preisig, "Underwater acoustic communication channels: Propagation models and statistical characterization", *IEEE Commun. Mag.*, vol. 47, no. 1, pp. 84–89, Jan. 2009.

- [28] M. D. Yacoub, "The  $\kappa$ - $\mu$  distribution and the  $\eta$ - $\mu$  distribution", *IEEE Antennas Propag. Mag.*, vol. 49, no. 1, pp. 68–81, Feb. 2007.
- [29] J. F. Paris, "Statistical characterization of  $\kappa$ - $\mu$  shadowed fading", *IEEE Trans. Veh. Technol.*, vol. 63, no. 2, pp. 518–526, Feb. 2014.
- [30] F. J. Lopez-Martinez, J. F. Paris, and J. M. Romero-Jerez, "The  $\kappa$ - $\mu$  shadowed fading model with integer fading parameters", *IEEE Trans. Veh. Technol.*, vol. 66, no. 9, pp. 7653–7662, Sep. 2017.
- [31] J. M. Romero-Jerez, F. J. Lopez-Martinez, J. F. Paris, and A. J. Goldsmith, "The fluctuating two-ray fading model: Statistical characterization and performance analysis", *IEEE Tran. Wireless Commun.*, vol. 16, no. 7, pp. 4420–4432, Jul. 2017.
- [32] C. Goutis and G. Casella, "Explaining the saddlepoint approximation", *Am. Stat.*, vol. 53, no. 3, pp. 216–224, 1999.
- [33] R. W. Butler and A. T. A. Wood, *Ann. Statist.*, vol. 32, no. 6, pp. 2712–2730, Dec. 2004.
- [34] H. E. Daniels, "Saddlepoint approximations in statistics", *Ann. Math. Statist.*, vol. 25, no. 4, pp. 631–650, Dec. 1954.
- [35] J. E. Kolassa, *Series approximation methods in statistics*. Springer Science & Business Media, 2006, vol. 88.
- [36] P. McCullagh, *Tensor Methods in Statistics*, ser. Monographs on statistics and applied probability. Kluwer Academic Publishers, 1987.
- [37] D. L. Wallace, "Asymptotic approximations to distributions", *Ann. Math. Statist.*, vol. 29, no. 3, pp. 635–654, Sep. 1958.
- [38] C. Field and E. Ronchetti, *Small Sample Asymptotics*, ser. Lecture notes-monograph. Institute of Mathematical Statistics, 1990, vol. 13.
- [39] S. B. Provost, "Moment-based density approximants", *Math. J.*, vol. 9, no. 4, pp. 727–756, 2005.
- [40] H. Sorenson and D. Alspach, "Recursive bayesian estimation using gaussian sums", *Automatica*, vol. 7, no. 4, pp. 465–479, 1971.
- [41] B. Everitt and D. Hand, *Finite mixture distributions*, ser. Monographs on applied probability and statistics. Chapman and Hall, 1981.
- [42] M. Wiper, D. Rios, and F. Ruggeri, "Mixtures of gamma distributions with applications", *J. Comput. Graph. Stat.*, vol. 10, pp. 440–454, Sep. 2001.
- [43] A. Bacharoglou, "Approximation of probability distributions by convex mixtures of Gaussian measures", *Proc. Amer. Math. Soc.*, vol. 138, pp. 2619–2619, Jul. 2010.
- [44] "Universal series induced by approximate identities and some relevant applications", *J. Approx. Theory*, vol. 163, no. 12, pp. 1783–1797, 2011.
- [45] D. Alspach and H. Sorenson, "Nonlinear bayesian estimation using gaussian sum approximations", *IEEE Trans. Autom. Control*, vol. 17, no. 4, pp. 439–448, Aug. 1972.
- [46] P. Ramírez-Espinosa, D. Morales-Jimenez, J. A. Cortés, J. F. París, and E. Martos-Naya, "New approximation to distribution of positive RVs applied to Gaussian quadratic forms", *IEEE Signal Process. Lett.*, vol. 26, no. 6, pp. 923–927, Jun. 2019.

- [47] P. Ramírez-Espinosa, L. Moreno-Pozas, J. F. París, J. A. Cortés, and E. Martos-Naya, "A new approach to the statistical analysis of non-central complex Gaussian quadratic forms with applications", *IEEE Trans. Veh. Technol.*, vol. 68, no. 7, pp. 6734–6746, Jul. 2019.
- [48] P. Ramírez-Espinosa, F. J. López-Martínez, J. F. París, M. D. Yacoub, and E. Martos-Naya, "An extension of the  $\kappa$ - $\mu$  shadowed fading model: Statistical characterization and applications", *IEEE Trans. Veh. Technol.*, vol. 67, no. 5, pp. 3826–3837, May 2018.
- [49] P. Ramírez-Espinosa, J. F. París, J. A. Cortés, and E. Martos-Naya, "The  $\kappa$ - $\mu$  shadowed fading model with arbitrary intercluster correlation", in *2018 15th Int. Symp. Wireless Commun. Syst. (ISWCS)*, Aug. 2018, pp. 1–5.
- [50] M. Abramowitz, I. A. Stegun, et al., *Handbook of Mathematical Functions with Formulas, Graphs, and Mathematical Tables*. Dover, New York, 1972, vol. 9.
- [51] I. S. Gradshteyn and I. M. Ryzhik, *Table of Integrals, Series, and Products*. Academic Press, 2007.
- [52] D. Williams, *Probability with Martingales*, ser. Cambridge mathematical textbooks. Cambridge University Press, 1991.
- [53] D. D. Boos, "A converse to Scheffe's theorem", *Ann. Statist.*, vol. 13, no. 1, pp. 423–427, 1985.
- [54] H. Scheffe, "A useful convergence theorem for probability distributions", *Ann. Math. Statist.*, vol. 18, no. 3, pp. 434–438, Sep. 1947.
- [55] E. B. Manoukian, *Mathematical Nonparametric Statistics*. CRC Press, 1986.
- [56] S. Resnick, *A Probability Path*, ser. A Probability Path. Birkhäuser Boston, 2003.
- [57] B. Sklar, *Digital communications: fundamentals and applications*, 2nd, ser. Prentice Hall Communications Engineering and Emerging Technologies Series. Prentice-Hall PTR, 2001.
- [58] R. Hankin, "The complex multivariate Gaussian distribution", *R Journal*, vol. 7, pp. 73–80, Jun. 2015.
- [59] N. R. Goodman, "Statistical analysis based on a certain multivariate complex gaussian distribution (an introduction)", *Ann. Math. Statist.*, vol. 34, no. 1, pp. 152–177, Mar. 1963.
- [60] H. Cramér, *Mathematical Methods of Statistics*, ser. Princeton landmarks in mathematics and physics. Princeton University Press, 1999.
- [61] G. Bolch, S. Greiner, H. de Meer, and K. Trivedi, *Queueing Networks and Markov Chains: Modeling and Performance Evaluation with Computer Science Applications*. Wiley, 2006.
- [62] C. Ming Tan, N. Raghavan, and A. Roy, "Application of gamma distribution in electromigration for submicron interconnects", *J. Appl. Phys.*, vol. 102, no. 10, p. 103 703, 2007.
- [63] N. Johnson, S. Kotz, and N. Balakrishnan, *Continuous Univariate Distributions*, 2nd, ser. Wiley Series in Probability and Statistics. Wiley, 1994, vol. 1.

- [64] V. Sundarapandian, *Probability, statistics and queuing theory*. PHI Learning Pvt. Ltd., 2009.
- [65] P. J. Smith, "A recursive formulation of the old problem of obtaining moments from cumulants and vice versa", *Am. Stat.*, vol. 49, no. 2, pp. 217–218, 1995.
- [66] A. Mathai and H. Haubold, *Special Functions for Applied Scientists*. Springer New York, 2008.
- [67] L. L. Scharf, *Statistical Signal Processing*. Addison-Wesley Reading, MA, 1991, vol. 98.
- [68] R. Horn and C. Johnson, *Matrix Analysis*. Cambridge University Press, 1990.
- [69] H. Robbins and E. J. G. Pitman, "Application of the method of mixtures to quadratic forms in normal variates", *Ann. Math. Statist.*, vol. 20, no. 4, pp. 552–560, Dec. 1949.
- [70] S. Kotz, N. L. Johnson, and D. W. Boyd, "Series representations of distributions of quadratic forms in normal variables. i. central case", *Ann. Math. Statist.*, vol. 38, no. 3, pp. 823–837, Jun. 1967.
- [71] —, "Series representations of distributions of quadratic forms in normal variables II. Non-Central case", *Ann. Math. Statist.*, vol. 38, no. 3, pp. 838–848, Jun. 1967.
- [72] B. Shah, "Distribution of definite and of indefinite quadratic forms from a non-central normal distribution", *Ann. Math. Statist.*, vol. 34, no. 1, pp. 186–190, 1963.
- [73] J. P. Imhof, "Computing the distribution of quadratic forms in normal variables", *Biometrika*, vol. 48, no. 3/4, pp. 419–426, 1961.
- [74] J. Gurland *et al.*, "Distribution of definite and of indefinite quadratic forms", *Ann. Math. Statist.*, vol. 26, no. 1, pp. 122–127, 1955.
- [75] F. J. Reifler, M. S. Rogers, and K. Malakian, "Distribution of general noncentral positive definite quadratic form in K-dimensions", *IEEE Trans. Aerosp. Electron. Syst.*, vol. 25, no. 3, pp. 411–414, 1989.
- [76] G. L. Turin, "The characteristic function of Hermitian quadratic forms in complex normal variables", *Biometrika*, vol. 47, no. 1/2, pp. 199–201, 1960.
- [77] K. H. Biyari and W. C. Lindsey, "Statistical distributions of Hermitian quadratic forms in complex Gaussian variables", *IEEE Trans. Inf. Theory*, vol. 39, no. 3, pp. 1076–1082, May 1993.
- [78] D. Raphaeli, "Distribution of noncentral indefinite quadratic forms in complex normal variables", *IEEE Trans. Inf. Theory*, vol. 42, no. 3, pp. 1002–1007, May 1996.
- [79] G. Tziritas, "On the distribution of positive-definite Gaussian quadratic forms", *IEEE Trans. Inf. Theory*, vol. 33, no. 6, pp. 895–906, 1987.
- [80] H. Ruben, "A new result on the distribution of quadratic forms", *Ann. Math. Statist.*, vol. 34, no. 4, pp. 1582–1584, 1963.
- [81] G. D. Durgin, T. S. Rappaport, and D. A. de Wolf, "New analytical models and probability density functions for fading in wireless communications", *IEEE Trans. Commun.*, vol. 50, no. 6, pp. 1005–1015, Jun. 2002.



- [82] S. O. Rice, "Statistical properties of a sine wave plus random noise", *Bell Syst. Tech. J.*, vol. 27, no. 1, pp. 109–157, Jan. 1948.
- [83] R. Hoyt, "Probability functions for the modulus and angle of the normal complex variate", *Bell Syst. Tech. J.*, vol. 26, no. 2, pp. 318–359, Apr. 1947.
- [84] K. Bischoff and B. Chytil, "A note on scintillation indices", *Planet. Space Sci.*, vol. 17, no. 5, pp. 1059–1066, 1969.
- [85] P. Beckmann and A. Spizzichino, *The scattering of electromagnetic waves from rough surfaces*, ser. International series of monographs on electromagnetic waves. Pergamon Press, 1963.
- [86] Chun Loo, "A statistical model for a land mobile satellite link", *IEEE Trans. Veh. Technol.*, vol. 34, no. 3, pp. 122–127, Aug. 1985.
- [87] A. Abdi, W. C. Lau, M. Alouini, and M. Kaveh, "A new simple model for land mobile satellite channels: First- and second-order statistics", *IEEE Trans. Wireless Commun.*, vol. 2, no. 3, pp. 519–528, May 2003.
- [88] U. S. Dias and M. D. Yacoub, "The  $\kappa$ - $\mu$  phase-envelope joint distribution", *IEEE Trans. Commun.*, vol. 58, no. 1, pp. 40–45, Jan. 2010.
- [89] S. L. Cotton, "Human body shadowing in cellular device-to-device communications: Channel modeling using the shadowed  $\kappa$ - $\mu$  fading model", *IEEE J. Sel. Areas Commun.*, vol. 33, no. 1, pp. 111–119, Jan. 2015.
- [90] L. Moreno-Pozas, F. J. Lopez-Martinez, S. L. Cotton, J. F. Paris, and E. Martos-Naya, "Comments on "human body shadowing in cellular device-to-device communications: Channel modeling using the shadowed  $\kappa$ - $\mu$  fading model"", *IEEE J. Sel. Areas Commun.*, vol. 35, no. 2, pp. 517–520, Feb. 2017.
- [91] L. Moreno-Pozas, F. J. Lopez-Martinez, J. F. Paris, and E. Martos-Naya, "The  $\kappa$ - $\mu$  shadowed fading model: Unifying the  $\kappa$ - $\mu$  and  $\eta$ - $\mu$  distributions", *IEEE Trans. Veh. Technol.*, vol. 65, no. 12, pp. 9630–9641, Dec. 2016.
- [92] F. J. Cañete, J. López-Fernández, C. García-Corrales, A. Sánchez, E. Robles, F. J. Rodrigo, and J. F. Paris, "Measurement and modeling of narrowband channels for ultrasonic underwater communications", *Sensors*, vol. 16, no. 2, 2016.
- [93] A. Goldberger, *Econometric theory*. J. Wiley, 1964.
- [94] F. Bornemann, "Accuracy and stability of computing high-order derivatives of analytic functions by Cauchy integrals", *Found. Comput. Math.*, vol. 11, no. 1, pp. 1–63, 2011.
- [95] Y. Ma, J. Yu, and Y. Wang, "Efficient recursive methods for partial fraction expansion of general rational functions", *J. Appl. Math.*, vol. 2014, 2014.
- [96] A. V. Oppenheim, A. S. Willsky, and S. H. Nawab, *Signals & Systems (2Nd Ed.)* Upper Saddle River, NJ, USA: Prentice-Hall, Inc., 1996.
- [97] R. K. Mallik and N. C. Sagias, "Distribution of inner product of complex Gaussian random vectors and its applications", *IEEE Trans. Commun.*, vol. 59, no. 12, pp. 3353–3362, Dec. 2011.
- [98] Yao Ma, "Impact of correlated diversity branches in Rician fading channels", in *IEEE Int. Conf. Commun. ICC 2005*, vol. 1, May 2005, 473–477 Vol. 1.

- [99] P. Bithas, N. C. Sagias, and P. T. Mathiopoulos, "Dual diversity over correlated Ricean fading channels", *J. Commun. Netw.*, vol. 9, pp. 67–74, Mar. 2007.
- [100] M. Ilic-Delibasic and M. Pejanovic-Djurisic, "MRC dual-diversity system over correlated and non-identical Ricean fading channels", *IEEE Commun. Lett.*, vol. 17, no. 12, pp. 2280–2283, Dec. 2013.
- [101] A. Goldsmith, *Wireless Communications*. Cambridge university press, 2005.
- [102] F. J. Lopez-Martinez, E. Martos-Naya, J. F. Paris, and U. Fernandez-Plazaola, "Generalized BER analysis of QAM and its application to MRC under imperfect CSI and interference in Ricean fading channels", *IEEE Trans. Veh. Technol.*, vol. 59, no. 5, pp. 2598–2604, Jun. 2010.
- [103] G. K. Karagiannidis, D. A. Zogas, and S. A. Kotsopoulos, "On the multivariate Nakagami-m distribution with exponential correlation", *IEEE Transactions on Communications*, vol. 51, no. 8, pp. 1240–1244, Aug. 2003.
- [104] S. L. Loyka, "Channel capacity of MIMO architecture using the exponential correlation matrix", *IEEE Commun. Lett.*, vol. 5, no. 9, pp. 369–371, Sep. 2001.
- [105] Y. Wu, R. H. Y. Louie, and M. R. McKay, "Asymptotic outage probability of MIMO-MRC systems in double-correlated Rician environments", *IEEE Trans. Wireless Commun.*, vol. 15, no. 1, pp. 367–376, Jun. 2016.
- [106] A. Abdi and M. Kaveh, "On the utility of gamma PDF in modeling shadow fading (slow fading)", in *IEEE 49th Veh. Technol. Conf.*, vol. 3, May 1999, pp. 2308–2312.
- [107] P. W. K. H. M. Srivastava, *Multiple Gaussian Hypergeometric Series*. John Wiley & Sons, 1985.
- [108] D. Morales-Jimenez and J. F. Paris, "Outage probability analysis for  $\eta$ - $\mu$  fading channels", *IEEE Commun. Lett.*, vol. 14, no. 6, pp. 521–523, Jun. 2010.
- [109] E. Martos-Naya, J. M. Romero-Jerez, F. J. Lopez-Martinez, and J. F. Paris, "A MATLAB program for the computation of the confluent hypergeometric function  $\Phi_2$ ", Repositorio Institucional Universidad de Malaga RIUMA., Tech. Rep., 2016.
- [110] J. Abate and W. Whitt, "Numerical inversion of Laplace transforms of probability distributions", *ORSA J. Comput.*, vol. 7, no. 1, pp. 36–43, 1995.
- [111] S. O. Rice, "Mathematical analysis of random noise", *Bell Syst. Tech. J.*, vol. 23, no. 3, pp. 282–332, 1944.
- [112] N. C. Beaulieu and S. A. Saberali, "A generalized diffuse scatter plus line-of-sight fading channel model", in *Proc. 2014 IEEE Int. Conf. Commun.*, Jun. 2014, pp. 5849–5853.
- [113] F. Ramos-Alarcon, V. Kontorovich, and M. Lara, "On the level crossing duration distributions of Nakagami processes", *IEEE Trans. Commun.*, vol. 57, no. 2, pp. 542–552, Feb. 2009.
- [114] P. Ramírez-Espinosa and F. J. López-Martinez, "On the utility of the inverse gamma distribution in modeling composite fading channels", *arXiv preprint arXiv:1905.00069*, 2019.



- [115] H. Al-Hmood and H. S. Al-Raweshidy, "Performance analysis of physical layer security over fluctuating Beckmann fading channels", *arXiv preprint arXiv:1904.08230*, 2019.
- [116] J. Chen and C. Yuan, "Coverage and rate analysis in downlink L-tier hetnets with fluctuating Beckmann fading", *IEEE Wireless Commun. Lett.*, 2019.